The Role of ICAM-1 Mediated T cell:T cell Interactions on CD8+ T cell Effector Function and Differentiation

A DISSERTATION
SUBMITTED TO THE FACULTY OF THE GRADUATE SCHOOL
OF THE UNIVERSITY OF MINNESOTA
BY

Nicholas Alan Zumwalde

IN PARTIAL FULFILLMENT OF THE REQUIREMENTS
FOR THE DEGREE OF
DOCTOR OF PHILOSOPHY

Yoji Shimizu, Ph.D., Advisor

April 2013

ACKNOWLEDGEMENTS

"If I have seen further it is by standing on the shoulders of giants."
- Isaac Newton to Robert Hooke (1676)

The work contained within the pages of this thesis dissertation could not have been obtained without the experimental and intellectual efforts of many individuals. My graduate school experience has been enriched through the collaborative efforts of my fellow Shimizu laboratory colleagues and more importantly friends, to which I recognize individually; Dr. Eisuke Domae, Dr. Brandon Burbach, Dr. Jason Mitchell, Dr. Chris DeNucci, Jessica Fiege, True Lee, Dr. Rupa Srivastava, Matthew Schwartz, Dr. Molly Thomas, Fernanda Shoyama, and many undergraduates. Other close collaborators that contributed to either my thesis project or overall scientific growth are Deb Lins, Dr. Julie Curtsinger, Dr. Gretta Stritesky, Dr. Janelle Olson, Dr. Lynn Heltemes-Harris, Dr. Sara Hamilton, Dr. Michael Gerner, Dr. James McLachlan, and Dr. Pujya Agarwal. To those names that I have forgotten, I remain sincerely apologetic. I would also like to recognize my fellow peers in the Microbiology, Immunology, and Cancer Biology (MICaB) program for making this arduous journey manageable; especially the entering class of 2007. Annette Bethke and Louise Shand must also be acknowledged for their Center for Immunology and MICaB efforts, respectively.

The University of Minnesota – Twin Cities has an outstanding list of extremely knowledgeable professors who prioritize the ambitions and needs of their students above all other noise. I sincerely appreciate the honest efforts of my thesis committee; Dr. Chris Pennell, Dr. Matthew Mescher, and Dr. Steve Jameson. Their experimental prowess and insight have immensely helped during my graduate education. Other collegial professors that have shaped my thinking and helped me succeed over the last several years include Dr. Kris Hogquist, Dr. Steve Rice, and Dr. Kim Mansky for their involvement on my preliminary committee; Dr. Erik Peterson and Dr. Marc Jenkins for their helpful discussions during lab meetings or data clubs/journal clubs; Dr. Chris Mohr and Dr. Mike Sadowsky for their role in helping me as a teaching assistant; and finally Dr. Christina Petersen for her role as an outstanding Preparing Future Faculty instructor.

My most important scientific acknowledgement is reserved for my mentor, Dr. Yoji Shimizu. His patience and high level of expectations during my development have molded me into the critical independent scientist that I am now. I am thankful for the tools and collaborations he afforded me. He is an outstanding example of strong work ethic fused with endless scientific intellect. His love of science is rivaled only by his love of baseball. I will miss our fruitful discussions about science, sports and Springsteen.

My upbringing and nurturing by my parents, Alan and Diana Zumwalde, deserves the highest level of recognition. My thankfulness for their unconditional love and support for all of my endeavors can never fully be put into words. Their guidance led by strong faith, great morals, and wonderful family values are above all the most crucial skills needed to navigate the path of life; I thank them for instilling in me those same strengths. Their commitment to their children is second to none. They are the best parents that a young man could ever ask or wish for and I consider myself beyond lucky to call them my mom and dad.

My younger brother, Colin Zumwalde, has been my best friend my entire life. I admire him for his positivity and sense of humor. I had the unique and blessed situation to be a graduate student on campus when he was also an undergraduate. My best memories at the University of Minnesota involved us walking through the state fairgrounds with our morning coffee. For those 20-30 minutes each day, our world revolved around the jokes and stories that we would tell each other; just like we used to when we were kids. Even though four years separate us in age, I'm thankful for the bond that I have with my brother that allows me to look up to him as an inspiration.

My younger sister, Bailee Zumwalde, is a gymnast for the University of Arkansas. I admire her passion and enthusiasm for every bend and curve that life provides. Her experiences as an athlete and my experiences as a graduate student have many parallels and I have appreciated the opportunity to be able to share these moments with her over the last few years. Her work ethic, in both athletics and academics, is top notch. She works hard to attain her goals and she deserves every ounce of recognition for exemplifying what hard work can do; I thank her for being a beacon of enthusiasm and a great example of how hard work really does pay off.

My wife, Katie Zumwalde, is my everything. She has sacrificed for my graduate education and has been my rock day in and day out. The little luxuries in life that we get to enjoy together are because of her. She shares in my successes with science, as well as talks me back up when there is "no light at the end of the tunnel". Putting science aside, the real important things in life are seeing her smile and making her happy. Over the past 6 years, I've focused on becoming someone to the world (through my science), when in reality my world has always been sitting right next to me at the dinner table, at church, on car rides, in movie theaters, and the list goes on. I want to thank my wife for allowing me to invest in our future through my graduate work and I apologize for my incessant babbling over T cells and graduate requirements. I want to recognize that no matter how big, she has always allowed me to dream; the exciting thing about her is that her dreams are just as big. Thank you for supporting my aspirations outside of and beyond science. I'm excited for our continued life together. Thank you for being a wonderful and understanding wife. I love you.

I want to once again thank my wife and family for their continued support, as well as my grandparents (Ralph and Linda Zumwalde & Frank and Shirley Weierke) and my in-laws (Jeff, Cheryl, Kathy, Craig, and Mark Christiansen) for all their prayers.

DEDICATION

"Your eyes must not determine what you see. Play more. Stand tall. Imagine."
- Mary Anne Radmacher

This written dissertation is dedicated to:

Frank "Pops" Herman Weierke
my guardian angel.

&

Katie Jayne Zumwalde
my love.

&

Baby Zumwalde in utero
my world.

ABSTRACT

CD8+ T cells are vital components to the immune system and serve as crucial effectors in the elimination of infected cells and pathogens. During the course of an immune response many interactions occur among antigen presenting cells and T cells, as well as, eventual contacts between activated T cells and target cells. However, during the stimulation of T cells, interactions exist among T cells themselves. These adhesion molecule mediated T cell activation clusters occur both *in vitro* and *in vivo*. Here we demonstrate the role of CD8+ T cell clusters on the eventual effector function and differentiation of CD8+ T cells. Our findings reveal that T cell clusters mediated via ICAM-1:LFA-1 interactions, help to dampen the immune response by regulating expression levels of the effector markers interferon-γ and granzyme B, as well as, cytotoxicity.

Understanding the mechanisms by which this effector regulation occurs is complex. Our data suggest that unclustered T cells sense an increased amount of antigen as shown through Nur77-GFP studies. In addition, our findings demonstrate a dependence on T cell cluster formation and contact in general for the upregulation of the immune inhibitory protein CTLA-4. CTLA-4 suppresses CD8+ T cell immunity via the downregulation of the transcription factor eomesodermin and thereby regulates the production of both interferon-γ and granzyme B. Similar effector function studies, under certain conditions, are indeed shown *in vivo* as well. Thus, T cell clusters regulate the tuning of CD8+ T cell function and terminal differentiation. These studies contribute to our knowledge of the necessity of T cell interactions and crosstalk during priming and potentially, via cluster manipulation, we hope to augment vaccine efficacy and anti-tumor immunotherapeutics.

TABLE OF CONTENTS

LIST OF FIGURES

CHAPTER 1: INTRODUCTION

CD8+ T cell Immunity

Stages of a CD8+ T cell immune response

Physiologically, the CD8+ naïve T cell precursor frequency for any given epitope has been estimated to be approximately 10-1200 per individual (1-8). These naïve or antigen inexperienced T cells, defined as $CD44^{low}$, migrate throughout the host via the circulatory and lymphatic systems. An assortment of differentially expressed proteins facilitates these T cell migration patterns from the blood into the lymph nodes and back into the blood stream. Specifically, T cell entry into lymph nodes from high endothelial venules (HEVs) is regulated by a multi-step process. The first step is the binding of T cell expressed L-selectin (CD62L) to HEV expressed peripheral node addressin (PNAd). This protein interaction leads to a slowing of T cell velocity and a rolling phenotype. T cell rolling aids in the process of chemokine receptor, namely CCR7 on the T cell surface, engagement of the chemokines CCL19 and CCL21 present on the surface of the endothelium. Chemokine receptor ligation mediates activation of integrins and subsequently strong adhesion to the HEV (9, 10). These strong adhesion, and eventual de-adhesion kinetics, facilitate T cell diapedesis into the lymph node either paracellularly (between two endothelial cells) or transcellularly (through endothelial cells) (11-13).

Once inside a lymph node, a naïve T cell will scan for cognate antigen in the context of major histocompatibility complex (MHC) presented on the surface of professional antigen presenting cells (APCs) such as dendritic cells (DCs), B cells, or macrophages. Under steady state conditions, a T cell will scan for antigen at a velocity of approximately 10-12 μm/minute (14, 15). If no antigenic signal is acquired, the T cell will sense gradient concentrations of phospholipid spingosine-1-phosphate (S1P)

through sphingosine-1-phosphate receptor 1 ($S1P_1$) and emigrate from the lymph node (16-18). However, if an immunological insult breaches the innate host defenses and a CD8+ T cell senses antigen presented via MHC-I on an APC a very different result occurs.

T cell receptor (TCR) triggering, in combination with co-stimulation and a third signal inflammatory cue, leads to the optimal activation of a T cell (19-21). This priming event induces a myriad of intracellular signals that eventually results in the upregulation of the early activation protein, CD69, and T cell proliferation (19, 21). Interleukin (IL)-2 production transiently occurs during early CD8+ T cell stimulation (19). The division of a single activated T cell clone has been estimated to give rise to at least 10,000 daughter T cells over the course of infection (21). This newly generated T cell effector army can then eradicate infected host cells through the expression of interferon-γ (IFN-γ), granzyme B, perforin, and tumor necrosis factor-α (TNF-α) (22). The peak of T cell expansion has been correlated with the clearance of pathogen (23, 24); at which time, a rapid T cell contraction will occur over several weeks yielding 5-10% of the peak T cell population to patrol the host as lifelong immunity (21, 25).

Long-lived T cell immunity or more aptly, T cell memory, exists in several flavors with an ever-expanding number of speculative models for their differentiation. Briefly, the strongest of the prevailing theories of memory induction are the uniform model, the signal strength model, the latecomer model, and the asymmetric division model. The uniform model speculates that all activated effector T cells acquire the potential to become memory precursors, but extrinsic factors limit the actual number of memory cells that are produced (23). The signal strength model hypothesizes that the T cells activated with the strongest combination of antigen, co-stimulation, and inflammation will become terminally differentiated effector cells; whereas the weaker combination of

signals leads to a memory phenotype (7, 23, 26). The latecomer model postulates that the last responding naïve T cells to infection will acquire the weakest signals during priming and subsequently be less terminally differentiated and attain a memory profile (7). Finally, the asymmetric division model speculates that the first division of an activated T cell will asymmetrically divide into a proximal and a distal T cell (relative to the APC). The proximal T cell fuels the effector T cell lineage; whereas the distal T cell can give rise to the memory lineage (7, 23, 27, 28).

To complicate these models, evidence has shown that a single precursor can give rise to multiple lineages (29). Additionally, short lived effector T cells (SLECs; KLRG-1^{high}CD127^{low}) and memory precursors (MPECs; KLRG-1^{low}CD127^{high}) can be observed during infection (30-33). SLECs tend to die during contraction and MPECs tend to seed the long-lasting memory population; however, conversion may occur between populations. Furthermore, memory cells can also be categorized based upon expression patterns of CD62L and CCR7. Central memory T cells (CD62L^{high}CCR7^{high}), which vigorously expand during antigen re-encounter, patrol lymphoid organs and have recently been shown to be prelocalized (34) or can rapidly relocalize (35) to peripheral lymph node regions upon pathogen re-exposure (7, 26). Effector memory T cells (CD62L^{low}CCR7^{low}), although inefficient at re-expansion, patrol the periphery of the host and rapidly exert effector functions upon antigen re-exposure (7, 26).

CD8+ T cell activation and immune regulation

In order for the aforementioned CD8+ T cell immune response to proceed, several important cues during priming must be achieved. The first step is T cell recognition of cognate peptide displayed by mature APCs (“signal one”). This TCR triggering step induces reorganization events at the interface of the APC:T cell junction.

More specifically, a “bulls-eye” structure consisting of a central supramolecular activation cluster (cSMAC) and a peripheral supramolecular activation cluster (pSMAC) become apparent and form the immunological synapse (IS) (36, 37). Evidence suggests that activation is induced by microclusters consisting of the TCR and several signaling kinases, which eventually move inward toward the cSMAC and either sustain or quench signaling (37-40). The pSMAC is primarily made up of integrins that help in the stabilization of a productive conjugate between the T cell and APC (36, 37); however, the relevance of integrin clustering at the IS beyond firm adhesion has yet to be deduced.

Besides TCR triggering, T cell stimulation is augmented via a variety of co-stimulation “signal-two” mechanisms. The canonical co-stimulation protein expressed by the CD8+ T cell is CD28. CD28 interactions with CD80 and CD86 (B7-1 and B7-2, respectively) expressed on the mature APC surface play a role in initiating T cell expansion, T cell survival, and IL-2 generation (41, 42). Other T cell surface molecules can serve co-stimulation purposes, such as 4-1BB (43), LFA-1 (44), OX40 (45), CD27 (45), and ICAM-1 (46) to name a few.

A “third major signal” that is imperative for optimal CD8+ T cell stimulation is the acquisition of an inflammatory cue. Recent evidence shows that this signal can take the form of interleukin (IL)-12 (47), IL-21 (48, 49), or type I interferon (IFN-α/β) (50). The third signal helps in significantly augmenting the clonal expansion and effector capabilities of primed CD8+ T cells. Mescher and colleagues have elegantly shown using microarray assays that different signal three cues may promote different T cell differentiation programs. Using three day *in vitro* activated OT-I (CD8+ T cells specific for chicken ovalbumin peptide (OVAp) in the context of H2-K^b) cells stimulated with IL-12 or type I interferon, they showed that IL-12 stimulated T cells promoted differential

expression patterns of ~730 genes, whereas type I interferon regulated ~610 genes. However, there were still ~355 genes commonly regulated between both conditions (perforin, granzyme B, IFN-γ, and several effector associated transcription factors to name a few) (51, 52). It has also been shown that certain pathogens exert different signal three responses by the immune system. For example, the clearance of *Listeria monocytogenes*, an intracellular bacterium, is heavily dependent upon IL-12 (53); whereas, lymphocytic choriomeningitis virus initiates a type I interferon response (54). Additionally, studies from Yi *et al.* have shown a requirement for IL-21 in CD8+ T cell mediated chronic viral immunity (49). The tuning of CD8+ T cell responses by different signal three cues may prove to be extremely beneficial for vaccine development and anti-tumor immunotherapies in the future.

Once activated, CD8+ T cells need inhibitory mechanisms to dampen immune responses from causing more destruction than necessary. The two most widely studied negative regulators of T cell responses are programmed cell death-1 (PD-1) and cytotoxic T-lymphocyte associated antigen-4 (CTLA-4; also referred to as CD152). PD-1 has two binding partners, programmed cell death ligand-1 and -2 (PD-L1 and PD-L2). PD-L1 is expressed among a broad spectrum of cell types such as (but not limited to) CD4+ and CD8+ T cells, myeloid DCs, and vascular endothelium; whereas PD-L2 is more restricted. PD-1 and PD-L1 are upregulated on CD8+ T cells after stimulation (55, 56). The ligation of T cell expressed PD-1 with PD-L1 (presumably on a DC, but maybe on another T cell or B cell) leads to a sequence of signaling events initiated by the tyrosine phosphorylation of immunoreceptor tyrosine inhibition and switch motifs (ITIM/ITSM) on the intracellular tail of PD-1. This leads to the binding of Src-homology 2 domain (SH2)-containing proteins, SHP-1 and SHP-2, which further dephosphorylates proximal signaling proteins and enhances PTEN expression (55, 56). Studies utilizing

PD-1 or PD-L1 blocking antibodies with exhausted T cells in chronic viral infection models have shown that blockade refreshes T cells so that viral control can be attained (57-59). This shows the efficacy in disrupting inhibitory molecule interactions for optimizing T cell responses.

The other inhibitory molecule of interest is CTLA-4 which binds to the same ligands as CD28 (60), albeit with a stronger affinity for both CD80 and CD86 when compared to CD28 (61-63). This affinity difference makes sense because both molecules need to compete for the same ligands; thus, by enabling the inhibitory protein to have a stronger binding affinity for ligand allows activation to be kept in check. CTLA-4 is upregulated both intracellularly and at the T cell surface after activation (60, 64-67) and the amount of expression has been correlated with both peptide affinity (65) for TCR, as well as, stimulation dosage (66). IL-2 has even been implicated in the induction of CTLA-4 expression in a dose dependent manner (66, 67). Many intrinsic and extrinsic models exist for understanding CTLA-4 function. Broadly speaking, the “inhibitory signaling” model states that negatively regulating signals are transduced through CTLA-4 upon ligation to CD80 or CD86; the second model, using a CTLA-4 splice variant that only expresses the cytoplasmic tail suggests that there are “ligand-independent inhibitory signals” (63). Another model hypothesizes that the ability of CTLA-4 to outcompete CD28 for ligand allows for a disruption in CD28 signaling (63). CTLA-4 has even been shown to augment LFA-1 adhesion to ICAM-1 (68). Extrinsic models suggest that CTLA-4 might be working to induce the production of inhibitory cytokines or to prevent ligand availability via soluble CTLA-4 to name several (63). Nonetheless, much work is needed to sort out the role of CTLA-4 on T cells and the signaling dynamics which mediate T cell inhibition.

More specifically, the role of CTLA-4 on CD8+ T cells has been examined using CTLA-4 ablation. These studies show that IFN-γ production, granzyme B expression, and target cell killing are all augmented in CTLA-4 deficient CD8+ T cells both *in vitro* and *in vivo* (69-71) . Additionally, Hegel *et al.* linked CTLA-4 regulation of effector ability to the transcriptional regulator of effector differentiation, eomesodermin (EOMES) (72), by showing that CTLA-4 inhibits the accumulation of EOMES through an unknown mechanism at both the transcript and protein level (70). Furthermore, clinical studies have revealed that blocking human CTLA-4 with ipilimumab monoclonal antibody can initiate long standing responses in a small subset of metastatic melanoma patients. Results showed that treatment augmented IFN-γ and granzyme B on EOMES expressing CD8+ T cells (73); further suggesting that CTLA-4 engagement controls EOMES suppression. However, the downstream events from CTLA-4 that appear to modulate EOMES are unknown.

Role of ICAM-1 and LFA-1 on CD8+ T cells

T cell:Dendritic cell interactions

As stated earlier, integrins (namely LFA-1 or $\alpha_L\beta_2$) expressed on the T cell surface promote firm adhesion to the counter ligand intercellular adhesion molecule-1, ICAM-1, expressed on endothelium (10). Additionally, LFA-1 on a T cell is important for optimal priming by facilitating a stable interaction with ICAM-1 expressed on DCs. Scholer *et al.* and Parameswaran *et al.* showed that ICAM-1 deficiency on APCs led to decreased T cell memory generation (74, 75). Additionally, IFN-γ expression by wt OT-I T cells was decreased when primed in ICAM-1 deficient hosts compared to wt hosts (75). Using an acute LCMV model, Cox *et al.* showed evidence of aberrant recall of ICAM-1 deficient memory T cells (76). Those studies also demonstrated that ICAM-1 on

non-lymphocytes was necessary for the contraction of MPEC CD8+ T cell populations (76). In sum, the combination of these data illustrates a critical need for both LFA-1 and ICAM-1 during optimal T cell activation.

Historically, ICAM-1 and LFA-1 interactions have been viewed in the context of ICAM-1 expressed on the DC and LFA-1 expressed on the T cell. However, the hematopoietic lineage specific integrin LFA-1 is also expressed on DCs and surface ICAM-1 is produced by T cells. Thus, the importance of these molecules from this new perspective must also be evaluated.

Active LFA-1 on T cells resides within lipid rafts; however, the LFA-1 expressed on the surface of human DCs is inactive and excluded from lipid rafts (77). These human monocyte derived DCs cannot bind to plate bound ICAM-1, unless the cells receive exposure to the chemokine CCL21 (78). Thus, DCs presenting antigen can only ligate ICAM-1 on another cell under strict conditions.

ICAM-1 co-stimulation

ICAM-1 expression on T cells is augmented upon TCR stimulation (79); however, the importance of this upregulation is unclear. Studies performed by Benedict and colleagues have shown utilizing stimulatory antibodies that ICAM-1 on human CD4+ and/or CD8+ T cells can serve as a co-stimulation molecule (46, 79-81). Specifically, co-stimulation through ICAM-1 initiated, among others, T cell division (46, 79, 80), upregulation of CD69 (46), activation of PI3K (46), and activation of the IL-2 and IFN-γ gene loci (46). It also promoted the generation of memory T cells (79, 80) and the differentiation of T-regulatory CD4+ T cells (Tregs) (81). These studies suggest that ICAM-1 on a T cell can play a role as a co-stimulatory signal during T cell antibody

stimulation. To our knowledge, these studies have not been demonstrated using *in vivo* models.

T cell:T cell interactions

ICAM-1 and LFA-1 have also been shown to play a role in allowing T cells to interact during activation *in vitro*. These T cell:T cell interactions result in the formation of T cell activation clusters that are now regularly regarded as hallmarks of T cell priming both *in vitro* and *in vivo* (82-89). Krummel and colleagues concluded that T cell:T cell contacts exhibit similarities to T cell:APC synapses based upon the observation that T cell:T cell contacts were stabilized yet dynamic, utilized LFA-1, maintained a gap between adjacent membranes, and secreted cytokines directionally (87). By performing elegant confocal microscopy and antibody capture assays, Sabatos *et al.* demonstrated that IL-2 signaling is polarized at T cell:T cell contact points via staining for CD25 and phosphorylated STAT5, as well as, IL-2 capture (87). These studies were performed using PMA / ionomycin treatment of a homogenous population of DO.11.10 TCR transgenic CD4+ T cells specific for an ovalbumin peptide (87). These studies and others have showed clustering *in vivo* using multi-photon microscopy.

Clusters *in vivo* most prevalently surround antigen presenting DCs. Thus, these clusters are multicellular in nature and could hypothetically be made up of DCs, antigen specific CD4+ and CD8+ T cells, B cells, and maybe Tregs; however, Tregs only make transient contact with other CD4+ T cells during activation *in vivo* and thus are thought to not be involved in these activation induced clusters (88).

The importance of T cell:T cell crosstalk within activation clusters is vastly understudied. Directed IL-2 signaling between T cells during initial stimulation (87) *in vivo* may help in the programming of memory recall as speculated by Cox *et al.* which is

based upon the ineptitude of ICAM-1 deficient T cells to re-expand upon re-exposure to antigen (76). Blazar and colleagues, using T cells that overexpress B7-2, showed a reduction in graft versus host disease mediated death presumably through T cell:T cell facilitated B7-2 and CTLA-4 interactions (90). Speculative roles for T cell clusters are numerous; however, polarization of CD4+ T helper differentiation, mediation of T cell contraction via Fas/TNF interactions, and T cell:T cell mediated immune regulation appear to be the leading candidates (88).

Structure and function of ICAM-1

Structure and putative signaling pathways of ICAM-1

ICAM-1 (or CD54) was discovered in the mid-1980's using the JY EBV transformed B cell lymphblastoid line (83). ICAM-1 is ubiquitously expressed by a wide variety of cells such as (but not limited to) fibroblasts, keratinocytes, leukocytes, and endothelial cells (91). This is unlike the integrin counter-ligands for ICAM-1 (LFA-1 or $\alpha_L\beta_2$ and MAC-1 or $\alpha_M\beta_2$), whose expression is restricted to cells of hematopoietic origin (92). The binding of ICAM-1 to LFA-1 and MAC-1 is reliant upon the integrin being active, thereby exposing a high affinity ICAM-1 binding region (93). Additionally, studies suggest that ICAM-1 dimerization allows for the proper orientation that enables LFA-1 ligation (94-96).

ICAM-1 is a transmembrane glycoprotein consisting of a cytoplasmic tail, a transmembrane region, and an extracellular portion that is made up of five immunoglobulin (Ig)-like domains with Ig5 proximal to the plasma membrane and Ig1 distal (95). LFA-1 binds to Ig1 and MAC-1 binds to Ig3 to promote adhesion (95, 97). ICAM-1, although rather simple in its structure, can be expressed quite differentially. ICAM-1 can be found in soluble form (sICAM-1) circulating in the bloodstream in both

healthy and diseased individuals (98-101); however, the source of this sICAM-1 is still unclear. It seems most reasonable that it is cleaved from the surface of endothelial cells during inflammatory conditions (presence of TNF-α, IL-1β, lipopolysaccharide (LPS), or IFN-γ) in which ICAM-1 upregulation can occur (95, 102, 103).

Circulating sICAM-1 can be found in mice that are deficient in wild-type ICAM-1 surface expression (102). These genetically manipulated mice are readily available, as opposed to cryopreserved, from The Jackson Laboratories. Our laboratory used these mice crossed to the OT-I background for the majority of this thesis research. They were generated by Xu *et al.* (C57BL/6^{tm1jcgr}) by inserting a neomycin cassette into exon four (which encodes Ig3) (97). Full length ICAM-1 expression is completely disrupted; however, several laboratories have shown evidence for differential splice variants with potential function (102, 104-106). The splice variants of ICAM-1, observed via reverse transcriptase polymerase chain reaction, are termed 3→6, 2→5, and 2→6. The 3→6 form is a fusion of domain 2 to domain 5, resulting in a potential protein with domains 1, 2, and 5 intact; this product can bind LFA-1 quite similarly to full length ICAM-1 (105). The 2→5 form is a fusion of domain 1 to domain 4 which yields a product with domains 1, 4, and 5. This isoform cannot bind LFA-1 (105). The last isoform expressed in the (C57BL/6^{tm1jcgr}) ICAM-1 mutant mouse (2→6), is a fusion of domain 1 and domain 5 to produce a small product that has intermediate LFA-1 binding ability (105); however, Robledo *et al.* did not observe the production of this isoform in the same strain (104). Another ICAM-1 deficient mouse (C57BL/6^{tm1Bay}), cryopreserved at The Jackson Laboratories, was generated by Sligh Jr. *et al.* by targeting exon 5 instead of exon 4 (107). Again, differential ICAM-1 isoforms were observed (102, 104-106). Wild-type mice have also been shown to express different spice variants encoded by mRNA (102).

The previously described isoforms denote variants in the extracellular domains of

ICAM-1; however, importance has also been ascribed to the short (28 amino acid) cytoplasmic tail. Even though this tail does not have enzymatic activity, there is a sequence, containing the only tyrosine residue within the tail, which shows homology to an ITIM motif (96). Depending on the cells (human lymphoblastoid B cells, human umbilical vein endothelial cells (HUVECs), brain microvascular endothelial cells, etc.) used for experimental study, signaling through ICAM-1 has been observed (95, 96, 108, 109). There is mounting evidence that ICAM-1 ligation on HUVECs is linked to rearrangement of the actin cytoskeleton via the GTPase Rho in a somewhat unclear mechanism (95, 96, 109). It is known *in vitro*, however, that the cytoplasmic tail of ICAM-1 expressed in brain endothelium is required for T cell transendothelial migration (TEM) because ICAM-1 tail mutants can still bind LFA-1 on T cells through the extracellular region but cannot deliver a signal to endothelial cells to allow for T cell TEM (110). Additional studies suggest that the phosphorylation of the sole tyrosine residue in the short cytoplasmic tail allows for an association with SHP-2 (108) which allows for events that lead to the activation of the small G-protein Ras (96). These signals feed into the activation of MAP kinase (MEK-1), which thereby activates Erk and helps promote the induction of the AP-1 transcription factor complex (95, 96). AP-1 plays an important role in regulating cytokines needed during cell proliferation (111). It is important to indicate that ICAM-1 signaling is not limited to the pathways and proteins listed above, as well as, ICAM-1 signaling may be different when comparing cells of different lineages such as endothelial cells and CD8+ T cells.

Pathogenesis associated with ICAM-1

As stated earlier, sICAM-1 can be seen escalated in individuals with disease. Specifically, high levels of sICAM-1 have been linked to cardiovascular disease (98-101)

and have also been observed in atherosclerotic lesions whereby it can play a role in promoting lesion size. Circulating sICAM-1 levels can also be increased in patients with graft versus host disease (112) , breast cancer (113), idiopathic pulmonary fibrosis (114), cystic fibrosis (115), and inflammatory disorders of the central nervous system (116).

The extracellular portion of membrane bound ICAM-1, aside from binding LFA-1 and MAC-1, also have docking sites for *Plasmodium falciparum* (causative agent of malaria) erythrocyte membrane protein-1 (PfEMP-1) and rhinovirus (causative agent of the common cold). Human rhinovirus and PfEMP-1 bind to the Ig1 domain of ICAM-1 (similar to LFA-1) (95). Studies have shown that the addition of sICAM-1 *in vitro* can neutralize rhinovirus infection (117). The commercially available zinc-based therapeutic Zicam (made by Zicam, LLC a subsidiary of Matrixx Initiatives, Inc.) focuses on disrupting rhinovirus entry by presumably decreasing ICAM-1 levels and inhibiting viral binding to ICAM-1 (118).

Scientific *in vivo* modeling using mice and matrigel matrix are effective ways to start to understand the progression of human disease. Using ICAM-1 deficient models, studies have linked ICAM-1 ablation to decreased vascular lesions during heart disease (119). Other studies have shown the importance of certain ICAM-1 isoforms over others in the progression of experimental autoimmune encephalomyelitis (106). Xu *et al.* has shown the importance of ICAM-1 in mediating resistance to LPS induced shock (97). Matrigel assays have shown that ICAM-1 is utilized by human breast cancer cells during invasion (120). In sum, ICAM-1 plays a significant role in the progression of multiple diseases and continues to be an important molecule to study in order to understand potential crosstalk among leukocytes, tumors, and pathogens.

Thesis summary

The broad objective of this thesis study was to illuminate the relationships and interplay that occur between T cells during activation. More physiologically, the goal was to understand how interactions between T cells themselves can contribute to overall immunity with the eventual intent on exploiting T cell:T cell crosstalk in order to optimize vaccine development and anti-tumor immunotherapeutics. Our specific hypothesis was that ICAM-1 mediated T cell:T cell interactions were necessary for the regulation of CD8+ T cell responses. Originally, we speculated that responses would be enhanced in the presence of T cell clusters; on the contrary, we observed that T cell clusters work to dampen CD8+ T cell effector function and tune differentiation.

Our early studies in Chapter 2 focused on the expression kinetics of ICAM-1 on T cells and the importance of a third signal cue in allowing for optimal upregulation which evidently correlated with T cell clustering during activation. Real time imaging of cluster formation allowed us to understand that clusters are indeed dynamic and that cluster formation can occur by several different methods. By utilizing ICAM-1 deficient CD8+ T cells, we also determined the dispensability of ICAM-1 on T cells in both forming a stable contact with antigen-laden APCs, as well as migrating in a naïve wild-type recipient.

Chapter 3 utilizes ICAM-1 deficiency, as well as antibody blockade as tools to examine additional roles for T cell clusters. The loss of clustering did not affect activation or T cell division, but surprisingly led to striking increases in effector function. These changes can be partially attributed to enhanced antigen sensing due to the lack of three-dimensional clustering. Furthermore, our studies show both decreased expansion and decreased long term survival of unclustered T cells compared to clustered T cells after co-transfer into naïve hosts. This result, in combination with augmented effector

capabilities, argues that enhanced terminal differentiation persists in the absence of T cell clustering.

Additional experiments support an immunoinhibitory role for T cell clusters. Although, PD-1 and PD-L1 do not seem to function aberrantly in the absence of clustering, we indeed observed an increased CTLA-4 expression profile if T cells were clustered. This contact mediated upregulation of CTLA-4 via T cell:T cell clustering was decreased using both ICAM-1 deficient T cells and cluster blocking antibodies. This increase of CTLA-4 observed with clustered T cells correlated with a diminution in intracellular EOMES expression when compared to unclustered T cells.

In chapter 4 we performed *in vivo* experiments in attempts to determine whether the enhanced effector function with unclustered T cells could lead to decreased tumor burden. Using a melanoma mouse model we did not observe augmented tumor control by the ICAM-1 deficient T cells when compared to wild-type. We also did not observe any major differences between low initial precursors of wild-type and ICAM-1 deficient OT-I T cells responding to *Listeria monocytogenes* expressing ovalbumin. However, we did observe effector differences, increased granzyme B and KLRG-1, in the ICAM-1 deficient OT-I T cells compared to wild-type when a high precursor frequency was used in combination with a single antigen/adjuvant administration. These results potentially suggest that ICAM-1 can play a role in tempering a CD8+ T cell response *in vivo*. Enhanced ICAM-1 deficient responses were only apparent when the endogenous (ICAM-1 sufficient) antigen specific T cells were outnumbered by the transferred T cells.

Taken together, the studies herein contribute evidence supporting the hypothesis that T cell activation clusters dampen CD8+ T cell immune responses. Disrupting these interactions may serve to strengthen an effector response. However, this might come at the expense of increased terminal differentiation and poor memory maintenance.

CHAPTER 2: Characterization of expression kinetics and adherent properties of ICAM-1 on CD8+ T cells

INTRODUCTION

Historically, there are two classical representations of contacts that T cells make with other cells. The first is a T cell circulating in the blood stream, whereby an encounter between the L-selectin (CD62L) expressed on the T cell occurs between peripheral lymph node addressin (PNAd) expressed on the surface of the endothelium. This interaction leads to a rolling and tethering event that allows for chemokines expressed on the surface of the endothelium to engage chemokine receptors on the naïve T cell, thereby changing the conformational status of the integrin $\alpha_L\beta_2$ (LFA-1) from an inactive to an active state. This active LFA-1 mediates tight adhesion and attachment to the ICAM-1 that is expressed on the surface of the endothelium. Upon strong ligation between LFA-1 and ICAM-1, the T cell can extravasate from a high endothelial venule (HEV) into the lymph node parenchyma (9, 10).

The second type of T cell interaction is usually illustrated as a naïve T cell scanning cells in a lymph node for cognate antigen being presented via a major histocompatibility complex molecule (MHC) (14). Once a CD8+ T cell recognizes peptide and MHC-I presented by a professional antigen presenting cell (APC), the T cell receptor (TCR) via inside-out signaling mechanisms mediates the affinity and avidity of integrins through conformational changes and integrin clustering, respectively (121). These changes allow for tight adhesion to the ICAM-1 expressed on the APC. Both of these interactions are tightly regulated by LFA-1 on the T cell binding to ICAM-1 on the recipient cell (75).

Even though the two major types of T cell contacts are detailed above, it is important to denote that lymphocytes can also make interactions between themselves. A well accepted interaction needed for high affinity antibody responses of B cells can occur between follicular helper CD4+ T cells and B cells (122). However, this T cell:B cell interaction is regulated by the SAP-SLAM pathway (123) and appears to rely less on LFA-1:ICAM-1 ligation. Another increasingly important, but severely understudied T cell association is the contact that T cells can make with other T cells. During activation, these contacts result in the formation of aggregates or clusters of interacting T cells. Krummel and colleagues recently utilized integrin deficient CD4+ T cells to reconfirm observations performed in the 1980's (82, 83) showing that these aggregates are mediated through LFA-1 on one T cell binding to, presumably, ICAM-1 expressed on another T cell (87). Recent studies have confirmed those initial *in vitro* studies (82, 83) by showing that these clusters form during *in vivo* T cell priming as well (85-87, 89).

All three of the LFA-1:ICAM-1 mediated interactions involving naïve or recently activated T cells listed above involves the upregulation of ICAM-1. ICAM-1 on endothelium is increased as a result of inflammation (91) and ICAM-1 on dendritic cells can become upregulated as the cell matures (124, 125). Studies have also shown that T cell activation through antigen recognition, or IL-2 and IFN-γ on memory cells, can lead to the upregulation of ICAM-1 on T cells (51, 79, 126). However, the function of this upregulation and the impact of the third signal inflammatory cue in augmenting ICAM-1 expression at the protein level on CD8+ T cells are not completely clear.

In this study we show that ICAM-1 expressed on naïve CD8+ T cells is critical for the formation of homotypic T cell activation clusters; whereas ICAM-1 is dispensable on the T cell for the formation of a T cell:APC conjugate. Interestingly, we also demonstrated that the highest expression of ICAM-1 on T cells is dependent on the

hallmark third signal, IL-12, and as a result mediated the most robust T cell activation aggregates even though LFA-1 surface expression is independent of IL-12 exposure.

MATERIALS AND METHODS

Mice

ICAM-1 deficient mice (B6.129S4-ICAM1^{tm1Jcgr}/J) were generated as previously described (97) and purchased from The Jackson Laboratories (Jackson Laboratory, Bar Harbor, ME). They were backcrossed to the OT-I TCR transgenic on the C57BL/6 background (>10 generations). In colony wild-type OT-I mice were used as controls. Recipient C57BL/6 mice were purchased from The Jackson Laboratories. Mice were housed and bred under specific-pathogen free conditions and generally used between the ages of 6-12 weeks. Experimental procedures, involving the use of mice, were approved by the Institutional Animal Care and Use Committee at the University of Minnesota – Twin Cities.

Cell preparation and flow cytometry

Single cell suspensions of mouse spleens and lymph nodes were prepared by mashing tissues through cell strainers or using an Automated gentleMACS^{TM} Dissociator (Miltenyi Biotec, Auburn, CA) into phosphate buffered saline (PBS)/2% bovine serum. Cell counts were attained using a Countess® Automated Cell Counter (Life Technologies, Grand Island, NY). Purified CD8+ OT-I T cells were obtained by depleting non-CD8+ leukocytes and red blood cells from the bulk population with the following negatively selecting antibodies (FITC conjugated – anti-CD4, anti-B220, anti-CD16/CD32, anti-F4/80, anti-I-A^{b}, anti-Ter119, and anti-CD44 (eBioscience, San Diego, CA and BioLegend, San Diego, CA)), then incubated with anti-FITC microbeads

(Miltenyi Biotec), and later applied to a MACS LS column (Miltenyi Biotec). The product obtained after column enrichment was generally ≥95% pure based upon CD8α+Vα2+ staining of 5-10x10^4 T cells using a FACS Calibur (BD Biosciences, San Jose, CA). Dendritic cell (DC) enrichment was performed similarly as above except that anti-CD11c microbeads (Miltenyi Biotec) were used for positive selection. After positive selection, DC enrichment was generally 45-50% using CD11c and I-A^b as positive markers. For flow cytometry experiments, usually 1-5x10^6 cells were stained in Hank's balanced salt solution (HBSS)/0.2% sodium azide/2% bovine serum (FACS buffer) for 30 minutes at 4° C. Surface antibody stains, unless stated, were performed as noted above and antibodies purchased from either BioLegend, eBioscience, or BD Biosciences. Surface staining antibodies of special interest include ICAM-1 (clone: YN1/1.7.4, eBioscience) and CD11a (clone: M17/4 eBioscience). Samples were run and collected using a FACS Calibur, LSRII, or Fortessa (BD Biosciences) and analyzed with FlowJo software (Tree Star, Inc., Ashland, OR).

Dendritic cell:T cell conjugate assay

2x10^5 wild-type or ICAM-1 deficient DCs enriched from non-transgenic mice were pulsed with chicken ovalbumin (OVA) peptide (SIINFEKL) (Life Technologies) and mixed with 2x10^5 purified wild-type or ICAM-1 deficient naïve CD8+ OT-I T cells for 5, 10, 30, or 60 minutes at 37° degrees C. At which time, the plates were briefly spun, supernatants dumped, wells vortexed for 20 seconds, and cells fixed with 1% paraformaldehyde at room temperature for 20 minutes. Cells were then washed several times with HBSS/2% bovine serum, stained with surface antibodies, and prepared for flow cytometry. The percentage of conjugates was assessed by evaluating the percentage of CD11c+I-A^b+ cells present in the CD8α+Vα2+ gate.

In vivo T cell homing assay

$1.3x10^6$ unpurified naïve wild-type (CD45.1+) or ICAM-1 deficient (CD45.1+) OT-I CD8+ T cells were adoptively transferred intravenously (i.v.) into recipients (CD45.2+). Three hours post transfer, recipients were sacrificed, and tissues harvested into PBS/2% bovine serum. Single cell suspensions were performed, stained with surface antibodies, and prepared for flow cytometry.

Emulsified OVA and adjuvant challenge into mouse ear pinna

$2.25x10^5$ unpurified wild-type OT-I CD8+ T cells (CD45.1+CD45.2+) were adoptively transferred i.v. into recipient C57BL/6 non-transgenic hosts (CD45.2+). One day later, mice were anesthetized with a mixture of ketamine/xylazine. Anesthetized mice were injected in ear pinna with 3 µg OVA emulsified in Incomplete Freund's Adjuvant (IFA) (Sigma-Aldrich, St. Louis, MO) in a total volume of 10 µLs. Control mice were injected with 10 µLs of PBS/IFA. One to five days post priming, recipients were sacrificed and the draining superficial cervical lymph node was harvested, stained with surface antibodies, and prepared for flow cytometry. Emulsions were prepared by mixing IFA and PBS/OVA using glass syringes (Popper and Sons, Inc., New Hyde Park, NY) and rapidly freeze thawing multiple times. Emulsifications were transferred from glass syringes into insulin syringes for ear pinna injections.

In vitro T cell stimulation

In vitro activation conditions were designed similarly to previous studies (51, 127). DimerX H-$2K^b$:Ig fusion protein (BD Biosciences) was diluted to 2 µg/mL in sterile PBS and recombinant B7-1/Fc chimeric protein (R&D Systems) was diluted to 0.4 µg/mL in sterile PBS. Flat-bottomed microtiter 96-well plates (Sigma-Aldrich) received 50 µLs

of each reagent and incubated for at least 2 hours at room temperature. Wells were washed twice with sterile PBS and once with alloclone media. Alloclone media was RPMI 1640 (Life Technologies) supplemented with 10% fetal calf serum, 4 mM L-glutamine (Mediatech, Inc., Manassas, VA), 0.1 mM nonessential amino acids (Mediatech, Inc.), 1 mM sodium pyruvate (Mediatech, Inc.), 100 U/mL penicillin and streptomycin (Mediatech, Inc.), 10 mM HEPES (Mediatech, Inc.), and 5 μM 2-Mercaptoethanol (Life Technologies). SIINFEKL (0.375 μg/mL) was loaded onto DimerX H-2K^{b}:Ig fusion protein by adding 100 μLs/well. Plates were incubated at 37° C for at least 2.5 hours and then washed several times with alloclone. Purified wild-type or ICAM-1 deficient OT-I CD8+ T cells were added at a concentration of 5x10^{4} cells/well in a total volume of 210 μLs alloclone supplemented with 0.05 μg/mL of IL-12 (R&D Systems). Plates were then incubated at 37° C until harvested at 24-, 48-, and 72-hour time points.

Anti-LFA-1 blocking antibody treatment

The disruption of T cell clusters *in vitro* was performed using the endotoxin-free/low azide anti-LFA-1 (anti-α_L) antibody M17/4 (BioLegend and eBioscience) at a final concentration of 2.5 μg/well. Control anti-LFA-1 (anti-β_2) antibody M18/2 (BioXCell, West Lebanon, NH) did not block clustering and was used at a final concentration of 2.5 μg/well. Blocking antibodies were added to wells at the same time T cells were plated.

CFSE labeling

Carboxyfluorescein succinimidyl ester (CFSE) labeling was performed by adding an equal volume of 10 μM CFSE to T cells (resuspended at 20x10^{6}/mL in PBS/5% bovine serum). The mixture was vortexed and labeling proceeded in the dark for 5

minutes. Then the cell mixture was washed three times with 20-35 mLs PBS/5% bovine serum. Cells were resuspended in PBS/2% bovine serum, counted, and brought to the concentration of $2.5x10^5$ T cells/mL in alloclone for plating.

Microscopy

Images of activated T cells were either taken with a light microscope equipped with a camera or using live content imaging and analysis with an IncuCyte™ ZOOM imager (Essen Bioscience, Inc., Ann Arbor, MI). Images were taken with a 10X objective lens every two hours for cluster quantification and every 15 minutes for single cell analysis using a CFSE labeled T cell spiking strategy. The parameters used in determining the number of clusters/mm^2 with IncuCyte™ ZOOM software were an area >2000 μm^2 and an eccentricity of <0.8. These parameters were chosen based on analysis troubleshooting with a trained professional.[1] Once a T cell cluster met these conditions it was "masked" yellow. The amount of separate masked clusters was enumerated by the software every two hours. Once the entire field was made up of a confluent lawn of masked T cells it was considered to be a single cluster. Four different locations were imaged in each well over the entire time course and clustering analysis was dependent upon the quantification of at least 8-16 total movies.

Statistics

GraphPad Prism version 5.03 software (GraphPad Software, Inc., La Jolla, CA) was utilized to determine statistical significance using Student's unpaired two-tailed *t* test. P value cutoffs and notation were used as follows (unless otherwise denoted in figure captions): *, p value<0.05; **, p value<0.01; ***, p value≤0.0008.

RESULTS

Confirmation of ICAM-1 deletion and normal LFA-1 expression

In order to perform our experiments, we took advantage of a previous ICAM-1 deficient mouse model that was designed by inserting a neomycin cassette into exon 4 (which translates to the third immunoglobulin (Ig) domain at the protein level) of the ICAM-1 gene as previously described (97). We then backcrossed (> 10 generations) the ICAM-1 deficient mouse to the OT-I CD8+ TCR transgenic on the C57BL/6 background to generate an ICAM-1 deficient OT-I mouse (ICAM-1 KO). This model is useful because we know the antigen specificity of the TCR for all of the CD8+ T cells used in this study. Wild-type (wt) OT-I mice were used as experimental controls.

We first wanted to confirm the ablation of ICAM-1 expressed on the T cell surface from the ICAM-1 KO OT-I mice. Lymph nodes from ICAM-1 KO and wt mice were stained for CD8+ OT-I T cells using CD8α and Vα2 antibodies that recognize the co-recepter and α-chain of the TCR, respectively. ICAM-1 staining on naïve wt OT-I T cells was positive and, as expected, ICAM-1 was not detected on the ICAM-1 KO T cells (Fig. 2-1A). The α_L subunit of LFA-1, the counter receptor for ICAM-1, was also stained for on both subsets of T cells and was found to be expressed at equal levels (Fig. 2-1B). We show here that ICAM-1 is undetectable on ICAM-1 KO T cells, whereas LFA-1 expression remains intact.

ICAM-1 KO T cells do not exhibit migratory defects to peripheral lymph nodes

Next, we wanted to examine whether the ablation of ICAM-1 on CD8+ T cells affected the ability of those cells to migrate to peripheral lymph nodes. It has been established that LFA-1 on T cells is critical for efficient transendothelial migration, as well as trafficking to peripheral lymph nodes (128, 129). Additionally, some recent evidence

using CD4+ T regulatory (Treg) cells suggested that migration to infected lung tissue is unaffected by the loss of ICAM-1 on the Treg (130). To test this question with naïve CD8+ OT-I T cells we used congenic markers that allow the differentiation of a transferred population from the recipient without affecting the biology in order to observe the wt or ICAM-1 KO T cells from the host after transfer. Three hours after intravenous (i.v.) adoptive transfer of $1.3x10^6$ T cells, the transferred populations were recovered from a single inguinal lymph node, a single cervical lymph node, and the spleen. The absolute numbers of T cells enumerated between the wt and ICAM-1 KO cells harvested from lymph nodes were determined to be statistically insignificant (Fig. 2-2A). However, absolute numbers recovered for ICAM-1 KO T cells were higher in the spleen than for wt T cells (Fig. 2-2B). These data suggest that ICAM-1 on T cells is not necessary for migration through HEV and into lymph node tissue. Additionally, since more ICAM-1 KO T cells were recovered in the spleen compared to wt T cells this might suggest that ICAM-1 on T cells might be important for the migration into other tissues not examined and as a result of not reaching that tissue(s), ICAM-1 KO T cells preferentially reside instead in the spleen.

Even though lymph node migration is unaffected, we consistently enumerated reduced amounts of naïve CD8+ OT-I ICAM-1 KO T cells from all lymph nodes when compared to wt controls post MACS purification (Fig. 2-2C). Decreased numbers may be indicative of a lymphopenic environment that can sometimes be filled by T cells that homeostatically proliferate and present themselves as activated (CD44hi) in an antigen independent manner (131, 132). ICAM-1 KO T cells taken from lymph nodes did not display evidence of homeostatic proliferation as evidenced by equal expression of the activation marker CD44 pre- and post-MACS when compared to wt T cells (Fig. 2-2D). We did not determine CD44 levels on naïve T cells post transfer into new recipients.

ICAM-1 is dispensable on T cells for binding antigen-laden wt dendritic cells

We next sought to understand whether ICAM-1 deficiency on the T cell ablates the ability of T cells to form stable contacts with antigen-pulsed dendritic cells (DCs) *in vitro*. As stated previously, these interactions are mediated extensively by the LFA-1 integrin on the T cell binding to ICAM-1 on the APC (75). We adapted a well-established conjugate assay (133, 134) in which enriched DCs from C57BL/6 non-transgenic mice are pulsed *in vitro* with SIINFEKL peptide (a short antigenic fragment derived from chicken ovalbumin (OVA)) and incubated with purified wt or ICAM-1 KO OT-I T cells for a short duration, fixed, and then assayed via flow cytometry for stable conjugate formation. In Figure 2-3A, the upstream gating strategy used to define conjugate efficiency is shown by determining the percentage of DCs (I-A^b+CD11c+) in the OT-I T cell (CD8α+Vα2+) gate. The wt DCs from C57BL/6 non-transgenic mice used in this assay show high levels of ICAM-1 expression and are LFA-1 positive (Fig. 2-3B), while ICAM-1 deficient DCs from ICAM-1 KO C57BL/6 non-transgenic mice show an ablation of ICAM-1 but similar levels of LFA-1 compared to wt DCs (Fig. 2-3B).

As proof of principle that the assay faithfully recapitulates previous literature (75), ICAM-1 deficient DCs were enriched from ICAM-1 KO non-transgenic mice, pulsed with SIINFEKL, and incubated with purified wt OT-I T cells. When compared to wt OT-I T cells incubated with non-transgenic wt DCs pulsed with SIINFEKL, we observed a striking difference in the conjugate efficiency that was statistically significant at every antigen dose experimentally tested (Fig. 2-3C). These data corroborate evidence that ICAM-1 on the DC is absolutely critical for T cell:APC interactions to persist (75).

Next, we used wt DCs pulsed with SIINFEKL and incubated them with ICAM-1 KO OT-I T cells. We determined that wt and ICAM-1 KO OT-I T cells produce equal levels of conjugates with antigen-laden wt DCs at all antigenic doses examined (Fig. 2-

3D). These similar conjugate efficiencies persist even when the incubation time is altered (Fig. 2-3E); in addition, it is interesting to denote that overall binding efficiency inversely correlates with incubation time (Fig. 2-3E). Although this is a striking result, it is not entirely unexpected given that there is some precedence in the literature that suggests that the LFA-1 present on DCs is held in an inactive state and does not bind ICAM-1 (77, 78). Furthermore, to our knowledge, this is the first time that conjugate efficiency of ICAM-1 deficient T cells has been tested in this manner. In summary, these studies reconfirm the importance of ICAM-1 expressed on DCs in stabilizing a T cell:APC interaction; whereas the ICAM-1 on T cells is dispensable for the stability of this contact.

Optimal ICAM-1 upregulation on T cells is dependent on the third signal

We next sought to determine the expression kinetics of surface ICAM-1 on activated T cells. By utilizing an established *in vitro* T cell activation system whereby plate bound H2-K^b:SIINFEKL (signal 1) and plate bound recombinant B7-1 (signal 2) are used to stimulate purified OT-I T cells in the presence or absence of soluble IL-12 (signal 3) (51, 127), we were able to ask how signal 3 alters the expression of ICAM-1 and LFA-1 on wt OT-I T cells over three days of T cell stimulation.

We observed rapid upregulation of ICAM-1 on wt T cells as early as five hours post stimulation that was not dependent upon IL-12 exposure (Fig. 2-4A). After one day of activation, ICAM-1 expression had increased but did not reach maximal expression until two days post stimulation (Fig. 2-4B). Interestingly, IL-12 exposure did not play a role in ICAM-1 expression after one day of activation; however, there was greater than a two-fold difference in ICAM-1 upregulation at day two between the +IL-12 and –IL-12 conditions (Fig. 2-4B). These IL-12 induced ICAM-1 expression differences were also

seen at three days post priming; a time in which total ICAM-1 expression is decreasing under both conditions (Fig. 2-4b). These results correlate with a previous study in which increased ICAM-1 transcript levels were also seen under T cell activation conditions in which signal 3 was present versus absent (51).

When LFA-1 expression was determined, we surprisingly noticed that the kinetics were unaltered by the presence or absence of signal 3 (Fig. 2-4C). LFA-1 upregulation peaked sometime between days two and three post *in vitro* stimulation (Fig. 2-4C). Unlike ICAM-1 kinetics on T cells, LFA-1 expression remained elevated and did not appear to decrease at any point throughout the experimental time course (Fig. 2-4C).

We next wanted to determine whether ICAM-1 upregulation kinetics *in vivo* were similar to the *in vitro* results. Using an established ear pinna administration model (135) with antigen/adjuvant which may mimic physiological conditions of vaccine immunizations into the sub-cutaneous or dermal layers of human skin, we sought to determine ICAM-1 kinetics on T cells in the activated draining cervical lymph node. On day -1, $2.25x10^5$ wt OT-I T cells (CD45.1+CD45.2+) were injected i.v. and allowed one day to park in the recipients (CD45.2+) before 3 µg OVA emulsified in Incomplete Freund's Adjuvant (IFA) were injected into the ear pinna. IFA was used because it serves as a signal to induce the maturation of dendritic cells to release IL-12 (136) among other signal 3 mediators of CD8+ T cell activation. Phosphate buffer saline (PBS) emulsified in IFA was used as a negative control. Within 24 hours, ICAM-1 expression on transferred T cells had started to increase based upon geometric mean fluorescence intensity (gMFI) above the control PBS/IFA hosts (Fig. 2-5A). Day 2 ICAM-1 gMFI showed approximately a 3-fold difference from day 1 and appeared to reach maximal expression at day 2 (Fig. 2-5A). Even 5 days after stimulation, the activated T cells still showed an elevated ICAM-1 protein level above the PBS/IFA control (Fig. 2-

5A). Adjuvant and PBS alone do not seem to enhance ICAM-1 expression at any time point; this reveals the necessity of TCR triggering for ICAM-1 expression to initiate (Fig. 2-5A). Interestingly, peak ICAM-1 expression correlated with peak CD69 upregulation (Fig. 2-5B), as well as the onset of T cell division based upon the absolute number of recovered cells (Fig. 2-5C). These data suggest that an increase in ICAM-1 expression may be a strong indicator of early activation of antigen specific CD8+ T cells. In sum, ICAM-1 expression kinetics *in vitro* mimic the *in vivo* response by peaking two days post priming. This optimal expression pattern is very much dependent upon both a TCR signal and a third signal such as IL-12.

T cell:T cell homotypic clusters are critically dependent upon IL-12 and ICAM-1:LFA-1 interactions

Using the previously described *in vitro* activation system for OT-I T cells, we wanted to monitor the formation of T cell:T cell homotypic clusters that are hallmarks of T cell priming *in vitro* and *in vivo* (82-89). In this reductionist APC-independent system, we were able to assess the role of T cell:T cell contacts. We chose this model because in an APC-dependent system of stimulation it is not possible to rule out the role of T cell:APC contacts and therefore not possible to solely interrogate a T cell:T cell interaction. Since peak ICAM-1 expression occurred at two days post *in vitro* stimulation (Fig.2-4B), we chose to image T cells at this time in order to capture T cell:T cell interactions. At two days post priming, we observed wt T cell aggregates (Fig. 2-6A).

Since optimal ICAM-1 expression kinetics were dependent upon IL-12 exposure, we sought to determine qualitative differences in T cell clustering as a result of the IL-12 third signal. Using 48 hours as our time point of interest, we imaged wt T cells that had been activated in the absence of IL-12. Under these priming conditions we observed a

decrease in the amount of T cells clustering and an increase in the total number of T cells not involved in clusters (Fig. 2-6B). This result suggests that IL-12 plays a role in mediating T cell clustering by regulating ICAM-1 expression on activated T cells. Though not examined here, it is possible that the affinity and avidity of LFA-1 could be altered in the presence of IL-12 and thereby contributes to cluster production.

Although ICAM-1 expressed by T cells did not play a critical role in promoting T cell:APC contacts (Fig. 2-3D), we hypothesized that cluster formation using our ICAM-1 deficient OT-I T cells might be reduced compared to wt because the ligand for the LFA-1 integrin was ablated. Using the same *in vitro* stimulation system as above, we activated purified ICAM-1 KO OT-I T cells and imaged cluster production at day two. As expected, we did not observe cluster formation (Fig. 2-6C).

We also utilized two different anti-LFA-1 antibodies in combination with wt OT-I T cells to test the disruption of wt T cell aggregates. The first antibody (M17/4) targets the α_L (CD11a) component of LFA-1, while the second antibody (M18/2) binds to the β_2 (CD18) chain of LFA-1. The M17/4 antibody disrupted wt T cell clusters to a similar extent as the ICAM-1 KO T cells (Fig. 2-6D); whereas, the M18/2 antibody did not inhibit clusters (Fig. 2-6E) and served as a control condition. In sum, ICAM-1 expression on T cells, and to a lesser extent acquisition of IL-12, co-mediate T cell cluster formation.

T cell:T cell clustering kinetics and composition

Extending our previous observation, we next sought to understand clustering kinetics. We performed this by quantitatively determining T cell clustering (parameters for determining clustering are outlined in Chapter 2 - Materials and Methods) using an IncuCyte™ ZOOM live imager (an incubator equipped with an imaging camera) which was able to take images of clusters every two hours for the extent of our *in vitro* time

course. Our results show a strong clustering phenotype, represented by the number of clusters/mm^2, that peaks around two days post stimulation for the wt T cells. ICAM-1 KO T cells show minimal to no T cell clustering (Fig. 2-7A[1]). Additionally, the M17/4 LFA-1 blocking antibody showed comparable cluster disruption to ICAM-1 deficiency (Fig. 2-7B[1]). The M18/2 anti-LFA-1 treatment did not disrupt clusters and aggregate formation was elevated above ICAM-1 KO conditions (Fig. 2-7C[1]). We also highlighted representative images at the end of each day in culture that are used in the quantitation shown in Figures 2-7A-C for each of our four T cell conditions; wt (Fig. 2-7D[1]), ICAM-1 KO (Fig. 2-7E[1]), wt with M17/4 blocking antibody (Fig. 2-7F[1]), and wt with M18/2 non-blocking antibody (Fig. 2-7G[1]). These images depict the lack of clustering at day one, as well as, illustrate the formation of a confluent lawn of T cells generally observed at three days post priming. This time course analysis also confirms that the time point used in Figure 2-6 is optimal for observing the presence or absence of T cell clustering.

Finally, it was of interest to determine the makeup of *in vitro* T cell clusters. Once again, utilizing the IncuCyte^{TM} ZOOM imaging technology, we sought to track the movement of individual cells as clustering occurred in order to understand whether clusters were an accumulation of daughter cells after division or whether clusters were the result of several activated T cells coming together. In order to perform these experiments, we labeled a population of purified wt OT-I T cells with the cell tracker dye CFSE and spiked them into a population of unlabeled wt OT-I T cells at a ratio of 2.5% labeled to 97.5% unlabeled. As shown in the sequence of images following one labeled T cell (indicated by *straight arrow*) throughout the experimental time course (Fig. 2-8A[1], starting from the *top image* and moving down) we show, qualitatively, that a single cluster is heterogeneous and can be made up of several different activated OT-I T cell clones. Additionally, we show that cluster formation can result from the merging of two

separate T cell clusters, as shown by two individual clusters at 32:15 hours in Figure 2-8A[1] (*straight arrow cluster* shows the location of the original T cell from the *top image* and one *rounded backside arrow* shows another cluster) that merge into a single cluster at 34 hours (indicated by the *straight arrow*). These sequences of merging events continue over the course of the experiment and contribute heavily to the masked yellow clusters that meet the parameters outlined for quantification of a cluster by the IncuCyte™ ZOOM analysis software. Furthermore, it is important to state that individual clones have the capacity to migrate over the plate (Figure 2-8A[1], location of *straight arrowed* cell in *top image* compared to the same T cell illustrated by a *straight arrow* in the *second image*).

The formation of a small cluster based solely on the division of a single labeled T cell is harder to assess. By following the labeled T cell (indicated by the *straight arrow*) in Figure 2-8B[1] (*top image* at 33:30 hours presumably shows an individual clone that is dividing in the *second image down* at 33:45 hours and eventually forms a small cluster in the *third image down* at 37:15 hours) we speculate that a small cluster might be produced as a result of a single division. Once again, these separate clusters merge rapidly together into larger clusters (Fig. 2-8B[1], merging of a *round backside arrow* and a *straight arrow*) that eventually become quantifiable. To more accurately assess the ability of a single T cell clone to form a single homogeneous cluster it would be better to perform these spiking experiments at a lower density of total cells/plate *in vitro* with a more frequent image rate than every fifteen minutes.

DISCUSSION

Here we demonstrate the role of ICAM-1 on T cells for both *in vivo*

migration and the formation of functional cell:cell interactions. We also monitor ICAM-1 upregulation in response to optimal CD8+ T cell stimulation conditions, as well as the effects of this expression on the ability of T cells to form clusters with one another.

ICAM-1 deficiency on a naïve CD8+ T cell does not alter the ability of T cells to traffic into peripheral lymph nodes of wt recipient mice based upon short-term adoptive transfer T cell homing assays. These data corroborate literature indicating that ICAM-1 on Tregs is dispensable for T cell migration to *Mycobacterium tuberculosis* infected lung tissue (130). This result is not completely unexpected because endothelial cells do not express the hematopoietic lineage specific ICAM-1 counter receptor, LFA-1; which is necessary to engage ICAM-1 on a T cell. Interestingly, more ICAM-1 KO T cells were recovered from spleens than wt T cells. This observation indicates that there might be a tissue that relies on ICAM-1 being expressed on the T cell to either efficiently migrate or to be retained at that currently underappreciated site.

Even though migration appears to be similar between wt and ICAM-1 deficient T cells, the absolute number of purified OT-I T cells from wt mice is statistically higher when compared to numbers recovered from ICAM-1 KO OT-I mice. This issue can most likely be explained using a combination of two rationales. First, in an ICAM-1 KO OT-I mouse, all of the cells (not just T cells) are deficient in ICAM-1 production. As previous literature suggests, T cell extravasation into tissue is heavily dependent upon LFA-1 on a T cell binding to ICAM-1 expressed on the endothelium (128, 129). If ICAM-1 expression on endothelial cells is ablated, the expectation would be that less T cells would enter into the desired tissue and thus recovery of ICAM-1 KO OT-I T cells would be reduced in the peripheral lymph nodes compared to wt OT-I mice. Another explanation would be that T cell development in an ICAM-1 KO mouse is not as efficient as it is in a wt mouse, since ICAM-1 would not be present on thymic cells that are

important for positive and negative selection. In order to test this, a mixed bone marrow chimera with an equal ratio of wt to ICAM-1 KO bone marrow could be employed. This would allow wt and ICAM-1 KO T cells to develop together with the expectation of a skewing toward wt if ICAM-1 on a T cell is necessary for development. The other expectation would be no difference between wt and ICAM-1 KO output because at least half of the thymic cells would be ICAM-1 sufficient and thus allow for adequate binding and selection.

We also determined, for the first time, the dispensability of ICAM-1 on T cells in binding to antigen-pulsed DCs. It is important to denote that both wt non-transgenic DCs and wt OT-I T cells express both ICAM-1 and LFA-1. Previous reports have shown that ICAM-1 on the APC is vital for a productive T cell interaction to occur (75). Not only does our data support those findings, it also extends those studies and examines the importance of T cell expressed ICAM-1 in mediating APC:T cell contacts. Surprisingly, the ablation of ICAM-1 on a T cell does not affect the ability of a T cell to form a conjugate with an antigen-laden DC. Even though DCs express LFA-1, previously published results suggest that it is not in an active and functional state until the DC acquires a chemokine signal (77, 78). Thus, it might be expected that LFA-1 deficient DCs when asked to bind to wt OT-I T cells would behave similarly to wt DCs combined with ICAM-1 KO OT-I T cells.

ICAM-1 is highly upregulated during inflammatory conditions on endothelial cells (91). It has also been shown to increase on leukocytes such as DCs (124, 125) and macrophages (137) after adjuvant exposure; in addition, some reports have shown that ICAM-1 becomes upregulated at the protein and transcript level on T cells (51, 79, 126). However, the kinetics of ICAM-1 expression on activated T cells and the impact of signal three in the regulation of ICAM-1 on the surface of T cells have not been adequately

examined. Here we demonstrate that ICAM-1 expression on CD8+ T cells is rapidly upregulated, sometime between two and five hours post priming. This early increase in expression is independent of third signal exposure. IL-12 independent effects on ICAM-1 expression extend to one day post activation; however, the dependency on IL-12 is vital for peak ICAM-1 expression and overall maintenance of ICAM-1 on activated T cells at days two and three post stimulation. In the presence of IL-12, ICAM-1 is upregulated 2.4-fold at day two and 3.6-fold at day three when compared to no IL-12 conditions. Our *in vivo* data demonstrates the necessity of TCR engagement for ICAM-1 upregulation. Adjuvant alone (IFA/PBS) does not lead to a striking upregulation of ICAM-1 and therefore suggests that antigen-sensing is the primary initiator of ICAM-1 expression on T cells. Using this model we were not able to clearly deduce whether IFA *in vivo* augments ICAM-1 expression as seen *in vitro* with IL-12. However, both *in vitro* and *in vivo* ICAM-1 expression maintains at an elevated state above naïve at three days post *in vitro* priming and five days post *in vivo* priming. Interestingly, ICAM-1 expression patterns closely mimic CD69 expression in such a way that ICAM-1 should be viewed as an additional hallmark biomarker of early T cell activation. Additionally, since CD69 acts to inhibit $S1P_1$ and lymphocyte emigration from activated lymph nodes (138), we speculate that the rapid upregulation of ICAM-1 on the T cell surface may facilitate strong interactions with other activated lymphocytes in the lymph node that could play a combinatorial role with the ability of CD69 to regulate $S1P_1$ in order to limit the immediate egress of activated T cells from lymphoid organs.

Even though ICAM-1 showed an increase in expression when exposed to a third signal, LFA-1 showed no preferential increase in upregulation whether IL-12 was present or absent. We speculate that these expression differences might be a mechanism by which T cells are able to sense the environment in which they are trafficking, such as an

activated draining lymph node where T cell expressed ICAM-1 may heavily engage upregulated LFA-1 on other T cells or leukocytes. Further experimentation is required to assess the validity of this hypothesis.

Although ICAM-1 is dispensable on the T cells for forming contacts between APCs and T cells, it is absolutely critical for T cell:T cell interactions and the immunological phenomenon of T cell clustering. ICAM-1 is a central mediator of T cell cluster formation during activation as evidenced in both the still images and the number of clusters forming over time. Previous literature has shown the importance of integrins in this process (87), as well as the actual discovery of ICAM-1 came as a result of a similar type of experiment (83). But to our knowledge this is the first time that cluster formation has been examined over the course of at least three days of stimulation *in vitro*. Additionally, our third signal inflammatory cue IL-12, albeit to a lesser extent than ICAM-1, also plays a role in cluster production. Here we have illustrated a link between peak expression of ICAM-1 as influenced by IL-12 and clustering as evidenced by time-lapse cluster quantification at approximately two days post T cell priming. T cell clustering dynamics as a result of IL-12 or another third signal cue *in vivo* is a more rigorous process and will require a stringent time course of T cell activation using multi-photon microscopy.

Finally, the process of cluster formation and the makeup of individual clusters has been a long-standing issue. Using the IncuCyte^{TM} ZOOM technology which allows images of activated T cells in incubating plates to be imaged every 15 minutes for the entirety of the experiment, we were able to follow the process of cluster formation. With this time-lapse imaging we were able to highlight three important points involving T cell clusters. The first was the formation of a cluster by at least two interacting activated clones. This shows evidence that clusters, even early on, are most readily produced by

the accumulation of multiple clones, instead of the division of a single cell. Secondly, a single cell appears to have the capacity to form a single cluster, as depicted by observing the sequence of images pertaining to the T cell indicated by the straight arrow in Figure 2-8B[1]; however, this interpretation assumes that the T cell of interest at 33:30 hours is dividing at 33:45 hours in Figure 2-8B[1]. Instead, this presumed daughter cell could actually be an unlabeled cell that has migrated in the time in which the images were taken to form an interaction with the labeled cell. If this latter interpretation is the case, the result still corroborates the data shown in Figure 2-8A[1] indicating that the interactions of multiple clones make up a large number of observed clusters. Further experimentation will be needed to assess single T cell division and cluster formation.

As a final point, we were able to demonstrate the coming together of separate clusters into one larger cluster. We believe that the majority of T cell clusters are produced by many interacting T cells from different clones eventually joining together to form small heterogeneous clusters that merge with other small clusters to produce larger clusters that can eventually be quantified using stringent parameters. This merging observation is the likely means by which a sharp decline in the amount of clusters is seen after two days in culture (Fig. 2-7A[1]) and the rationale by which a confluent lawn of T cells forms after three days of priming (Fig. 2-7D-G[1]). We speculate that the cell density at day three has reached a critical threshold that makes the detection of individual clusters difficult. However, it is plausible that LFA-1 mediated adhesion at day three could decline and thus facilitate the formation of a confluent layer of activated T cells. Even though the parameters to define a wt cluster were stringent, we feel that our quantification of cluster number is an underestimate. If we were to try and quantify all clusters formed by enabling the software to count clusters at more of an infancy stage of cluster formation in the wt condition, we would have presumably seen a much higher

background in the ICAM-1 KO T cell conditions. This would have most likely occurred because the stringency for identifying a cluster would have been reduced to an easier threshold for ICAM-1 KO T cells to achieve. Our attempts to reduce this background, although not completely perfect, convince us that wt T cells produce clusters and ICAM-1 KO T cells do not. Furthermore, the M17/4 wt cluster blocking antibody conditions also show a small amount of clustering that is comparable to ICAM-1 KO deficiency; thus corroborating the plausibility that these clusters shown in Figure 2-7A-C[1] are background. Also, at day one post stimulation shown in Figure 2-7E[1], we can clearly see that the software is defining strands of both wt and ICAM-1 KO T cells as clusters because they are masked in yellow. These strands or collections of wt and ICAM-1 KO T cells show no resemblance to our defined wt T cell clusters shown in Figure 2-6A and at day two in Figure 2-7D[1] and thus we consider them background.

In summary, we highlighted the dispensability of ICAM-1 on T cells during *in vivo* migration, as well as, during the formation of APC:T cell conjugates. We also illustrated the expression kinetics of ICAM-1 after T cell stimulation both *in vitro* and *in vivo* and demonstrated that peak expression occurs two days post priming. Optimal expression and maintenance of ICAM-1 expression is dependent upon a third signal cue. ICAM-1 expression is indispensable on T cells in forming contacts and mediating cluster production; however, the importance of these clusters is largely unknown and will be explored in Chapter 3.

FOOTNOTES

[1]Micheal Conley (Midwest Regional Sales for Essen Bioscience) contributed to cluster analysis and masking thresholds involving the use of the IncuCyte™ ZOOM imager (Figures 2-7 and 2-8).

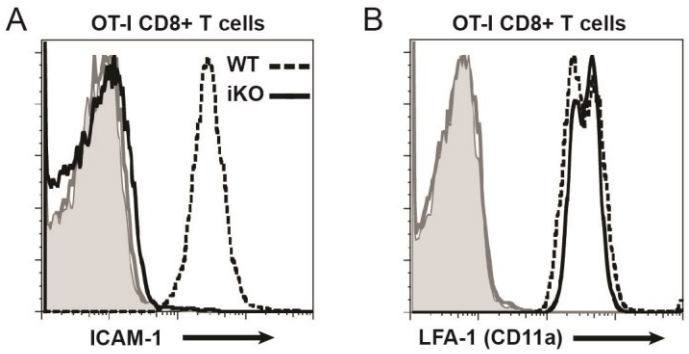

Figure 2-1: ICAM-1 and LFA-1 expression levels on wt and ICAM-1 KO OT-I T cells.

Naïve wild-type (WT) and ICAM-1 KO (iKO) CD8+ OT-I T cells from lymph nodes were stained for surface expression of **(A)** ICAM-1 and **(B)** the α_L subunit (CD11a) of the LFA-1 integrin. Isotype control staining for both subsets is indicated by the gray filled histogram and the bolded gray line.

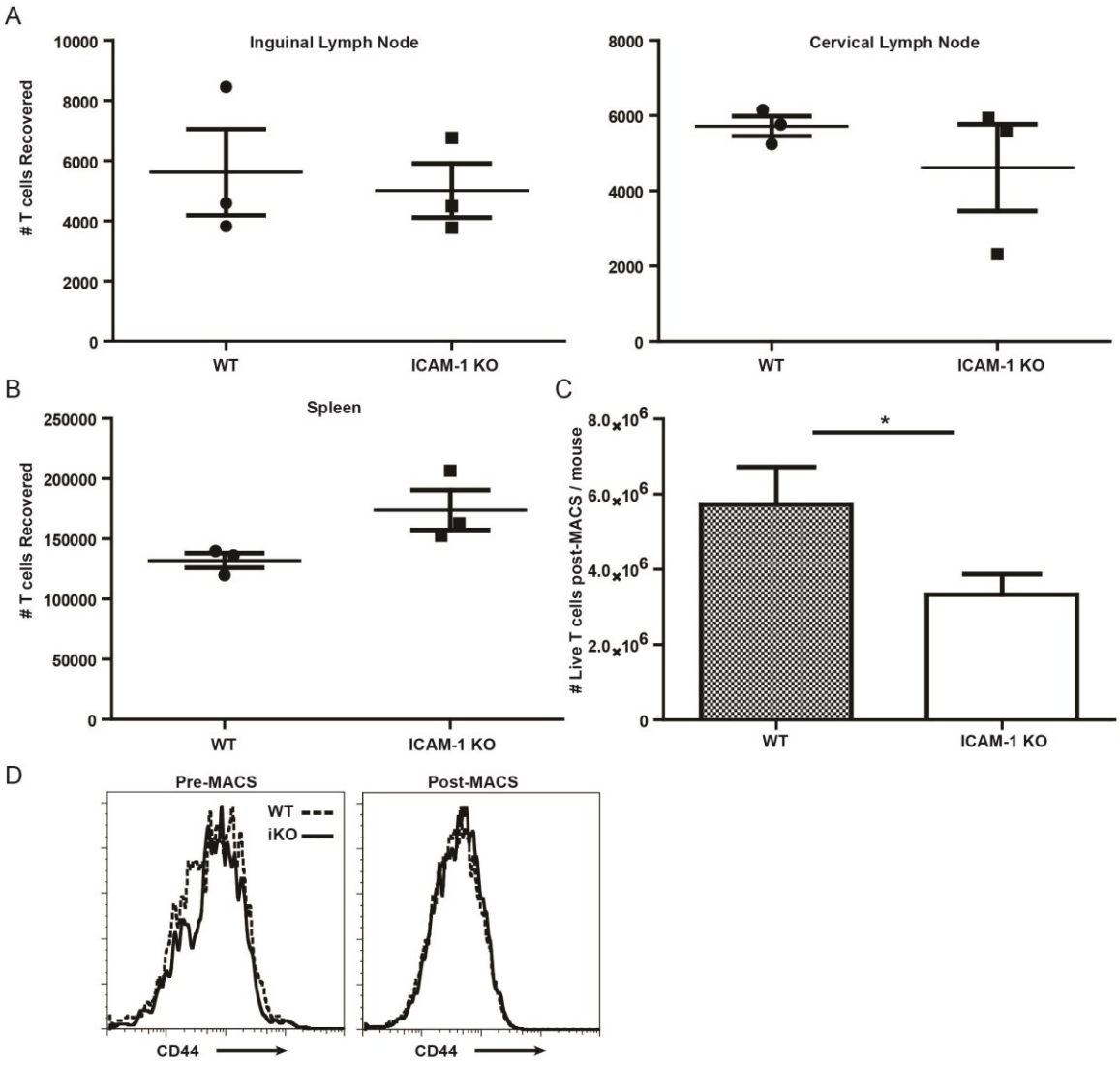
A
Inguinal Lymph Node
T cells Recovered
10000
8000
6000
4000
2000
0
WT
ICAM-1 KO
Cervical Lymph Node
8000
6000
4000
2000
0
WT
ICAM-1 KO
B
Spleen
T cells Recovered
250000
200000
150000
100000
50000
0
WT
ICAM-1 KO
C
Live T cells post-MACS / mouse
8.0x10^6
6.0x10^6
4.0x10^6
2.0x10^6
0
*
WT
ICAM-1 KO
D
Pre-MACS
Post-MACS
WT
iKO
CD44
CD44

Figure 2-2: ICAM-1 deficiency leads to normal lymph node migration in a wt host, despite reduced T cell recovery in ICAM-1 deficient hosts.

Naïve unpurified wt or ICAM-1 KO CD8+ OT-I T cells were transferred into wt hosts and three hours later **(A)** single inguinal (not significant (ns), p value=.7361) and cervical (ns, p value=.4034) lymph nodes, as well as **(B)** spleens (ns, p value=.0768) were harvested and T cell numbers enumerated. **(C)** Total amount of live naïve post-MACS purified OT-I T cell numbers recovered after combining peripheral and mesenteric lymph nodes from wt or ICAM-1 KO OT-I mice. Average of 11 recent experiments (*, p value=.0479). **(D)** Surface expression of CD44 pre- and post-MACS negative selection of wt or ICAM-1 KO OT-I T cells from peripheral and mesenteric lymph nodes.

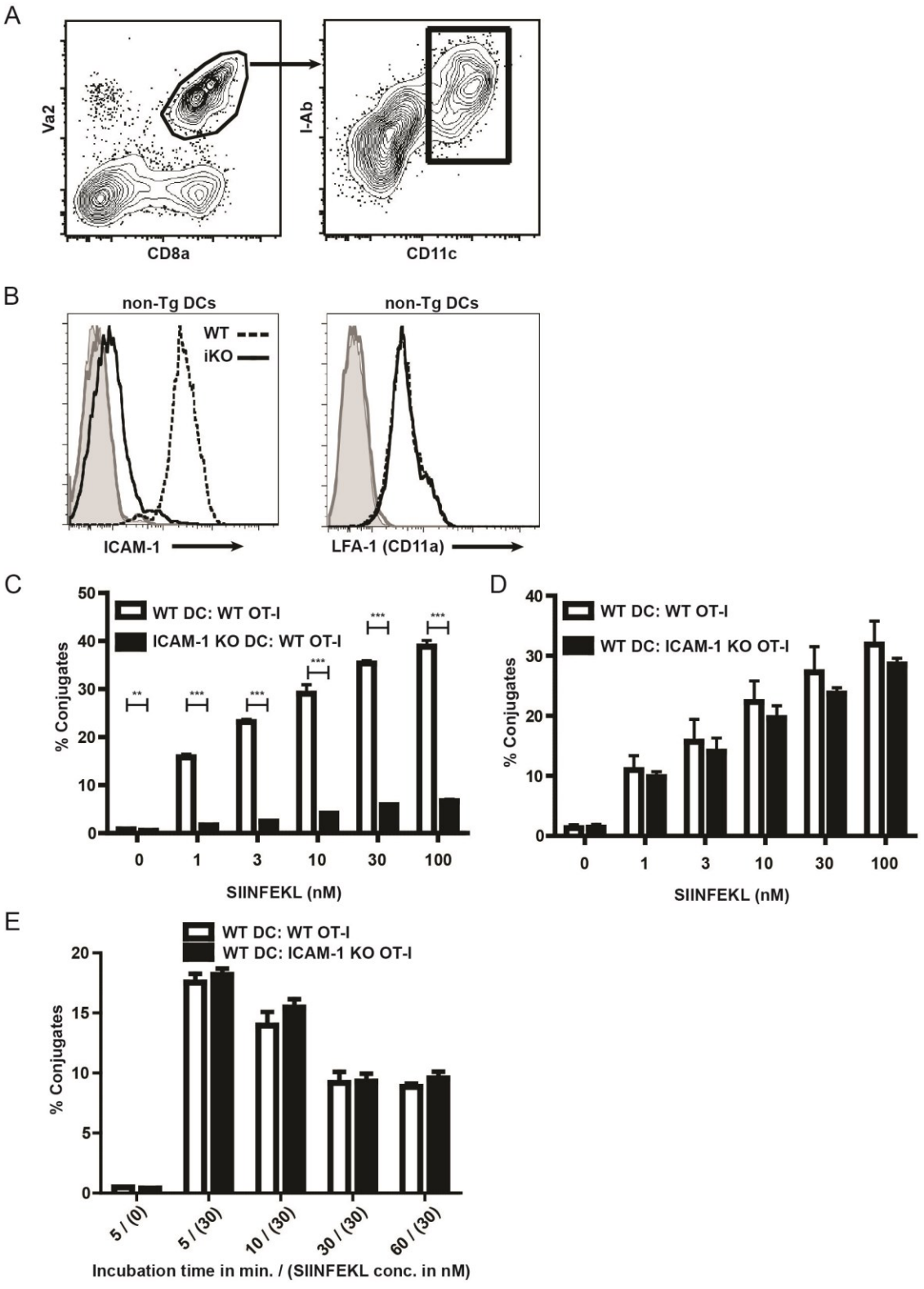
A
Va2
CD8a
I-Ab
CD11c
B
non-Tg DCs
WT
iKO
ICAM-1
non-Tg DCs
LFA-1 (CD11a)
C
WT DC: WT OT-I
ICAM-1 KO DC: WT OT-I
% Conjugates
SIINFEKL (nM)
D
WT DC: WT OT-I
WT DC: ICAM-1 KO OT-I
% Conjugates
SIINFEKL (nM)
E
WT DC: WT OT-I
WT DC: ICAM-1 KO OT-I
% Conjugates
5 / (0)
5 / (30)
10 / (30)
30 / (30)
60 / (30)
Incubation time in min. / (SIINFEKL conc. in nM)

Figure 2-3: ICAM-1 expressed on T cells is dispensable for binding antigen-laden dendritic cells.

Naïve purified wt or ICAM-1 KO CD8+ OT-I T cells were incubated with peptide-pulsed enriched dendritic cells (DCs) in a conjugate assay. **(A)** The gating strategy for identifying conjugates. The example shown above illustrates wt T cells and wt DCs at a 30 nM SIINFEKL dose. **(B)** CD11c+I-A^b+ DCs from non-transgenic (non-Tg) wt and ICAM-1 KO mouse spleens were stained for ICAM-1 and the α_L (CD11a) subunit of LFA-1. **(C)** Enriched non-Tg peptide-pulsed wt and ICAM-1 KO DCs were incubated with purified wt OT-I T cells or **(D)** wt DCs were incubated with wt and ICAM-1 KO OT-I T cells for 10 minutes at different antigen doses. In *(C)* the data is shown from triplicate wells from one of two independent experiments (**, p value<0.01; ***, p value≤0.0002); data in *(D)* is an average of three independent experiments. **(E)** Time course of conjugate incubation ranging from 5-60 minutes with either 0 or 30 nM SIINFEKL dose.

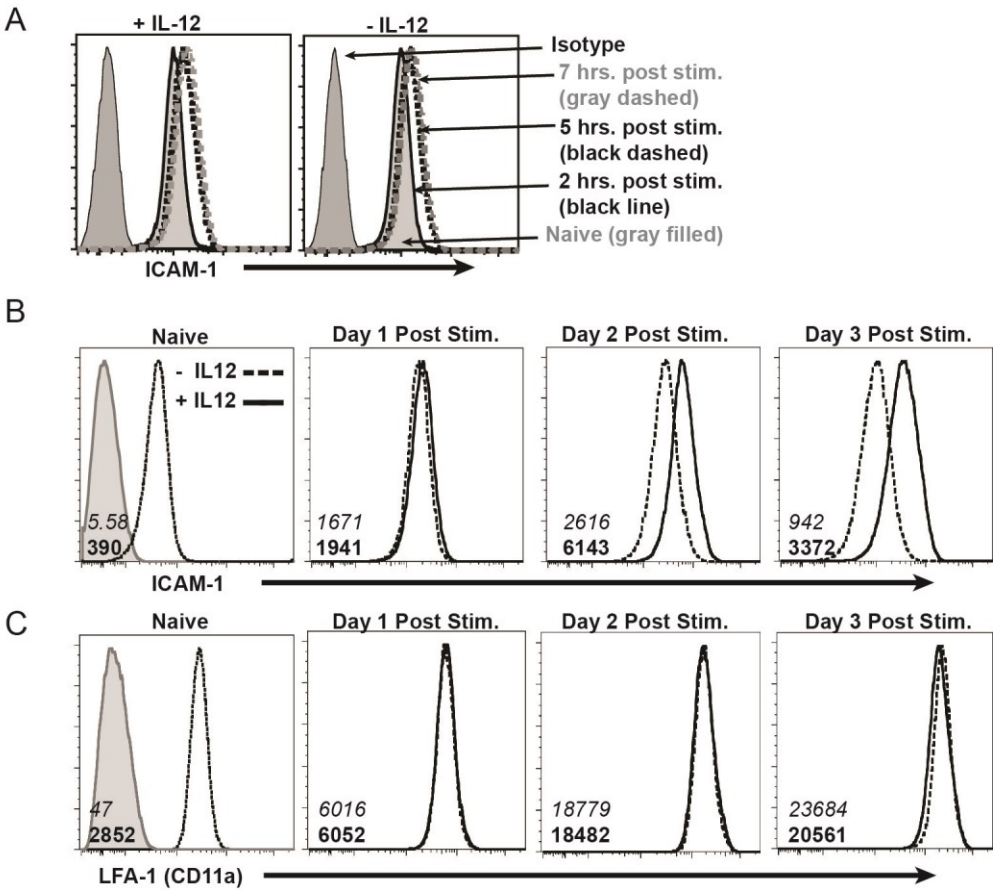

Figure 2-4: Long-term, but not short-term, ICAM-1 upregulation *in vitro* is dependent upon IL-12 exposure, whereas LFA-1 expression is IL-12 independent.

Naïve purified wt OT-I T cells were stimulated *in vitro* using plate-bound H2-K^{b}:SIINFEKL and recombinant B7-1, with or without soluble IL-12. **(A)** Early ICAM-1 expression kinetics. Naïve (gray filled), 2 hours post stimulation (black line), 5 hours post stimulation (black dashed), 7 hours post stimulation (gray dashed), and isotype are depicted with or without IL-12. **(B)** Three day ICAM-1 and **(C)** LFA-1 expression kinetics with IL-12 (black line) or without IL-12 (black dashed) post T cell activation. Italicized numbers refer to geometric mean fluorescence (gMFI) intensity values of –IL12 conditions on days 1-3. Bold numbers refer to gMFI of +IL12 conditions on days 1-3. The gMFI values in naïve histogram plots refer to isotype (italicized) and naïve (bold) ICAM-1 or LFA-1 staining.

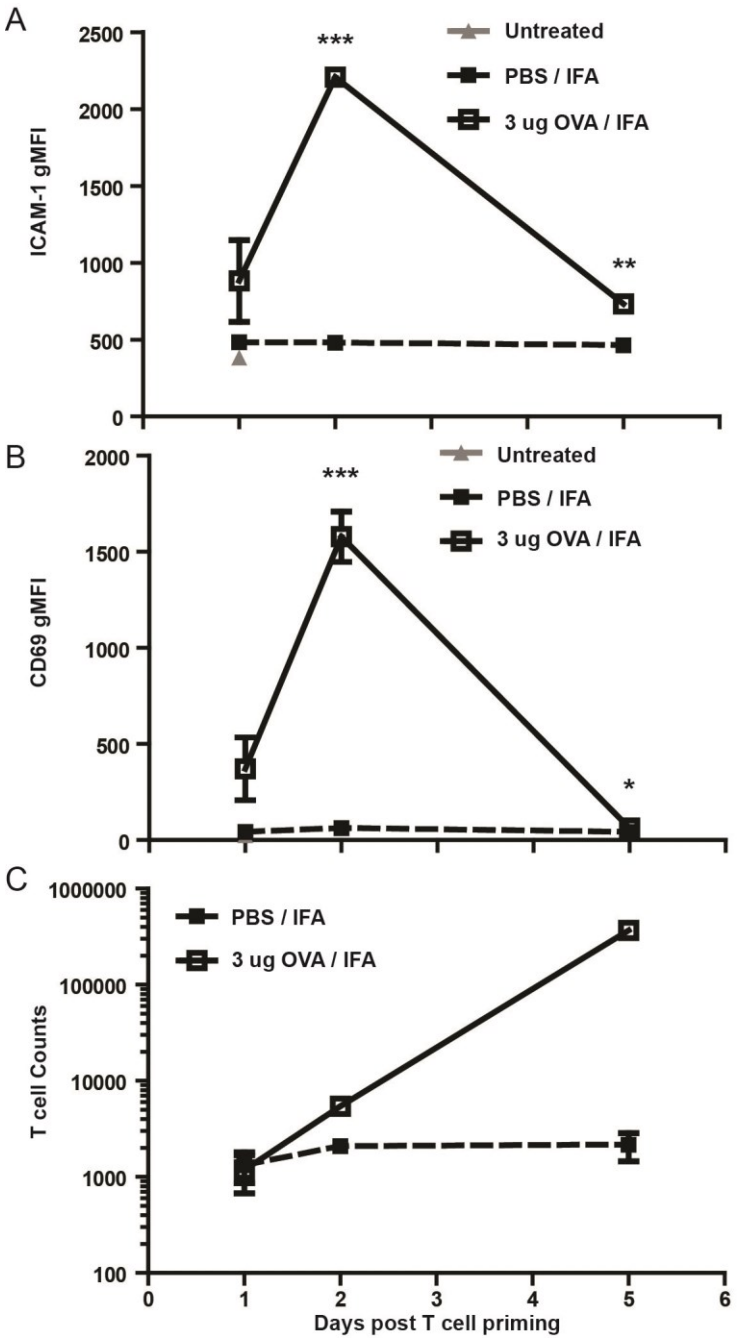
A
ICAM-1 gMFI
2500
2000
1500
1000
500
0
***
**
Untreated
PBS / IFA
3 ug OVA / IFA
B
CD69 gMFI
2000
1500
1000
500
0
***
*
Untreated
PBS / IFA
3 ug OVA / IFA
C
T cell Counts
1000000
100000
10000
1000
100
PBS / IFA
3 ug OVA / IFA
0
1
2
3
4
5
6
Days post T cell priming

Figure 2-5: ICAM-1 on T cells is upregulated after *in vivo* priming.

$2.25x10^5$ naïve unpurified wt OT-I T cells were transferred intravenously and one day later primed with 3 µg OVA/IFA or PBS/IFA as a control into the ear pinna. Mice were sacrificed one day, two days, or five days post priming and draining cervical lymph node (dcLN) harvested and stained for **(A)** ICAM-1 (**, p value=0.002; ***, p value<0.0001) and **(B)** CD69 (*, p value=0.0291; ***, p value=0.0003). **(C)** Recovered T cell numbers were obtained from the dcLN. All peripheral lymph nodes were taken from the untreated (transfer only) recipients. Data shown is from one of at least three *in vivo* ICAM-1 T cell expression experiments. Student's unpaired two-tailed *t* test statistically compared the OVA/IFA and PBS/IFA conditions.

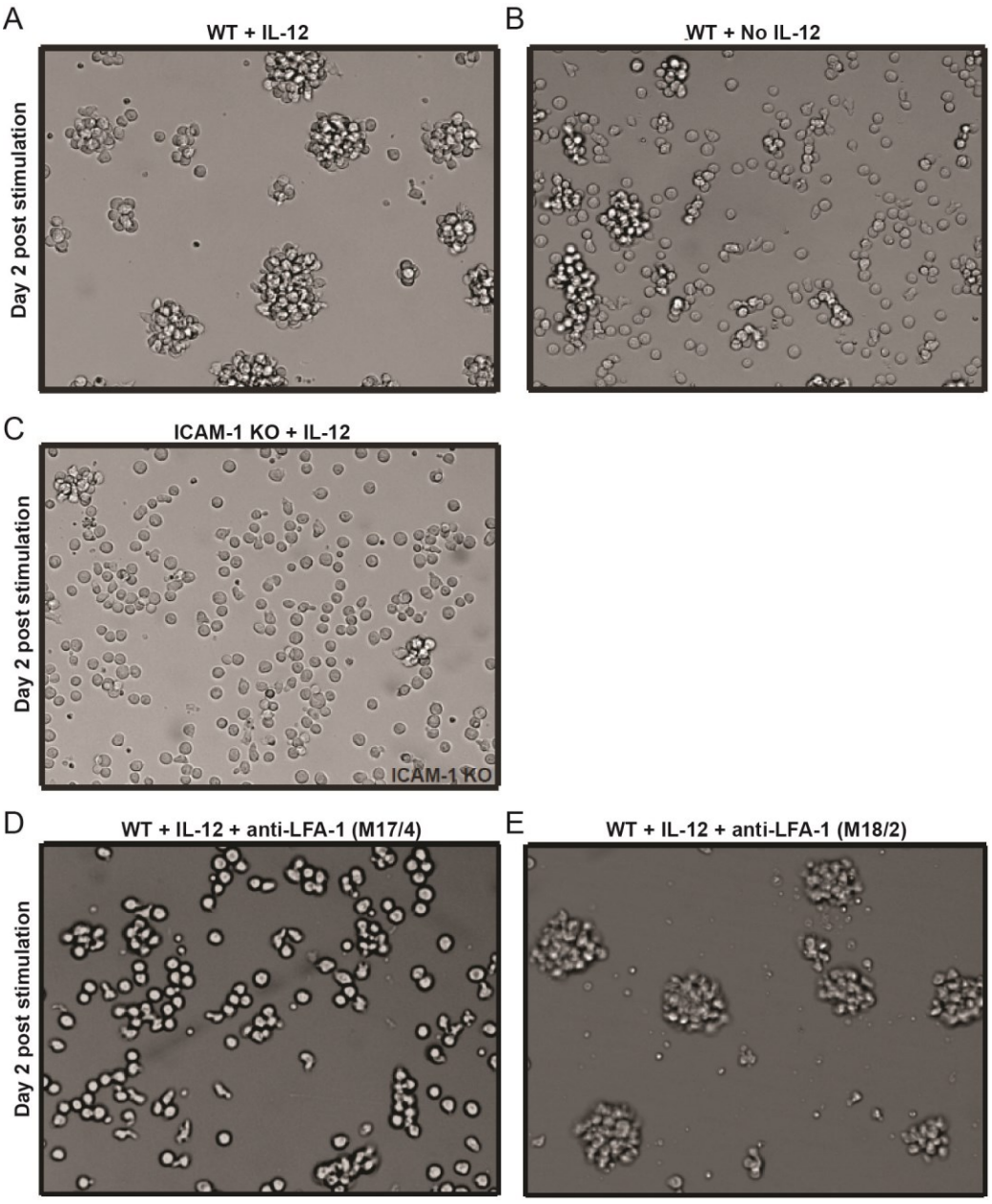

Figure 2-6: T cell:T cell homotypic clusters are mediated by the third signal cue, IL-12, and ICAM-1:LFA-1 ligation.

Images were taken of naïve purified wt OT-I T cells stimulated *in vitro* using plate-bound H2-K^b:SIINFEKL and recombinant B7-1, **(A)** with or **(B)** without soluble IL-12 after two days of activation. **(C)** Images were taken of naïve purified ICAM-1 KO OT-I T cells that were stimulated for two days *in vitro* as stated above. Day two images were taken of naïve purified wt OT-I T cells stimulated *in vitro* together with anti-LFA-1 antibodies that **(D)** disrupt clusters (M17/4) or **(E)** do not disrupt clusters (M18/2).

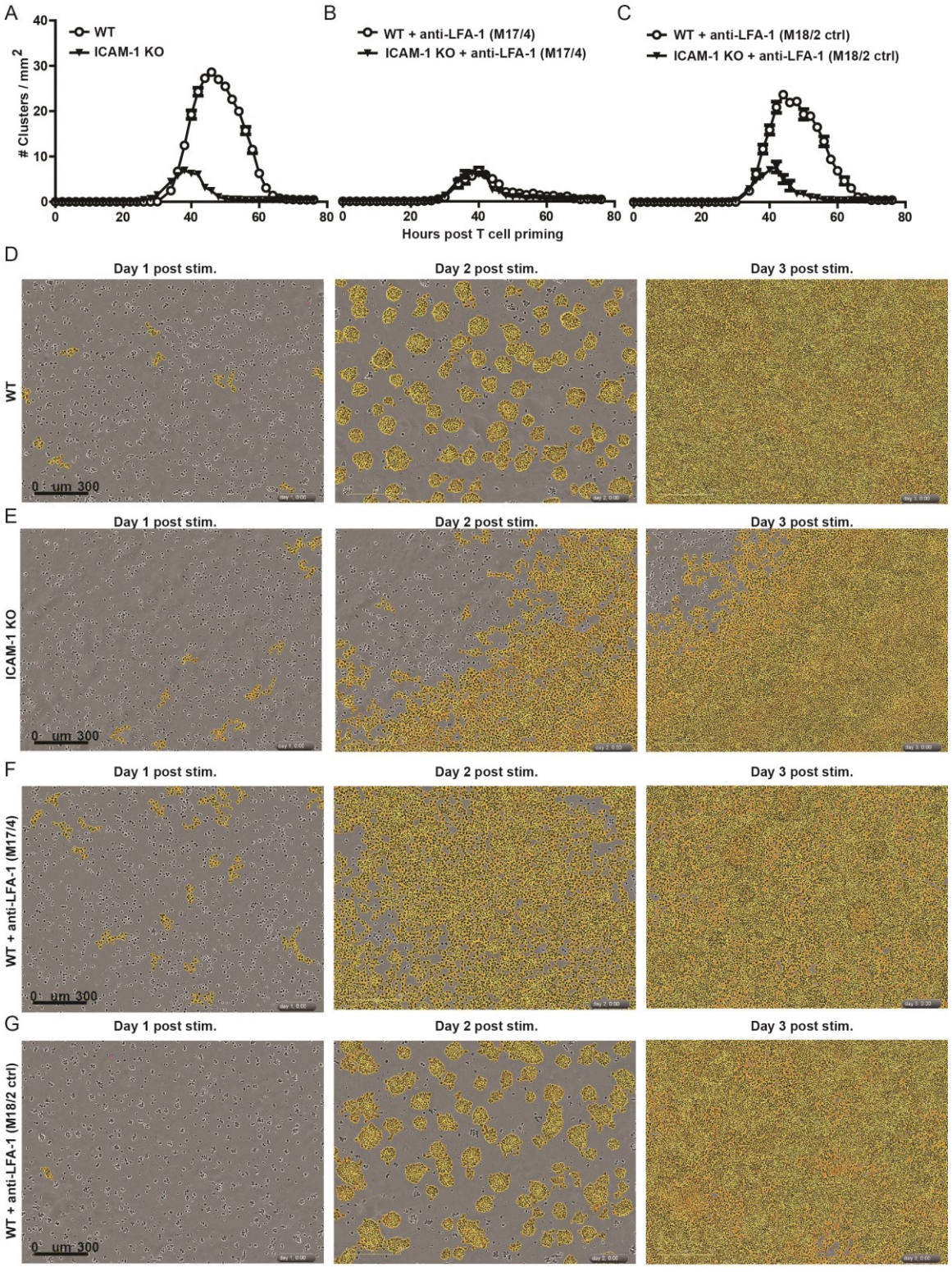
A
B
C
WT
ICAM-1 KO
WT + anti-LFA-1 (M17/4)
ICAM-1 KO + anti-LFA-1 (M17/4)
WT + anti-LFA-1 (M18/2 ctrl)
ICAM-1 KO + anti-LFA-1 (M18/2 ctrl)
Clusters / mm 2
Hours post T cell priming
D
E
F
G
Day 1 post stim.
Day 2 post stim.
Day 3 post stim.
WT
ICAM-1 KO
WT + anti-LFA-1 (M17/4)
WT + anti-LFA-1 (M18/2 ctrl)
0 um 300

Figure 2-7: T cell:T cell homotypic *in vitro* clustering kinetics.

Naïve purified wt and ICAM-1 KO OT-I T cells were stimulated *in vitro* using plate-bound H2-K^b:SIINFEKL, recombinant B7-1, and soluble IL-12. Using an IncuCyte^{TM} ZOOM incubator imager, images of each well were taken every two hours for <80 consecutive hours during T cell stimulation and the total number of clusters were enumerated based upon the following parameters: eccentricity (a measure of circularity) <0.8 and cluster area >2000 μm^2. Clusters were "masked" yellow after reaching these parameters. Four images were taken per well every two hours and the quantification of 16 movies for wt and ICAM-1 KO OT-I T cells are shown in **(A)** and 8 movies, also at four images per well, were quantified using anti-LFA-1 treated conditions and shown in **(B-C)**. **(D)** Representative images used in the quantification of wt T cell clusters as shown in *(A)*. **(E)** Representative images used in the quantification of ICAM-1 KO T cell clusters as shown in *(B)*. **(F)** Representative images used in the quantification of wt clusters using cluster blocking anti-LFA-1 (M17/4) as shown in *(B)*. **(G)** Representative images used in the quantification of wt clusters using control anti-LFA-1 (M18/2) as shown in *(C)*. A reference scale (in μm) is present in the bottom left hand corner of each day one image.

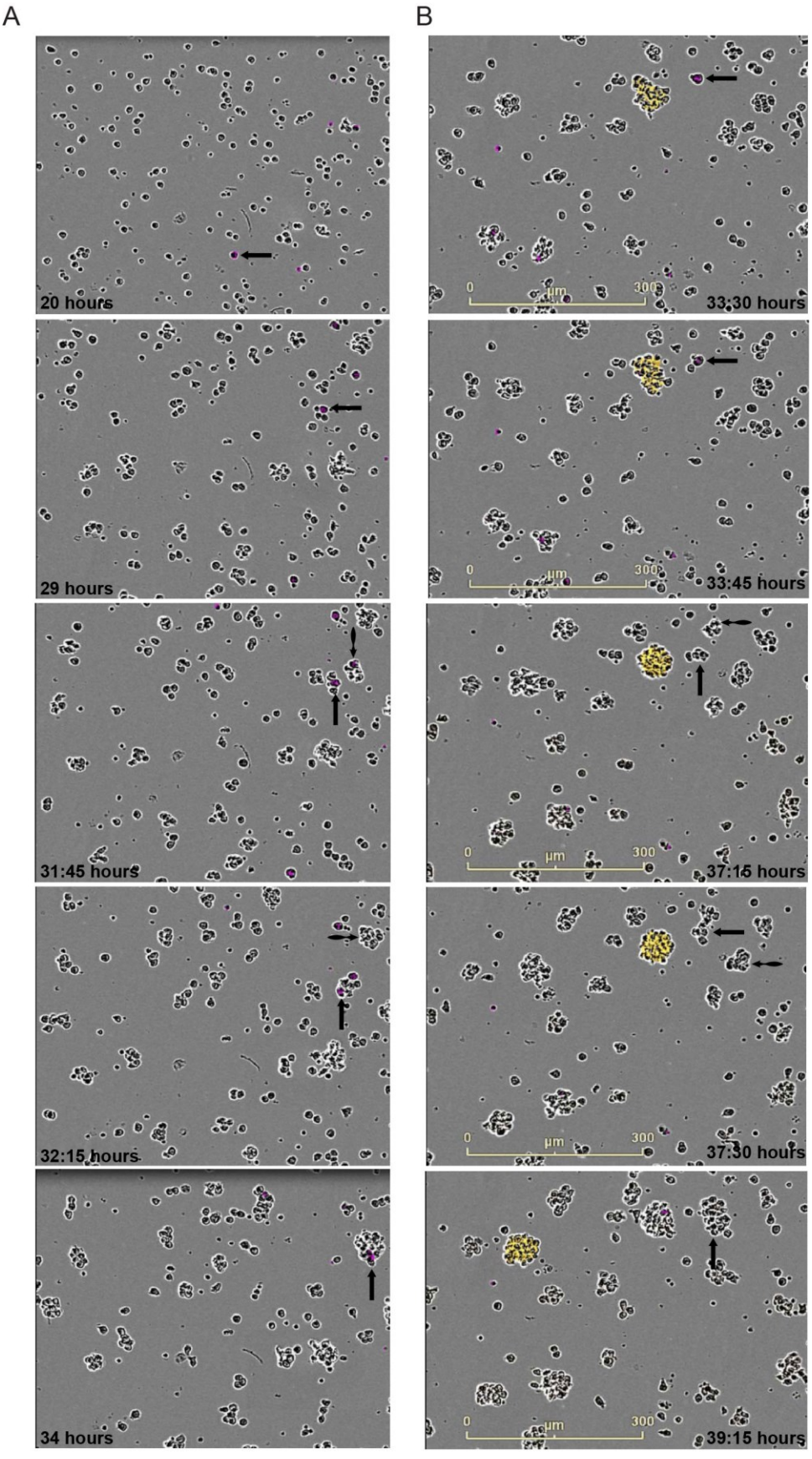
A
B
20 hours
29 hours
31:45 hours
32:15 hours
34 hours
33:30 hours
33:45 hours
37:15 hours
37:30 hours
39:15 hours
0
µm
300

Figure 2-8: T cell:T cell homotypic *in vitro* clustering composition.

(A-B) Naïve purified wt OT-I T cells were stimulated *in vitro* using plate-bound H2-K^b:SIINFEKL, recombinant B7-1, and soluble IL-12. A small wt population was labeled with CFSE and spiked into an unlabeled wt population at a 2.5%:97.5% ratio. Using an IncuCyte™ ZOOM imager, images of each well were taken every fifteen minutes. Using IncuCyte™ ZOOM analysis software, CFSE labeled cells were masked with a purple color. Clusters masked in yellow are aggregates that meet the stated parameters for a cluster to be counted. Straight arrows indicate the T cell that is of interest throughout the sequence of still images, even though that T cell may be a single cell or in a cluster. Arrows that have a rounded backside indicate a cluster that will merge with the T cell or cluster of interest (indicated with a straight arrow) to form a larger cluster. A reference scale (in μm) is present in the bottom left hand corner of *(B)*.

CHAPTER 3: ICAM-1 mediated homotypic T cell activation clusters regulate CD8+ T cell effector function and differentiation through antigen sensing and immune inhibition mechanisms

INTRODUCTION

One of the major features of a productive T cell interaction with a professional APC is the formation of an immunological synapse (IS) (37). A fully functional IS is preceded by initial T cell:APC contact that induces early TCR:MHC signaling events that occur in small microclusters. These microclusters are thought to be the active site for rapid (on the order of seconds) receptor-proximal signaling. As these microclusters merge (37-40), the development of a canonical “bulls-eye” structure is formed within several minutes. This “bulls-eye” is made up of a central and peripheral supramolecular activation cluster (c-SMAC and p-SMAC, respectively) (36). The p-SMAC is a distribution of LFA-1 integrin that surrounds the c-SMAC in a ring-like fashion (36). The c-SMAC is a centralized region of TCR, CD4 or CD8 co-receptors, and important downstream kinases such as Lck and Fyn (36). Although somewhat controversial, it is believed that signaling is quenched at the c-SMAC (39); however, based upon the quality of the ligand, TCRs at the c-SMAC may induce enhanced signaling (38). Other proteins such as the co-stimulatory molecule CD28 and the immunosuppressive protein CTLA-4 can rapidly polarize to the T cell:APC interface (65). These contacts during activation are not permanent and the T cell can engage other cells after detachment from the initial antigen-bearing APC.

Interestingly, T cell:T cell contacts show surprising similarities to this canonical T cell:APC IS using several different parameters. Briefly, T cell:T cell contacts and T cell:APC contacts share the ability to utilize LFA-1:ICAM-1 proteins for synapse

formation, they display directional secretion through the polarization of the microtubule organizing complex, they retain distinct identities between interacting cells, and the contacts formed are dynamic in nature but fundamentally stabilized (87). Krummel and colleagues recently showed evidence of these structural features between interacting T cells, as well as revealed the presence of directional IL-2 signaling from one T cell to another adjacent T cell using elegant antibody capture methods and confocal microscopy (87). They revealed for the first time a novel function for CD4+ T cell:T cell contacts during stimulation; presumably a T cell:T cell crosstalk mechanism by which the secretion and acquisition of a polarized IL-2 signal can be achieved. Other functions of T cell:T cell interactions during stimulation, and particularly CD8+ T cell:T cell contacts, have not been elucidated.

Since LFA-1:ICAM-1 interactions maintain stable T cell contacts between APCs or other T cells, some studies have focused on the importance of ICAM-1 ligation as a co-stimulatory molecule on T cells during activation. These studies revealed that stimulation of CD4+ and/or CD8+ human T cells from tonsils or peripheral blood using anti-CD3 and anti-ICAM-1 can lead to T cell proliferation, upregulation of CD69, activation of PI3K, regulation of the IL-2 locus, generation of memory cells, and differentiation of Tregs (46, 79-81) to name a few. The signaling mechanisms by which these processes are regulated by ICAM-1 are somewhat unclear, but studies suggest that it involves the phosphorylation of the sole tyrosine residue in the short cytoplasmic tail. This allows for an association with Src Homology Domain 2-containing Tyrosine Phosphatase 2 (SHP-2) (108) which yields further events that lead to the activation of the small G-protein Ras (96). These signals induce the activation of MAP kinase (MEK-1), thereby activating Erk and helping promote the induction of the AP-1 transcription

factor complex (95, 96). AP-1 plays a necessary role in regulating cytokines needed during cell division (111).

In the following study we chose to understand the importance of T cell clusters on a cellular level using ICAM-1 deficiency as a tool to investigate the necessity of a T cell:T cell interaction during priming. Our objective was to determine the role of CD8+ T cell clustering on the differentiation and effector function of CD8+ T cells. In our study we demonstrated that ICAM-1 deficient T cells showed similar division and activation marker phenotypes to wt T cells; however, effector function was strikingly increased when clusters were ablated. We reveal that the increase in effector status seen in unclustered T cells is due in part by two separate mechanisms. One mechanism focuses on antigen sensing and the other concentrates on the immune-inhibitory function of clusters that allows for the tempering of a CD8+ T cell response, namely through CTLA-4 and EOMES expression.

MATERIALS AND METHODS

Mice

ICAM-1 deficient mice (B6.129S4-ICAM1^{tm1Jcgr}/J) were generated as previously described (97) and purchased from The Jackson Laboratories (Jackson Laboratory, Bar Harbor, ME). They were backcrossed to the OT-I TCR transgenic on the C57BL/6 background (>10 generations). Nur77-GFP OT-I mice were created as described (139) and generously provided by Dr. Kris Hogquist (University of Minnesota – Twin Cities). Colony bred wild-type OT-I mice were used as controls. Recipient C57BL/6 mice were purchased from The Jackson Laboratories or the National Cancer Institute Mouse Repository (NCI-Frederick, Frederick, MD). Mice were housed and bred under specific-pathogen free conditions and generally used between the ages of 6-12 weeks.

Experimental procedures, involving the use of mice, were approved by the Institutional Animal Care and Use Committee at the University of Minnesota – Twin Cities.

Cell preparation

Single cell suspensions of mouse spleens and lymph nodes were prepared by mashing tissues through cell strainers or using an Automated gentleMACS^{TM} Dissociator (Miltenyi Biotec, Auburn, CA) into phosphate buffered saline (PBS)/2% bovine serum. Cell counts were attained using a Countess® Automated Cell Counter (Life Technologies, Grand Island, NY). Purified CD8+ OT-I T cells were obtained by depleting non-CD8+ leukocytes and red blood cells from the bulk population with the following negatively selecting antibodies (FITC conjugated – anti-CD4, anti-B220, anti-CD16/CD32, anti-F4/80, anti-I-A^{b}, anti-Ter119, and anti-CD44 (eBioscience, San Diego, CA and BioLegend, San Diego, CA)), then incubated with anti-FITC microbeads (Miltenyi Biotec), and later applied to a MACS LS column (Miltenyi Biotec). The enriched product was generally ≥95% pure based upon CD8α+Vα2+ staining of 5-10x10^{4} T cells using a FACS Calibur (BD Biosciences, San Jose, CA).

Flow cytometry

For flow cytometry experiments, usually 1-5x10^{6} cells were stained in Hank's balanced salt solution (HBSS)/0.2% sodium azide/2% bovine serum (FACS buffer) for 30 minutes at 4° C. Surface antibody stains, unless stated, were performed at 1:100 dilutions. Antibodies of special interest include CD69 (clone: H1.2F3, BioLegend), CD44 (clone: IM7, BioLegend), CD25 (clone: PC61, BioLegend), CD212 generously provided by Dr. Matthew Mescher (clone: 114, BD Biosciences), PD-1 (clone: J43, eBioscience), PD-L1 generously provided by Dr. Brian Fife (clone: MIH5, eBioscience), CD80 (clone: 16-

10A1, eBioscience), and CD86 (clone: GL1, eBioscience). All other surface or isotype staining antibodies were purchased from BioLegend, eBioscience, or BD Biosciences. Samples were run and collected using a FACS Calibur, LSRII, or Fortessa (BD Biosciences) and analyzed with FlowJo software (Tree Star, Inc., Ashland, OR).

Intracellular staining for flow cytometry

Intracellular (i.c.) staining for interferon-γ (IFNγ) (clone: XMG1.2, eBioscience), granzyme B (clone: GB11, Life Technologies), and CTLA-4 (clone: UC10-4F10-11, BD Biosciences) were performed per manufacturer's instructions using the BD Cytofix/Cytoperm kit (BD Biosciences). Briefly, T cells were stained with surface antibodies, washed with FACS buffer, fixed with 250 µLs of BD Cytofix/Cytoperm, and stored at 4° C for 20 minutes. Cells were then washed twice with 1X BD Perm/Wash buffer, i.c. staining antibodies added, and cells stored at 4° C. Granzyme B staining was generally performed at a 1:50 dilution for 60 minutes; while IFNγ and i.c. CTLA-4 were prepared at 1:100 dilutions for 30-60 minutes. At which time, cells were washed twice with 1x BD Perm/Wash buffer and resuspended in FACS buffer for flow cytometry. EOMES (clone: Dan11mag, eBioscience) staining was performed using the eBioscience FoxP3 staining buffer set (eBioscience) per manufacturer's instructions. Briefly, T cells were stained with surface antibodies, washed with FACS buffer, and resuspended in 1 mL fresh Fixation/Permeabilization working solution for 30 minutes at 4° C. Then cells were washed twice with 1 mL 1X Permeabilization buffer and EOMES antibody added and samples stored for 60 minutes at 4° C. Cells were washed twice with 1 mL 1X Permeabilization buffer and resuspended in FACS buffer for flow cytometry. Isotype stains were performed under similar conditions as the stain of interest.

In vitro T cell stimulation

In vitro activation conditions were designed similarly to previous studies (51, 127). DimerX H-2K^b:Ig fusion protein (BD Biosciences) was diluted to 2 µg/mL in sterile PBS and recombinant B7-1/Fc chimeric protein (R&D Systems) was diluted to 0.4 µg/mL in sterile PBS. Flat-bottomed microtiter 96-well plates (Sigma-Aldrich) received 50 µLs of each reagent and incubated for at least 2 hours at room temperature. Wells were washed twice with sterile PBS and once with alloclone media. Alloclone media was RPMI 1640 (Life Technologies) supplemented with 10% fetal calf serum, 4 mM L-glutamine (Mediatech, Inc., Manassas, VA), 0.1 mM nonessential amino acids (Mediatech, Inc.), 1 mM sodium pyruvate (Mediatech, Inc.), 100 U/mL penicillin and streptomycin (Mediatech, Inc.), 10 mM HEPES (Mediatech, Inc.), and 5 µM 2-Mercaptoethanol (Life Technologies). SIINFEKL (0.375 µg/mL) was loaded onto DimerX H-2K^b:Ig fusion protein by adding 100 µLs/well. Plates were incubated at 37° C for at least 2.5 hours and then washed several times with alloclone. Purified wild-type or ICAM-1 deficient OT-I CD8+ T cells were added at a concentration of 5x10^4 cells/well in a total volume of 210 µLs alloclone supplemented with 0.05 µg/mL of IL-12 (R&D Systems). Plates were then incubated at 37° C until harvested at 24-, 48-, and 72-hour time points. Co-cultures using wt and ICAM-1 KO OT-I T cells were performed by combining the subsets of naïve purified T cells at the indicated ratios (wt:ICAM-1 KO; 9:1, 3:1, 1:1, 1:3, 1:9) while keeping the total number of OT-I T cells at 5x10^4 cells/well in a total volume of 210 µLs alloclone supplemented with 0.05 µg/mL IL-12. For conditioned media dilutions, CFSE labeled (see below for procedure) purified naïve wt OT-I T cells were added to supernatants from wt or ICAM-1 KO day three cultures at 100%, 80%, 60%, 40%, 20%, or 0% conditioned media supplemented with fresh alloclone. IL-2 (R&D Systems) supplementation was performed at a final concentration

of 10 ng/mL. B7-2 (CD86; R&D Systems) activation conditions were performed at a final concentration of 2 µg/mL.

Blocking antibody treatment

The disruption of T cell clusters *in vitro* was performed using the endotoxin-free/low azide anti-LFA-1 (anti-α_L) antibody M17/4 (BioLegend and eBioscience) at a final concentration of 2.5 µg/well. Control anti-LFA-1 (anti-β_2) antibody M18/2 (BioXCell, West Lebanon, NH) did not block clustering and was used at a final concentration of 2.5 µg/well. Anti-PD-L1 blocking antibody (clone: 10F.9G2, BioLegend) was used at a final concentration of 10 µg/mL. Anti-CTLA-4 blocking antibody (clone: UC10-4F10-11, BD Biosciences) was used at a final concentration of 30 µg/mL. Low endotoxin, azide free anti-CD80 (clone: 16-10A1, BioLegend) was used at a final concentration of 3, 10, and 30 µg/mL. Blocking antibodies were added to wells at the same time cells were plated.

7-AAD viability staining

7-AAD (eBioscience) viability staining was performed using day two and day three *in vitro* activated wt and ICAM-1 KO T cells. Samples were stained with 10 µLs 7-AAD reagent and incubated for 10 minutes on ice. T cells were not washed before sampling by flow cytometry.

CFSE and cell trace violet labeling

Carboxyfluorescein succinimidyl ester (CFSE; Life Technologies) labeling was performed by adding an equal volume of 10 µM CFSE to T cells (resuspended at $20x10^6$/mL in PBS/5% bovine serum). The mixture was vortexed and labeling performed in the dark for 5 minutes. The cell mixture was washed three times with 20-35 mLs

PBS/5% bovine serum. Cells were resuspended in PBS/2% bovine serum, counted, and brought to $2.5x10^5$ T cells/mL in alloclone for plating. Cell trace violet (CTV; Life Technologies) labeling was performed by adding 10 µLs of dimethyl sulfoxide (DMSO)-reconstituted CTV to 3 mLs PBS and mixed well. An equal volume of CTV mixture was then added to T cells resuspended at $1x10^7$/mL in PBS/10% bovine serum. T cells were incubated for 15 minutes in 37° hot water bath with frequent mixing. Labeling was quenched with 30 mLs alloclone. Cells were then washed, counted, and resuspended.

T cell adoptive co-transfer

Two day *in vitro* activated wt and ICAM-1 KO OT-I CD8+ T cells were harvested under sterile conditions and washed at least twice with sterile PBS. T cells were counted and resuspended at $1x10^5$ OT-I cells/100 µLs. An equal volume of wt and ICAM-1 KO OT-I T cells were mixed to a final concentration of $2x10^5$ cells/200 µLs injection volume. T cells were adoptively co-transferred into naïve recipient C57BL/6 mice (CD45.2+) intravenously. Recipient mice were sacrificed at various time points post adoptive transfer (days 1-12), tissues harvested, and samples prepared for flow cytometry.

Cell culture of EL4 and EG7-OVA thymoma cell lines

EL4 and EG7-OVA cell lines were generously provided by Dr. Matthew Mescher. EL4 cells were grown in alloclone, while EG7-OVA cells were grown in alloclone supplemented with 250 µg/mL of the selective agent G418 (Mediatech, Inc.). Cells were thawed, plated, stored in a 37° incubator, and split every couple days. For experimentation, cells were split the day before to ensure the best viability.

In vitro cytotoxicity chromium^{51} release assay

EL4 (negative control) and EG7-OVA thymoma "target" cell lines were harvested and EG7-OVA cells pulsed with additional SIINFEKL (750 µg/mL) at 1 µL SIINFEKL/1x10^6 cells. If chromium^{51} (Cr^{51}) was brand new then 20 µLs were added; if not, 5-10 µLs were added for each additional week of aging. Cells were mixed well and stored at 37° for 1.5 hours with further mixing every 15 minutes. Target cells were washed three times with alloclone, counted, and resuspended at 1x10^5 cells/mL in alloclone. Additionally, day three *in vitro* activated wt and ICAM-1 KO OT-I "effector" T cells were harvested, washed, and resuspended in 1 mL of alloclone. Using a 96-well V-bottom plate, we performed a three-fold serial dilution with the activated T cells and added a total volume of 100 µLs to each well; T cells were counted after plating and back calculations were performed to attain the effector:target (E:T) ratio. Also, 100 µLs alloclone media only and 100 µLs 10X Triton were plated to separate wells; these served as spontaneous and total Cr^{51} release controls, respectively. Then 100 µLs of target cells (1x10^4 cells total) were added to each experimental well containing T cell effectors, as well as each control well. Plates were spun and incubated for 3.5-4 hours at 37°. After the incubation, the wells were spun, supernatants were recovered and transferred into new tubes, and samples run on a Packard Cobra II Auto Gamma Counter Model D5005 (Packard BioScience Company, Meriden, CT) to assess killing. Each E:T ratio was performed in triplicate and % lysis was calculated as follows: ((mean of triplicate wells – spontaneous) / (total – spontaneous)) x 100%.

Splenocyte activation of T cells

Purified wt and ICAM-1 KO OT-I CD8+ T cells were plated in 24-well flat bottom dishes at a density of 3x10^5/well (1X) in 1 mL of alloclone. Splenocytes from a non-

transgenic C57BL/6 mouse were harvested, mashed, and resuspended in alloclone. Concentrations of splenocytes ranged from 1/10X – 2X based upon the amount of T cells present in the well. Splenocytes were added to the wells in 1 mL of alloclone. The total volume/well was 2 mLs. SIINFEKL was added directly to the wells at a final concentration of 1 μg/mL. Plates were incubated at 37° for two days prior to harvest.

Microscopy

Mixed culture images of day two activated wt and ICAM-1 KO OT-I T cells were imaged using an inverted Olympus FluoView 1000 confocal microscope with a 10X dry lens. ICAM-1 KO T cells were labeled with cell trace violet (CTV) and visualized by excitation with the ultraviolet laser. Images were analyzed using the free software (ImageJ) supplied by the National Institutes of Health (Bethesda, MD) and available for download at http://rsbweb.nih.gov/ij/ (downloaded on 9/26/2012). Images were analyzed for % ICAM-1 KO T cells in contact with wt T cells by using the following equation: (# of ICAM-1 KO T cells in contact with wt T cells) / (total # of ICAM-1 KO T cells). Multi-photon microscopy was performed using an upright Leica TCS MP resonance scanning microscope with 4 non-descanned photomultiplier detectors and a Mai Tai DeepSee two-photon laser (15W; Spectra-Physics) was used for imaging with a 20X water immersion objective. Samples were excited with the two-photon laser at 840nm and emission wavelengths of 450-490 nm (for CTV), 500-560 nm (for CFSE) were collected in the detectors. The xy acquisition dimensions were 193.75 μm x 193.75 μm and were scanned at 8000 Hz with a pixel resolution of 0.28 μm. Z-stacks at a 0.25 μm step-size were acquired. Imaris software (version 5.7.2x64, Bitplane) was used for the generation of z-stack images.

Statistics

GraphPad Prism version 5.03 software (GraphPad Software, Inc., La Jolla, CA) was utilized to determine statistical significance using Student's unpaired two-tailed *t* test. P value cutoffs and notation were used as follows (unless otherwise denoted in figure captions): *, p value<0.05; **, p value<0.01; ***, p value≤0.0008.

RESULTS

Loss of T cell clustering does not affect T cell proliferation or activation marker upregulation

In Chapter 2 we elucidated the role of ICAM-1 as an adhesion molecule on T cells for the formation of T cell:T cell clusters. In the absence of ICAM-1, T cells cannot cluster (Fig. 2-6C). Whereas, the activation of ICAM-1 sufficient wt T cells led to dynamic T cell cluster formation that commenced at approximately 30-40 hours post priming (Figures 2-7A &D). Using our aforementioned *in vitro* three signal T cell stimulation conditions (H2-K^b:SIINFEKL, recombinant B7-1, and soluble IL-12) we assessed the importance of cluster formation on T cell division kinetics using CFSE labeled wt and ICAM-1 KO OT-I CD8+ T cells. We monitored CFSE dilution on the two T cell subsets every 24 hours for three days and observed that the CFSE profiles were nearly indistinguishable from one another (Fig. 3-1A). T cells had not started to divide at 24 hours post priming in either condition; furthermore, both subsets displayed at least two divisions at day two and between two and five divisions at day three (Fig. 3-1A).

We also wanted to determine if T cell activation was aberrant in the absence of cluster formation. Using the well-established T cell activation markers, CD44 (marker for antigen-experience), CD69 (early activation marker), and CD25 (high affinity IL-2 receptor α-subunit), we determined that wt and ICAM-1 KO T cells displayed equal

expression of these surface proteins (Fig. 3-1B). As additional proof of T cell naivety, we show that CD44, CD69, and CD25 were negative in expression on naïve T cells and equal between the wt and ICAM-1 KO populations (Fig. 3-1B).

Lack of T cell clustering promotes increased effector function

Although T cell clustering did not affect division and activation, we still sought to understand whether effector functions were altered between clustered and unclustered T cells. Thus, at two days post priming when the presence or absence of clustering was most evident (as shown in Figures 2-6A & C), we harvested T cells and performed intracellular staining for the effector molecules interferon-γ (IFNγ) and granzyme B. At two days post stimulation, we observed an increase in both IFNγ and granzyme B production in the ICAM-1 KO T cells (Fig. 3-2A). This exacerbation of effector function in the absence of clusters was also seen at three days post priming (Fig. 3-2B). Normalized fold changes in expression level of effector molecules seen in ICAM-1 KO T cells compared to wt (n≥14 experiments) at two and three days post priming showed a reproducibly enhanced effector status in ICAM-1 KO T cells (Fig. 3-2C).

Additionally, we performed cytotoxic killing assays with day three wt and ICAM-1 KO effector T cells to monitor the physiological significance of an increase in effector molecules. As performed by us and others (conversations with Dr. Julie Curtsinger and Deb Lins), day two effectors are not optimal for monitoring killing of peptide-pulsed target cells (*data not shown*). Using effectors in combination with Chromium^{51} (Cr^{51}) pulsed, antigen expressing thymoma cells (EG7-OVA) we compared the ability of wt OT-I T cells to kill relative to ICAM-1 KO OT-I T cells. We observed an increase in % specific target cell lysis at all E:T ratios tested (Fig. 3-2D[1]). In general, increased ICAM-1 KO killing compared to wt was most reproducible at the highest E:T ratios. If T cells were not

activated in the presence of IL-12 we demonstrated reduced overall killing for both wt and ICAM-1 KO T cells (Fig. 3-2E[1]); this finding corroborates previous studies (19). EL-4 negative controls showed little to no death when incubated with wt T cells; however, ICAM-1 KO T cells displayed increased ability to kill control targets (Fig. 3-2F[1]).

Next we wanted to assess whether these differences were due to the expression levels of the IL-12 receptor (CD212). Since IL-12 can drive cytotoxicity and effector function (19), we hypothesized that ICAM-1 KO T cells would express more IL-12 receptor throughout priming. However, IL-12 receptor expression was identical on both naïve and activated wt and ICAM-1 KO OT-I T cells (Fig. 3-2G).

Disruption of wt T cell clusters enhances effector molecule expression

Since we saw a difference in effector function between wt and ICAM-1 KO T cells during activation, we wanted to complement these results using wt T cells in combination with previously tested anti-LFA-1 antibodies. The rationale for this was three-fold; one, we wanted to eliminate the possibility that our finding was a by-product of ICAM-1 deletion; two, we wanted to exclude the chance that our finding was due to potential ICAM-1 isoform expression in the ICAM-1 KO T cells. Lastly, we wanted to perform a more physiological condition using wt T cells that were not genetically manipulated and thus more clinically relevant. Using the anti-LFA-1 CD11a-specific (M17/4) blocking antibody and the anti-LFA-1 CD18-specific (M18/2) non-blocking antibody we sought to determine if we could obtain comparable effector results to the ICAM-1 KO T cells. Images of wt T cells using the M17/4 and M18/2 antibodies are shown in Figure 2-6D-E and Figure 2-7F-G, respectively. In culture, the M17/4 and M18/2 anti-LFA-1 antibodies did not appear to alter T cell expansion based upon T cell recovery (Fig. 3-3A). When intracellular staining for IFNγ and granzyme B at two days post stimulation was

assessed, we saw an increase in effector molecule expression under the condition in which the T cell clusters were blocked (M17/4 – *black filled*) (Fig. 3-3B). T cell clustering conditions in which wt was alone (*gray line*) or in the presence of the control antibody (M18/2 – *gray filled*) condition showed decreased IFNγ and granzyme B expression compared to conditions in which clusters were disrupted (Fig. 3-3B). Normalizing IFNγ (p value<0.05) and granzyme B (p value<0.01) to wt for each of the treated conditions revealed statistical significance between the M17/4 and M18/2 antibody treatments using the Student's unpaired two-tailed *t* test (Fig. 3-3C).

In sum, T cell clusters appear to temper the expression of effector molecules and cytotoxic ability of activated CD8+ T cells. Using genetic manipulation and antibody blockade approaches to inhibit the formation of T cell:T cell clusters, we provide evidence that effector function is regulated by T cell:T cell contact.

ICAM-1 KO T cells can form mixed clusters with wt T cells

Next we wanted to assess whether ICAM-1 deficiency inhibits T cell capacity to form clusters with wt (ICAM-1 sufficient) T cells. We predicted that ICAM-1 KO T cells, which express LFA-1 (Fig. 2-4C), would form contacts with wt T cells. We validated this hypothesis by performing mixed culture experiments *in vitro*. By differentially labeling ICAM-1 KO OT-I T cells with cell trace violet (CTV) and mixing the cells at altered ratios with wt OT-I T cells we were able to assess and quantify the extent to which ICAM-1 KO T cells clustered with wt T cells. Figure 3-4A[2] shows a representative example of mixed cultures at five different wt:ICAM-1 KO ratios. Quantification of these images using ImageJ analysis software revealed that ICAM-1 KO T cells could indeed co-cluster with wt T cells (Fig. 3-4B). The ability of ICAM-1 KO T cells to cluster directly correlated with the amount of wt T cells in culture. To take these two-dimensional images further, we

employed the use of multi-photon microscopy to take z-stack slices in order to qualitatively delineate a three-dimensional appreciation for both clustering and cluster make up at a 1:1 ratio (Fig. 3-4C^2). CFSE labeled ICAM-1 KO T cells (*yellow cells*) could cluster with CTV labeled wt T cells (*blue cells*); however, there was an increased amount of unclustered ICAM-1 KO T cells compared to wt T cells (Fig. 3-4C^2).

ICAM-1 KO T cells in mixed cultures take on a wt T cell effector phenotype

Once we concluded that ICAM-1 KO T cells can make clusters with wt T cells, we wanted to understand the effector abilities of ICAM-1 KO T cells upon clustering. We mixed the T cells at altered wt:ICAM-1 KO ratios (9:1, 3:1, 1:1, 1:3, 1:9) and differentially examined each subset at day two by separating them via congenic markers. Our studies revealed that upon titrating wt T cells into the culture, the ICAM-1 KO T cells showed an IFNγ pattern that began to resemble the wt T cells (Fig. 3-5). The gMFI values attained are shown in the upper right hand corner for wt (*gray*) and ICAM-1 KO (*black*). Upon comparing the wt:ICAM-1 KO ratios at the two extremes (1:9 and 9:1) we showed that the ICAM-1 KO T cells dropped IFNγ expression by 31.2%, while the wt T cells only decreased 10.2%. These data suggest that the physical act of being in a T cell cluster contributes to the dampening of effector functions during CD8+ T cell stimulation *in vitro*.

Although viable in vitro, ICAM-1 KO T cells do not persist as well as wt T cells after co-adoptive transfer into naïve recipients

Our next step was to determine whether clustering mediated T cell viability. We performed 7-Aminoactinomycin D (7-AAD) staining, a fluorescent chemical compound that intercalates into double-stranded DNA and delineates a compromised cell

membrane, of day two and day three activated wt and ICAM-1 KO T cells. We determined that there was a similar, albeit small, total amount of 7-AAD+ T cells under both conditions at days two and three (Fig. 3-6A). Staining for the pro-survival protein, B-cell lymphoma extra-large (Bcl-X_L), also revealed no discernible differences between wt and ICAM-1 KO T cells during *in vitro* priming (Fig. 3-6B). These data suggest that T cell clustering does not play an immediate role on T cell viability during early activation.

A useful technique to determine T cell fates after *in vitro* stimulation has been to adoptively transfer T cells into naïve recipients and follow T cell maintenance (127). Thus, day two activated T cells were harvested, washed, and $1x10^5$ wt OT-I and $1x10^5$ ICAM-1 KO OT-I T cells were co-adoptively transferred intravenously into congenically different naïve recipients. Based upon recent studies, these transferred T cells expand and maintain if the T cell was exposed to the three important signals needed for optimal priming *in vitro* (127). In our studies, both the wt and the ICAM-1 KO T cells expanded, but the ICAM-1 KO T cells did not expand to the same extent based upon recovery in the spleen five days post transfer (Fig. 3-6C). Additionally, T cell maintenance in the ICAM-1 KO subset was also compromised compared to the wt population (Fig. 3-6C). After determining the recovery percentages of ICAM-1 KO and wt T cells, it became apparent that at three days or more post transfer the ICAM-1 KO T cells had a decreased potential to persist when compared to wt T cells as indicated by the ICAM-1 KO (%) / wt (%) recovery ratio decreasing below 1.0 (Fig. 3-6D). A similar trend occurred in the bone marrow, as well as in the peripheral and mesenteric lymph nodes (Fig. 3-6E). The lymph node data showed more variability than the spleen and bone marrow from experiment to experiment. These data suggest that in the absence of T cell clustering during priming, activated CD8+ T cells become imprinted with a terminal differentiation phenotype that does not allow for expansion or persistence *in vivo* to the

same extent as clustered cells. A slightly modified interpretation of these data is that the expansion is different and not the persistence because the percentage of cells maintaining at late time points relative to the peak of expansion (the slope) appears to be similar between the wt and ICAM-1 KO T cell subsets, if not even more so in the favor of ICAM-1 KO T cells.

Increased ICAM-1 KO effector phenotype is likely not due to soluble factors, alternative ICAM-1 binding, or antigen dose

We sought to understand why unclustered T cells showed an increase in effector function compared to clustered T cells. Since IL-2 has been shown to be a cytokine that is centrally localized at T cell:T cell contact points within T cell clusters (87), we hypothesized that IL-2 might be mediating the effector differences. We rationalized that differences in IL-2 production or acquisition might be driving these *in vitro* observations. We struggled to assess IL-2 intracellular staining in both the wt and the ICAM-1 KO activated OT-I T cells; instead we added exogenous IL-2 to the cultures and determined if the effector differences were less pronounced. When wt and ICAM-1 KO T cells were assessed for IFNγ and granzyme B production after two days post priming in the absence or presence of exogenous IL-2, we once again saw an increase in effector ability by the ICAM-1 KO T cells (Fig. 3-7A). Although differences were seen in the expression of IFNγ at day three between the absence and presence of IL-2 supplementation, there was a similar fold change in gMFI values from no IL-2 to +IL-2 conditions in both the wt and ICAM-1 KO T cells. This suggests that effector increases in the ICAM-1 KO T cells is not a direct result of an inadequate acquisition of IL-2 during activation especially at day two where clustering is most prevalent.

Another approach we took to understand if a different soluble factor played a role in increasing effector function on ICAM-1 KO T cells was to perform a conditioned media experiment. We took supernatants from day three activated wt and ICAM-1 KO T cell culture wells, and used this conditioned media to activate naïve CFSE labeled wt OT-I T cells. We expected that if the ICAM-1 KO T cells produced a factor that accelerated effector function or if the wt T cells produced a soluble factor that inhibited effector ability, we should be able to assess these outcomes using freshly purified naïve wt OT-I T cells. We tracked both granzyme B and IFNγ expression (Fig. 3-7B), as well as T cell division (Fig. 3-7C) over several different concentrations of conditioned media at two and three days post stimulation and observed no differences between the wt T cells in either day three wt or ICAM-1 KO conditioned media.

The data to this point have shown the importance of LFA-1:ICAM-1 interactions; however, MAC-1 ($\alpha_M\beta_2$ or CD11b/CD18) integrin can also bind mouse ICAM-1. The ICAM-1 KO that we experimentally utilize is not a complete knock-out and has been shown to produce truncated ICAM-1 isoforms (102, 104-106). Our particular ICAM-1 KO is deficient in the MAC-1 binding region (immunoglobulin region 3 of ICAM-1) (97); thus we needed to explore MAC-1 upregulation kinetics on activated T cells to determine whether or not wt ICAM-1 could bind wt MAC-1 and facilitate effector regulation. Using flow cytometry to examine CD11b kinetics on our *in vitro* activated T cells, we concluded that CD11b is not upregulated during *in vitro* activation in either the wt or ICAM-1 KO population (Fig. 3-7D). Therefore, the loss of the MAC-1 binding region of our ICAM-1 KO T cells is not relevant since MAC-1 is not elevated during T cell priming.

An additional concern of isoform expression is that transient interactions between ICAM-1 KO T cell expressed LFA-1 and ICAM-1 KO ICAM-1 isoforms could exist that may not be stable enough to allow for cluster stability but could permit signaling. To

verify that these hypothetically brief interactions do not mediate the augmentation of effector function in ICAM-1 KO T cells compared to wt T cells, we used the previously described anti-LFA-1 blocking antibody (M17/4) to block these potential LFA-1:isoform contacts. We observed no increases in IFNγ expression in the ICAM-1 KO anti-LFA-1 blocking condition compared to the ICAM-1 KO unblocked condition (Fig. 3-7E). These data suggest that the potential for LFA-1 to bind ICAM-1 isoforms is not regulating effector functions.

Lastly, we wanted to verify that our IFNγ differences seen between our two subsets of activated T cells was not a result of the current (1X) dosage of antigen used in culture. Thus, we titrated the amount of SIINFEKL used *in vitro* and kept all other concentrations of stimulatory reagents identical to previous experiments. We observed an increase in ICAM-1 KO expressed IFNγ compared to wt at all doses of antigen beginning at a 2X SIINFEKL dose and decreasing to a 1/30X SIINFEKL dose; indeed the 1/30X showed the smallest difference between the ICAM-1 KO and wt T cells (Fig. 3-8A). A comparative analysis of all doses demonstrated a gradual decrease in IFNγ expression as dosage was decreased (Fig. 3-8B); however the maintenance of enhanced IFNγ expression across all antigen doses remained elevated in the ICAM-1 KO subset. These data demonstrate that the effector difference seen between ICAM-1 KO and wt T cells is not due to one unique antigen dose, but rather a potential ability to sense more antigen. The collection of these results suggests that soluble factors, ICAM-1:MAC-1 binding, isoform binding, and antigen dose do not contribute to the differential regulation of effector functions observed between clustered and unclustered CD8+ T cells.

Unclustered T cells are exposed to more antigen than clustered T cells

Although different antigen doses and broad activation marker expression did not help in identifying the driver for increased effector functions between unclustered and clustered T cells, we still wanted to determine the strength of TCR triggering. Thus, we utilized Nur77-GFP OT-I mice that were created as described (139) and generously provided by Dr. Kris Hogquist. Nur77 is an immediate downstream target of TCR engagement and as a result is a faithful marker for the amount of antigen that is sensed by the TCR, irrespective of co-stimulation and inflammation (139). Since the Nur77-GFP OT-I mouse was not bred to the ICAM-1 KO, we instead utilized the anti-LFA-1 blocking antibodies with Nur-77-GFP wt OT-I T cells to disrupt cluster formation *in vitro*. When GFP expression was examined every 24 hours for three days post priming, we observed a modest but statistically significant (p value<0.01) increase in the amount of Nur77-GFP that was upregulated at days two and three on the wt T cells that were blocked for cluster formation with the M17/4 antibody compared to wt (+ M18/2) control antibody (Fig. 3-9A-B). This result shows that unclustered T cells can sense antigen longer and in part might explain the increased effector functions relative to clustered T cells.

Immune inhibitory proteins PD-1 and PD-L1 do not contribute to effector regulation

It appeared that enhanced antigen sensing in unclustered T cells played a partial role for increased effector status; however, we believed that decreased antigen sensing was not the only function for T cell clustering because antigen sensing differences were modest compared to effector molecule expression differences. Thus, we decided to look at immune-inhibitory proteins that might lead to effector control. Programmed cell death protein 1 (PD-1) is a marker that correlates with T cell activation (140). Using our *in vitro*

stimulation model, we examined PD-1 kinetics and determined that there were no differences between wt (*gray filled*) and ICAM-1 KO (*black line*) T cells at any time before and during activation (Fig. 3-10A[3]). The same result was observed for the PD-1 ligand, PD-L1 (Fig. 3-10B[3]); however, unlike PD-1, PD-L1 peaks at one day post stimulation and declines over the course of the next 48 hours.

Even though expression kinetics were unaltered between the T cell subsets, we wanted to determine whether ligation between PD-1 and PD-L1 was enhanced in the presence of clusters. We hypothesized that if this interaction was blocked during wt T cell cluster formation, there would be a disruption in PD-1:PD-L1 interactions and as a result might lead to an increased amount of IFNγ produced by the blocked condition. In order to test this idea, we used an anti-PD-L1 blocking antibody to eliminate the ability of PD-1 to bind PD-L1. When wt T cells were harvested at two days post priming, we saw that the PD-L1 blocked T cells did not exhibit enhanced IFNγ expression (Fig. 3-10C[3]). PD-L1 blockade using ICAM-1 KO T cells were performed as a control and also showed no increases in IFNγ regulation (Fig. 3-10C[3]). PD-L1 and PD-1 although upregulated after activation, do not appear to contribute to IFNγ control in clustered or unclustered T cells.

Expression of the CTLA-4 immune inhibitory protein is regulated by T cell clusters

A different hallmark immune-inhibitory protein that has recently been shown to be regulated by T cell interactions is cytotoxic T-lymphocyte antigen 4 (CTLA-4) (67). We stained day two stimulated wt and ICAM-1 KO OT-I T cells with anti-CTLA-4 and found a reduction in CTLA-4 expression both on the surface and intracellularly in the ICAM-1 KO T cells compared to the wt T cells (Fig. 3-11A[3]). CTLA-4 surface and intracellular staining were both performed because the activation of T cells mobilizes CTLA-4 to the

cell surface; however, surface mobilization does not necessarily lead to membrane stabilization and therefore turnover still exists (141). We also performed and obtained similar results with wt + anti-LFA-1 (M17/4) blockade conditions (Fig. 3-11B); these experiments were performed in order to rule out the loss of ICAM-1 artificially reducing CTLA-4 expression. Published studies have suggested that IL-2 can induce CTLA-4 expression in human and mouse T cells (64, 66). Therefore, we supplemented both wt and ICAM-1 KO cultures with exogenous IL-2 and once again observed decreased CTLA-4 expression in the ICAM-1 KO samples compared to the wt samples (Fig. 3-11C[3]). Furthermore, CTLA-4 appeared in our microarray as a candidate transcript of interest differentially regulated between wt and ICAM-1 KO T cells at two days post stimulation. This has been reconfirmed using reverse transcriptase quantitative polymerase chain reaction (*data not shown*[4]). Thus, T cell:T cell contact mediates overall CTLA-4 expression; whereas, IL-2 supplementation does not play a role in CTLA-4 regulation in our model.

CTLA-4 blockade leads to increased IFNγ expression on clustered T cells

Since CTLA-4 production on clustered T cells was augmented compared to unclustered T cells, we were curious if the counter ligands for CTLA-4, CD80 (B7-1) and CD86 (B7-2), were also differentially regulated. We observed upregulation of CD80 at day two and three after priming; whereas CD86 was barely detectable above isotype staining at day three (Fig 3-12A[3]). CD80 upregulation was experimentally performed several times for both activated wt and ICAM-1 KO T cells and expression was similar between the wt and ICAM-1 KO T cells, if not slightly elevated in the ICAM-1 KO subset.

Next we hypothesized that blocking CTLA-4 with antibody would disrupt ligation to CD80, either expressed on an adjacent T cell or bound to the plate, and thereby lead

to enhanced IFNγ expression on wt T cells. When anti-CTLA-4 blocking antibodies and T cells were added to the plate, we observed our expected increase in wt IFNγ staining at two days post priming (Fig. 3-12B[3]). Normalized values to untreated wt conditions showed an average of a 1.4-fold increase (Fig. 3-12C[3]), while the normalized values of treated ICAM-1 KO to untreated ICAM-1 KO showed an average fold change of 0.98 (Fig. 3-12C[3]). This suggests that anti-CTLA-4 antibody blockade disrupts an immunosuppressive signal in clustered T cells. Next, we wanted to determine the importance of T cell expressed CD80 (high affinity counter-receptor for CTLA-4). We therefore altered our T cell stimulation conditions (H2-K^b:SIINFEKL, CD86 (B7-2), IL-12) so that the only CD80 present in the culture was on the T cell surface. We added anti-CD80 blocking antibodies and did not observe IFNγ increases in the treated compared to the untreated conditions at three different concentrations of antibody with either the wt or ICAM-1 KO cells (Fig. 3-12D[3]). This does not completely rule out the importance of CD80 on T cells because CTLA-4 can still bind plate bound CD86 (low affinity counter-receptor for CTLA-4) and deliver an inhibitory signal. The data, however, does argue a role for T cell expressed CTLA-4 during stimulation.

Unclustered ICAM-1 KO T cells express increased levels of eomesodermin

Previous studies have shown that CTLA-4 can exhibit immunosuppressive effects on both IFNγ and granzyme B production (69-71). CTLA-4 regulates these events by suppressing the T-box transcription factor eomesodermin (EOMES) in both NK cells and CD8+ T cells (70, 71). Thus, we speculated that EOMES expression on day two activated wt T cells would be reduced compared to ICAM-1 KO T cells. When intracellular staining was performed on both subsets, we saw an increase in EOMES expression in the ICAM-1 KO T cells (Fig. 3-13A). After averaging multiple experiments,

we observed that wt T cells produced only 60-70% the amount of EOMES made by ICAM-1 KO T cells (Fig. 3-13B). As other studies have illustrated (70, 71), our data supports the idea that EOMES expression is inversely correlated with CTLA-4 expression.

In vitro splenocyte activation yields increased IFNγ expression in ICAM-1 KO T cells

Our model has been minimalistic using only purified T cells; thus, we chose to activate purified wt and ICAM-1 KO OT-I T cells with bulk splenocytes from a non-transgenic C57BL/6 mouse to observe effector abilities after a more physiological priming condition. Using $3x10^5$ purified wt or ICAM-1 KO OT-I T cells and a range of splenocytes ($3x10^4$ - $6x10^5$), we observed that the ICAM-1 KO T cells showed elevated IFNγ expression compared to wt (Fig. 3-14, *far right*). CD44 and, surprisingly, intracellular CTLA-4 were similar in expression levels (Fig. 3-14, *far left and middle*). This suggests that the contact between the ICAM-1 KO T cell and the APC is enough to induce contact mediated intracellular CTLA-4 expression; however, since these ICAM-1 KO T cells do not persist in T cell:T cell activation clusters, the ability of that CTLA-4 to regulate IFNγ is presumably disrupted.

DISCUSSION

Here in Chapter 3 we show evidence that T cell clusters play a role in affecting the effector status and differentiation of CD8+ T cells. Using a reductionist approach with purified CD8+ OT-I T cells, we demonstrate increases in effector capabilities when T cells cannot cluster even though activation markers and T cell proliferation remain unaffected. Furthermore, our data provide a novel model that illustrates the importance

of T cell:T cell contacts in mediating the upregulation of the immunosuppressive molecule, CTLA-4, which plays a role in the downregulation of the transcription factor EOMES and thereby mediates CD8+ T cell immunity by regulating IFNγ and granzyme B expression and subsequently target cell killing. The slight enhancement of killing with EL4 control target cells suggests a small amount of killing might be antigen non-specific; however, further experimentation will be needed to understand this observation.

Our original hypothesis for the role of T cell clustering was to facilitate optimal T cell responses, such as (but not limited to) enhanced T cell division and effector responses, as well as rapid upregulation of activation markers. Thus, we were surprised that unclustered ICAM-1 KO T cells diluted CFSE and upregulated the activation markers CD44, CD69, and CD25 to a similar extent as wt clustered T cells. Additionally, the fact that unclustered T cells actually produced a better effector response was completely unexpected. Some studies are showing compelling evidence that these T cell clusters persist *in vivo* (85-87, 89); we can speculate, for the first time, that clusters are a mechanism by which activated T cell effector profiles are regulated. It may be the case that it is physiologically unhealthy for T cells to produce maximal amounts of IFNγ and granzyme B at the site of priming when the site of insult is likely at a distal region.

Translating these results directly to *in vivo* physiology has several caveats. First, during an actual infection there are a multitude of different CD8+ antigen specific T cells with altered TCR affinities responding, as well as a plethora of CD4+ T cells, Tregs, B cells, macrophages, neutrophils, and antigen presenting DCs, to name a few. The combination of these leukocytes could contribute to the composition of multi-cellular clusters. The impact of many different naïve, effector, and memory T cells responding to antigen and inflammation has not been adequately depicted with our *in vitro* studies. Secondly, disrupting clusters *in vivo* using anti-LFA-1 blocking antibodies would be very

difficult without understanding the proper timing and kinetics of T cell activation. Even then, blocking LFA-1 during priming in order to disrupt T cell clusters, would also interrupt crucial APC:T cell interactions, as well as LFA-1 mediated tissue extravasation. If these concerns were circumvented, predicting the timing of a natural infection is nearly impossible and thus, blocking clusters during an actual immune response might prove to be very challenging.

The mixed culture experiments shed light on physical cluster composition by showing evidence that ICAM-1 KO T cells can engage wt T cells in T cell clusters. These mixed clusters point to the fact that the act of being involved in a cluster is enough to dampen CD8+ effector T cell responses *in vitro*. Our data support the idea that IFNγ increases in the ICAM-1 KO T cells is not due to the loss of ICAM-1 on the T cell. If the loss of ICAM-1 drove enhanced effector status, then we would have postulated that IFNγ expression for the ICAM-1 KO T cells would have looked identical between the 1:9 (wt:ICAM-1 KO) and the 9:1 mixed ratios. This was not the case and therefore excludes the loss of ICAM-1 as the driver of augmented CD8+ effector T cell responses. As for LFA-1 engagement, although not definitive, our data proposes that LFA-1 does not play a large role in IFNγ production. The rationale for this is that we observe a 31.2% decrease in gMFI values for IFNγ when comparing the 1:9 (wt:ICAM-1 KO) to the 9:1 ratio for ICAM-1 KO T cells. When the decrease is examined for the wt T cells under the same conditions (1:9 equates with less clustering; 9:1 equates with more clustering) we only see a 10.2% decrease. If LFA-1 ligation on a T cell strongly facilitated IFNγ expression in our model, we would have expected the wt to have a value that was similar to the 31.2% seen in the ICAM-1 KO. This interpretation assumes that there is less LFA-1 ligation on wt T cells under conditions in which the majority of the T cells present are ICAM-1 KO compared to wt only conditions because there is less total

ICAM-1 for wt LFA-1 to bind to. However, it is plausible that some wt LFA-1 will be ligated to ICAM-1 when wt T cells contact each other while dividing and clustering even at low wt amounts.

We also sought to determine whether the differentiation of unclustered T cells was altered compared to clustered T cells. In order to do so, we used an adoptive transfer model in which activated cells were transferred into naïve (antigen-free) mice and maintenance and expansion of those T cells analyzed over time. ICAM-1 KO T cells harvested at two days post priming were co-transferred at an equal ratio with wt T cells and showed equivalent ratios at days one and two post transfer; however, every day thereafter we recovered a skewing in favor of the wt T cells. These experiments support the idea that the ICAM-1 KO T cells are terminally differentiated in comparison to the activated wt T cells; or in other words, that clustering supports the tuning of terminal differentiation. The two major pieces of supporting evidence for this idea is that there are reduced amounts (ratio percentages and numbers) of ICAM-1 KO T cells that persist long term and that expansion kinetics are not as robust in the ICAM-1 KO T cells compared to wt. It is believed that longevity of T cells is influenced by a subset of T cells, termed memory precursors, which are identifiable during infection *in vivo*. These cells promote memory and harbor the characteristics of self-renewal and proliferation (23). Terminal differentiation is an end-stage for T cells and it would not be expected that terminally differentiated T cells would have self-renewal or long-lasting abilities to persist *in vivo* (23). Our data suggests, since we recover ratios that favor wt T cells over ICAM-1 KO T cells, that the majority of ICAM-1 KO T cells were not programmed for memory but rather terminal differentiation during *in vitro* stimulation. Secondly, expansion kinetics for the ICAM-1 KO T cells were not similar to the re-expansion of wt T cells post transfer. This again suggests that activated ICAM-1 KO T cells are terminally

differentiated. Thus, clusters play a role in regulating terminal differentiation; furthermore, the effector molecule increases in the ICAM-1 KO T cells also support this enhanced terminal differentiation hypothesis.

Attempting to understand the driver of effector function involving clustered and unclustered T cells led us to perform many experiments that led to results showing no difference between the wt and ICAM-1 KO T cells. Although, no single experiment can rule out definitively the role of one pathway versus another; we believe that our experiments in regards to soluble factors, alternative ICAM-1 binding, and antigen dose collectively suggest that these mechanisms play little to no role in the enhanced effector responses in the ICAM-1 deficient population. Based on the importance of IL-2 regulation within clusters (87), we originally predicted that IL-2 acquisition would be less than ideal in the ICAM-1 KO T cells because they could not interact with one another. However, adding sufficient amounts of exogenous IL-2 to culture dishes did not alter the data and therefore provides little support, although not contrasting evidence, for the importance of directionally secreted IL-2 as shown previously (87). The conditioned media experiment suggests that there is not a soluble factor produced by the ICAM-1 KO or wt T cells that promotes or inhibits effector function.

The ICAM-1 deficient mouse (B6.129S4-ICAM1^{tm1Jcgr}/J) that has been used in our experiments has been shown by other laboratories to express different isoforms of ICAM-1 (102, 104-106). The ICAM-1 deficient mouse strain used in our laboratory was created by inserting a neomycin cassette into exon four and thus disrupting the Ig3 protein domain (97). Using this mouse, van den Engel *et al.*, as well as others have shown that the following isoforms can be produced; 2 → 5 (exon 2 is spliced to exon 5 resulting in the Ig1 domain fusing to the Ig4 domain), 3 → 6 (exon 3 is spliced to exon 6 resulting in the Ig2 domain fusing to the Ig5 domain), and 2 → 5 (exon 2 is spliced to

exon 5 resulting in the Ig1 domain fusing to the Ig5 domain) (102, 104-106). Thus, the idea that ICAM-1 isoforms expressed on the ICAM-1 KO T cell surface could ligate to LFA-1 on another T cell seems possible. When we tested this by blocking LFA-1 on ICAM-1 KO T cells and compared IFNγ expression to ICAM-1 KO T cells under untreated conditions we did not see any alterations in effector function. Therefore, we speculate that the presence of ICAM-1 isoforms do not play a role in the absence of T cell clustering. Additionally, since the MAC-1 integrin was not upregulated on activated T cells, we postulate that the MAC-1 binding region (the Ig3 domain of ICAM-1), which is ablated on ICAM-1 KO T cells but present within the ICAM-1 that is on wt T cells, does not play a role in T cell clusters. Lastly, the specific antigen dose that we use for our experiments is not unique to exacerbating the ICAM-1 KO effector phenotype; rather, upon performing titrations we observe an increased ICAM-1 KO effector response with antigen doses ranging from 1/30X – 2X the original dosage.

We instead believe that antigen exposure plays a role in augmenting effector function in unclustered T cells. Using Nur77-GFP OT-I mice we show with anti-LFA-1 blocking conditions that Nur77-GFP increases above both wt untreated and wt + control anti-LFA-1 antibody. Since Nur77 is exclusively downstream of TCR and not regulated by inflammation or co-stimulation (139), our results suggest that unclustered T cells are actually sensing an increased amount of antigen, even though the concentration of SIINFEKL in culture is identical to clustered cells. In addition, we believe that TCR affinity or strength of peptide is not promoting these differences because all T cells under our experimental conditions (both wt and ICAM-1 KO) have the exact same OT-I TCR specific for SIINFEKL in the context of H2-K^b. Based upon multi-photon microscopic z-stack projections, we can see that unclustered T cells are localized closer to the plate, while clustered T cells appear to be in three-dimensional clusters that would physically

make it difficult for all clustered T cells to be receiving antigen at the same time. We have hypothesized and shown along with others (87) that these clusters are dynamic in nature and not static (Fig. 2-8A-B); thus, a T cell residing on top of a cluster is most likely not excluded from antigen for the entirety of the time course and might be rapidly moving within a cluster. We do not begin to see Nur77-GFP changes until after one day post stimulation. This correlates with the start of cluster formation. Nur77-GFP is the same among all cells at 24 hours because the physical separation from plate bound antigen via clustering has not initiated. Whether SIINFEKL has been stripped from plate bound MHC-I and re-presented by T cells themselves is not known. It is also important to denote that the half-life of GFP is longer than Nur77 (139); thus, our observed increase in GFP signal at two days and three days might not be the exact time points that Nur77 is actually differentially expressed. Nonetheless it is an appropriate readout for TCR triggering and under these model conditions demonstrates a statistically significant increase in antigen sensing.

As an additional mechanism, aside from antigen exposure, we show evidence of cluster mediated events inducing immunesuppression. Originally we examined PD-1:PD-L1 interactions and assessed that there was no role for this ligation pair in suppressing CD8+ T cells in our model. This prompted us to further investigate other immunosuppressive markers, such as CTLA-4. We were struck by the decreased amount of CTLA-4 expressed by ICAM-1 KO T cells both on the surface and intracellularly. We were able to reproduce increased CTLA-4 expression using wt T cells with cluster blocking anti-LFA-1 antibody. We determined that IL-2 acquisition is not the driver of decreased CTLA-4, but rather CTLA-4 upregulation is a function of activated T cell:T cell contacts. A recent publication in PNAS showed some evidence of this

phenomenon through the titration of unactivated T cells into cultures of activated T cells and observing the downregulation of CTLA-4 on the activated T cells (67).

Our laboratory and others have observed the upregulation of CD80 on T cells (60, 67) or alloreactive T cells (90); thus, we hypothesized that close contact between T cells could lead to the dampening of effector responses by ligating upregulated CTLA-4 and CD80. In fact, Blazer and colleagues have published studies regarding CTLA-4 mediated down regulation of T cell immune responses via T cell expression of B7 molecules (90). Anti-CTLA-4 blockade experiments did indeed promote increased IFNγ expression on wt T cells. Although ICAM-1 KO T cells showed no difference under anti-CTLA-4 treated or untreated conditions, it is tough to determine whether the low levels of CTLA-4 expressed on unclustered T cells is enough to induce an inhibitory signal. The lack of a difference in the ICAM-1 KO T cells might be a direct function of low expression of CTLA-4. Although interesting, this ICAM-1 KO data does not rule out a role for plate bound CD80 in the wt conditions. Thus, we swapped plate bound B7-1 (CD80; higher affinity for CTLA-4) for B7-2 (CD86; lower affinity for CTLA-4) and monitored T cell effector responses in the presence of a CD80 blocking antibody which would only block CD80 expressed on T cells because CD86 was now the co-stimulation reagent adsorbed to the plate. Under these conditions there were no differences observed between the treated and untreated conditions. Based upon this result, we speculate that under our conditions CD80 on a T cell does not play as large of a role as CTLA-4 in mediating immunosuppressive effects on clustered T cells. Even though the concentration of co-stimulatory B7-2 used was comparable to B7-1 in regards to several T cell activation readouts (*data not shown*), we must acknowledge the fact that it does not have the same affinity for CD28 and CTLA-4 and therefore could behave differently under certain conditions. Also, we might not see differences after anti-CD80 treatment

because the vast majority of T cell expressed CTLA-4 is binding plate bound CD86 and inducing inhibition in that manner. Our data confidently suggests a role for CTLA-4 in immunoinhibition via clustering; however the ability to ligate CD80 or CD86 on another T cell or to a plate and the importance of this precise interaction requires further experimentation. We believe that it is the absence of a CTLA-4 mediated signal and not an increase in co-stimulation in the ICAM-1 KO T cells that is driving enhanced effector functions for two reasons. The first is that EOMES expression is in part mediated by CTLA-4 inhibition (70, 71) and we subsequently see an increased EOMES signal in the ICAM-1 KO T cells during activation. And secondly, if ICAM-1 KO T cells were receiving an enhanced CD28 co-stimulation signal we might expect the T cells to express higher levels of Bcl-X_L (142, 143); however, this is not observed.

We also determined that this upregulation of CTLA-4, although pronounced when purified OT-I T cells were used, was not prominent when splenocytes were used to activate wt and ICAM-1 KO OT-I T cells. We speculate that under the conditions of splenocyte activation, the contact between an activating T cell and an APC is enough to induce CTLA-4 upregulation. An older study showed that adding IFNγ to human peripheral blood mononuclear cells led to the upregulation of CTLA-4, whereas, adding IFNγ to purified T cells did not lead to increased CTLA-4 (66). Those authors speculated that the IFNγ might activate monocytes, which in turn can activate T cells and induce CTLA-4 expression. This monocyte activation induced by IFNγ (produced by activated T cells in our model) may help explain why we do not observe differences in CTLA-4 expression between wt and ICAM-1 KO T cells when activated with splenocytes as opposed to plate bound antigen. However, we still observed increased effector function in the ICAM-1 KO splenocyte activated cultures compared to the wt cultures. We speculate that since ICAM-1 KO T cells cannot cluster with other ICAM-1 KO T cells, the

ability to inhibit IFNγ through CTLA-4 ligation does not occur as strongly when compared to wt. Since plate bound CD80 or CD86 is not present under these splenocyte stimulation conditions, these data indirectly suggest that CD80:CTLA-4 ligation within T cell clusters may play a role in immune-inhibition. A complication of these mixing experiments is the potential immunosuppression regulated through contacts other than T cell:T cell. It is for this reason, and the fact that ICAM-1 KO T cells can co-cluster with wt T cells that further complicates *in vivo* experiments that will be discussed in Chapter 4.

Egen and Allison demonstrated (65) that CTLA-4 expressed at the surface of a T cell is proportional to the intensity of the TCR signal. The authors showed this novel observation using 5C.C7 TCR transgenic T cells activated by peptide pulsed APCs. They showed that weak agonist peptides led to decreased surface expressed CTLA-4 compared to T cells stimulated with agonist peptides. The CTLA-4 differences that we showed using purified wt and ICAM-1 KO T cells may be explained by the absence of an APC during activation, because splenocyte induced activation of T cells led to equal levels of CTLA-4 expression. These data also suggest that there are no differences in the affinity for MHC-I:SIINFEKL between wt and ICAM-1 KO OT-I T cells. However, the data using purified T cells with plate bound antigen suggests that T cell contact during activation plays a prominent role in the expression level of CTLA-4 on an activating T cell. We did not perform CTLA-4 expression level experiments using altered peptide ligands for the OT-I TCR; however, we would predict that CTLA-4 expression differences would continue to persist between clustered and unclustered T cells even in the presence of a lower affinity peptide. Additionally, aside from TCR affinity for peptide dictating CTLA-4 expression, data using concanavalin A (66) (ConA; a T cell stimulatory agent that is similar to PMA or PHA) have been used to show positive correlations

between increasing ConA concentrations and CTLA-4 levels. Our data showing unclustered T cells display lower CTLA-4 levels even though the T cells are exposed to more antigen (as assessed via Nur77-GFP) suggests that contact dependent upregulation of CTLA-4 plays a prominent role in regulating CTLA-4 surface and intracellular levels during CD8+ T cell activation. The receptor(s), ligand(s), or soluble factor(s) involved in this contact mediated event are unknown. Our data would suggest that it is not IL-2 mediated or ICAM-1 mediated because the ICAM-1 KO T cells display different CTLA-4 levels under the plate bound and splenocyte activation conditions. If ICAM-1 ligation mediated this event, we would have expected CTLA-4 expression levels to be reduced relative to wt under both of these conditions. Some studies speculate that CTLA-4 ligation can lead to an increase in adherence to ICAM-1 through LFA-1 (68), but the opposite regulation event (LFA-1 → CTLA-4) has not been shown.

Since CTLA-4 clearly played a role (both on an expression and a suppression level), we wanted to define a downstream target of CTLA-4 inhibition between clustered and unclustered T cells. Previous studies have linked CTLA-4 suppression (via CTLA-4 ablation (70, 71) or inhibition through ipilimumab (an anti-CTLA-4 antibody) treatment (73) to Eomesodermin (EOMES) expression either on a protein or mRNA transcript level. Thus, we stained for EOMES expression between wt and ICAM-1 KO T cells at two days post priming and, as expected, observed an enhanced expression level in the ICAM-1 KO T cells.

Taking all of these data together we propose a model that demonstrates how T cell clustering regulates effector functions (Figures 3-15 & 3-16). These augmented functions in unclustered T cells are due in part to two separate mechanisms. The first being the enhanced physical exposure to antigen as defined by altered Nur77-GFP kinetics in unclustered T cells. Since unclustered T cells sense more antigen, the

increased effector functions are a direct readout of antigen exposure; however, the Nur77-GFP differences, although statistical, appeared to be overly modest to entirely account for the striking effector differences. Thus, we focused on immunosuppressive molecules that might be regulated as a result of T cell clusters. The second mechanism focuses on the role of contact-mediated upregulation of the suppressive molecule CTLA-4 that binds to CD80 on the plate (and possibly on another T cell depending on priming conditions) and thereby downregulates EOMES expression which in turn dampens effector functions on clustered T cells. In unclustered T cells, CTLA-4 is not as highly upregulated and as a result leads to enhanced EOMES expression, which subsequently allows for increased effector functions. The role of ICAM-1 on T cells *in vivo* will be explored in Chapter 4 using several different models.

FOOTNOTES

[1] Deb Lins (scientist in Dr. Matthew Mescher's laboratory, University of Minnesota - Twin Cities, Minneapolis, MN) supplied radioactive Cr^{51} for killing assays, as well as standard operating procedures and safety training for proper usage.

[2] Dr. Jason Mitchell (post-doctoral fellow in Dr. Yoji Shimizu's laboratory, University of Minnesota – Twin Cities, Minneapolis, MN) contributed to the acquisition of multi-photon images, as well as performed training for the use of the confocal microscope.

[3] Dr. Eisuke Domae (former post-doctoral fellow in Dr. Yoji Shimizu's laboratory, University of Minnesota – Twin Cities, Minneapolis, MN) contributed intellectually and experimentally to the IL-2 supplementation (Figure 3-7A), PD-L1/PD-1 (Figures 3-10A-B) and CTLA-4/CD80/CD86 (Figures 3-11A & C and Figures 3-12A-D) results.

[4]Dr. Brandon Burbach (research associate in Dr. Yoji Shimizu's laboratory, University of Minnesota – Twin Cities, Minneapolis, MN) contributed to microarray analysis and confirmation of candidate genes.

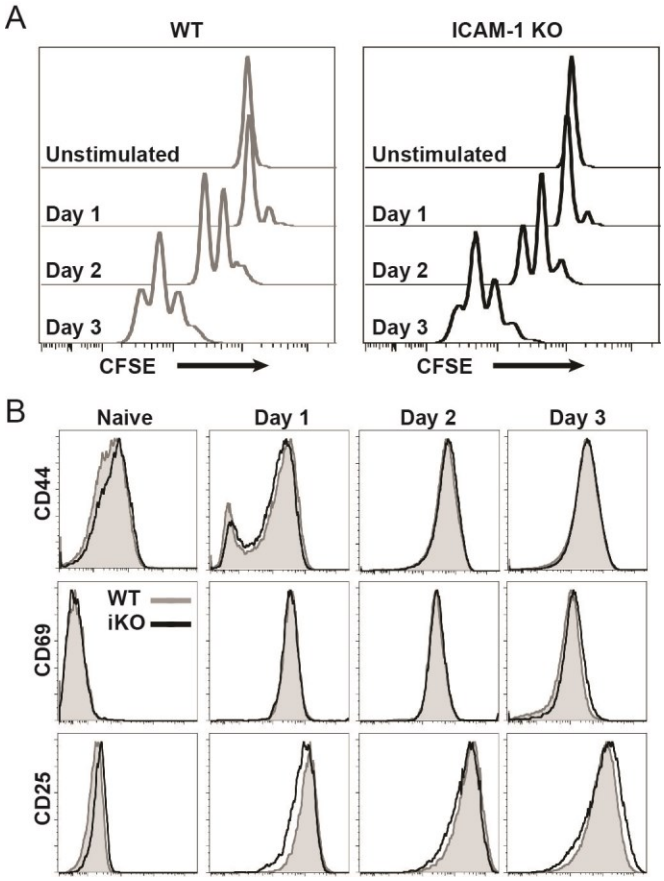

Figure 3-1: Absence of T cell clustering does not affect T cell proliferation or activation marker upregulation.

Naïve purified wt and ICAM-1 KO (iKO) OT-I T cells were stimulated *in vitro* using plate-bound H2-K^b:SIINFEKL, recombinant B7-1, and soluble IL-12. **(A)** CFSE dilution kinetics for unstimulated and activated wt (*gray*) and ICAM-1 KO (*black*) T cells. **(B)** Surface CD44, CD69, and CD25 activation marker upregulation kinetics on naïve and activated wt *(gray*) and ICAM-1 KO *(black*) T cells.

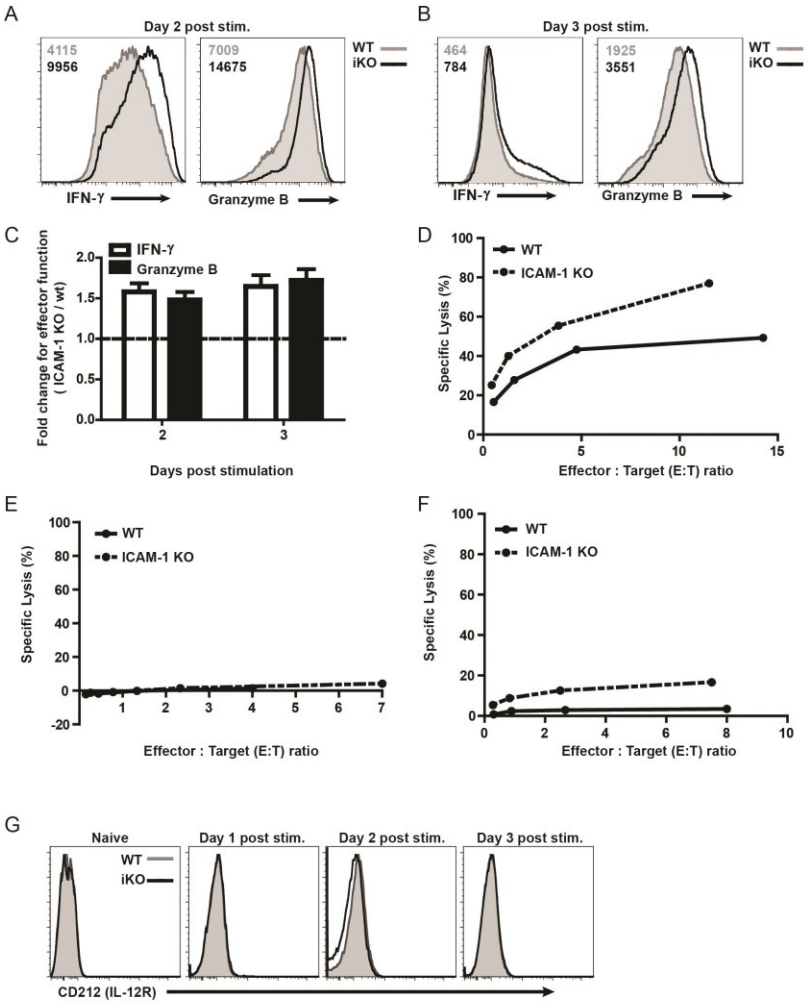
A
Day 2 post stim.
4115
9956
7009
14675
WT
iKO
IFN-γ
Granzyme B
B
Day 3 post stim.
464
784
1925
3551
WT
iKO
IFN-γ
Granzyme B
C
IFN-γ
Granzyme B
Fold change for effector function (ICAM-1 KO / wt)
Days post stimulation
D
WT
ICAM-1 KO
Specific Lysis (%)
Effector : Target (E:T) ratio
E
WT
ICAM-1 KO
Specific Lysis (%)
Effector : Target (E:T) ratio
F
WT
ICAM-1 KO
Specific Lysis (%)
Effector : Target (E:T) ratio
G
Naive
Day 1 post stim.
Day 2 post stim.
Day 3 post stim.
WT
iKO
CD212 (IL-12R)

Figure 3-2: ICAM-1 KO T cells display enhanced effector functions compared to wt clustered T cells.

Naïve purified wt and ICAM-1 KO (iKO) OT-I T cells were stimulated *in vitro* using plate-bound H2-K^b:SIINFEKL, recombinant B7-1, and soluble IL-12. **(A)** Intracellular expression of IFNγ and granzyme B for wt (*gray filled*) and ICAM-1 KO (*black line*) for day two and **(B)** day three post stimulation. **(C)** Normalized MFI or gMFI values for both IFNγ and granzyme B at each time point were performed in order to determine the ICAM-1 KO fold change compared to wt for n≥14 experiments. **(D)** Day three effector killing was determined using SIINFEKL-pulsed EG7-OVA thymoma cells as targets. **(E)** Day three effector killing (in the absence of IL-12 during stimulation) was determined using SIINFEKL-pulsed EG7-OVA thymoma cells as targets. **(F)** Control killing was determined using antigen-negative EL4 thymoma targets. **(G)** CD212 (IL-12 receptor) kinetics were determined on naïve and activated wt (*gray filled*) and ICAM-1 KO (*black line*) T cells.

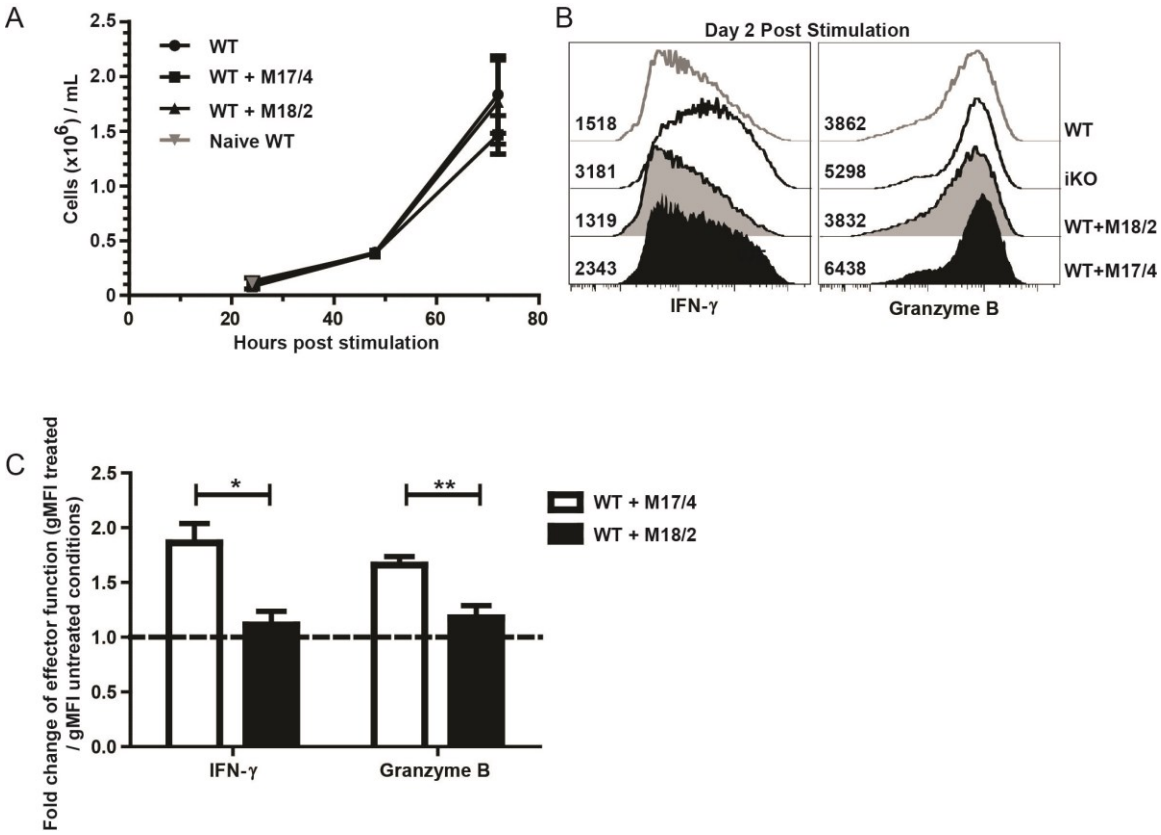

Figure 3-3: Disruption of wt T cell clusters enhances effector functions.

Naïve purified wt and ICAM-1 KO (iKO) OT-I T cells were stimulated *in vitro* using plate-bound H2-K^b:SIINFEKL, recombinant B7-1, and soluble IL-12. **(A)** T cell recovery (cell counts (x10^6) /mL) over the course of three days of activation using wt T cells (*black circle*), wt T cells + M17/4 anti-LFA-1 cluster blocking antibody (*black square*), wt T cells + M18/2 anti-LFA-1 cluster blocking control antibody (*black triangle*) and naïve wt T cells (*gray triangle*). **(B)** Intracellular expression of IFNγ and granzyme B two days post priming with wt (*gray*), ICAM-1 KO (*black*), wt + M18/2 (*gray filled*), and wt + M17/4 (*black filled*). gMFI values are indicated to the right of each histogram. **(C)** Normalized gMFI values to wt only. Statistically analyzed using a Student's unpaired two-tailed *t* test. Each M17/4 bar represents an n=7 (*, p value<0.05) and each M18/2 bar represents n=3 (**, p value<0.01).

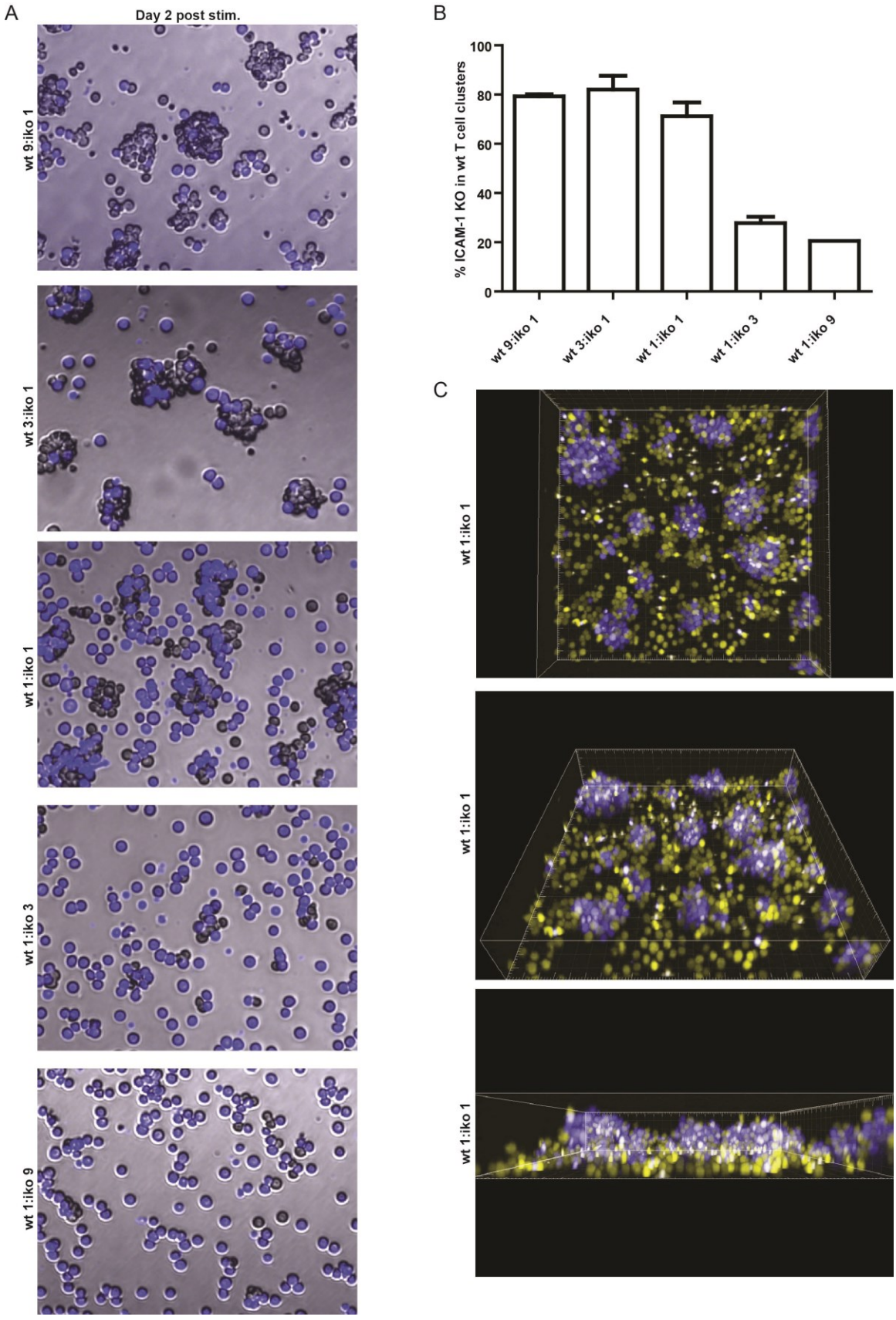
A
Day 2 post stim.
wt 9:iko 1
wt 3:iko 1
wt 1:iko 1
wt 1:iko 3
wt 1:iko 9
B
% ICAM-1 KO in wt T cell clusters
100
80
60
40
20
0
wt 9:iko 1
wt 3:iko 1
wt 1:iko 1
wt 1:iko 3
wt 1:iko 9
C
wt 1:iko 1
wt 1:iko 1
wt 1:iko 1

Figure 3-4: ICAM-1 KO T cells can co-cluster with wt T cells during activation.

Naïve purified wt and ICAM-1 KO (iKO) OT-I T cells were stimulated *in vitro* using plate-bound H2-K^b:SIINFEKL, recombinant B7-1, and soluble IL-12. **(A)** ICAM-1 KO T cells were labeled with cell trace violet (CTV) (*blue cells*) and mixed at altered ratios with wt T cells (*phase-contrast cells*). **(B)** The percentage of ICAM-1 KO T cells in contact with wt T cells was determined using ImageJ analysis and the following equation: (# of ICAM-1 KO T cells in contact with wt T cells) / (total # of ICAM-1 KO T cells). **(C)** ICAM-1 KO T cells were labeled with CFSE and wt T cells were labeled with CTV and mixed at a 1:1 ratio in scaled up culture dishes to allow for the immersion of a 20X objective lens and imaged via multi-photon microscopy with an upright Leica TCS MP resonance scanning microscope. A z-stack projection was acquired and three different angles of the same z-stack are shown above.

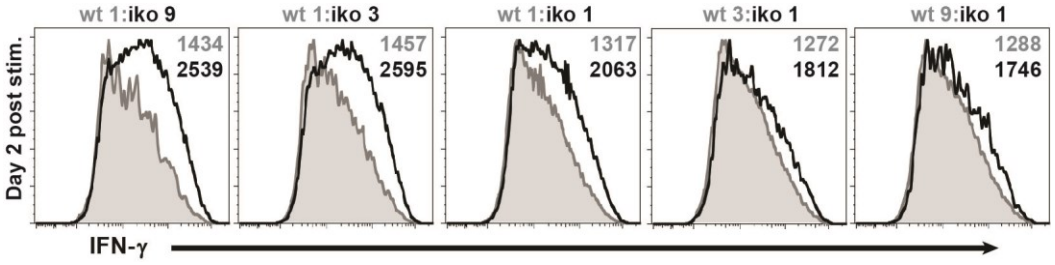

Figure 3-5: ICAM-1 KO T cells express effector molecules similar to wt T cells when engaged in mixed T cell clusters.

Naïve purified wt and ICAM-1 KO (iKO) T cells were stimulated for two days *in vitro* using plate-bound H2-K^b:SIINFEKL, recombinant B7-1, and soluble IL-12. T cell subsets were mixed at indicated wt:ICAM-1 KO ratios, starting with 1:9 (*far left histogram*) and ending with 9:1 *(far right histogram*). gMFI values for wt (*gray*) and ICAM-1 KO (*black*) are listed in the upper right hand corner of each flow plot. T cell histograms refer to wt (*gray filled*) and ICAM-1 KO (*black line*), respectively.

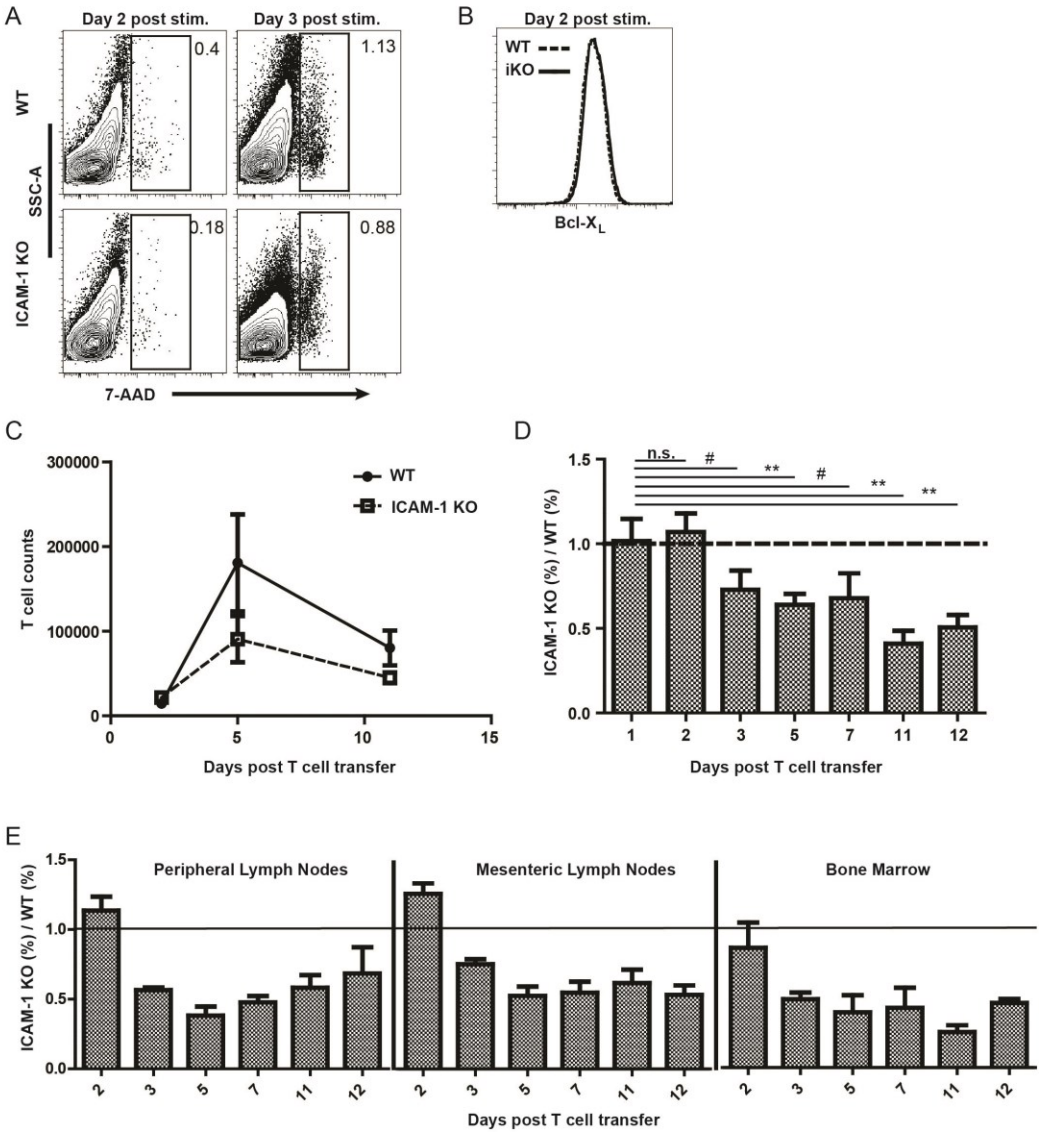

Figure 3-6: Despite equal viability *in vitro*, unclustered T cells do not persist as well as clustered T cells *in vivo*.

Naïve purified wt and ICAM-1 KO (iKO) T cells were stimulated *in vitro* using plate-bound H2-K^b:SIINFEKL, recombinant B7-1, and soluble IL-12. **(A)** Viability of T cells was assessed by using 7-AAD at two and three days post T cell priming. **(B)** The pro-survival protein Bcl-X_L was assessed by intracellular staining at two days post priming. **(C)** Two day activated wt and ICAM-1 KO T cells were adoptively co-transferred at similar ratios ($1x10^5$ of each subset per recipient) and expansion and maintenance were assessed. **(D)** A ratio of ICAM-1 KO (%) to wt (%) of recovered T cells for four experiments is shown (**, p value<0.01; #, p value<0.13; n.s., not significant). **(E)** A ratio of ICAM-1 KO (%) to wt (%) of recovered T cells for the peripheral lymph nodes, mesenteric lymph nodes, and bone marrow.

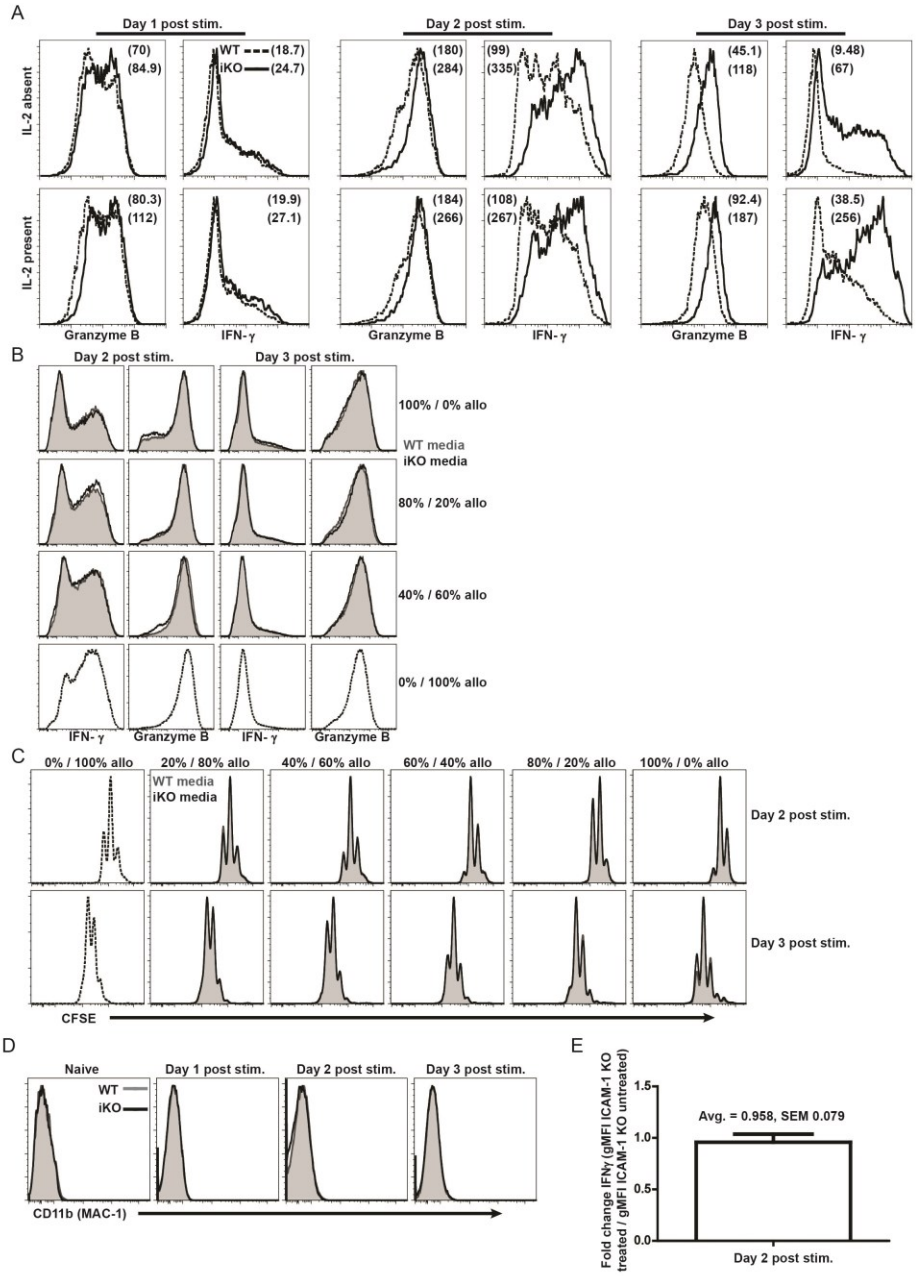
A
Day 1 post stim.
Day 2 post stim.
Day 3 post stim.
IL-2 absent
IL-2 present
WT
iKO
(70)
(84.9)
(18.7)
(24.7)
(180)
(284)
(99)
(335)
(45.1)
(118)
(9.48)
(67)
(80.3)
(112)
(19.9)
(27.1)
(184)
(266)
(108)
(267)
(92.4)
(187)
(38.5)
(256)
Granzyme B
IFN- γ
B
Day 2 post stim.
Day 3 post stim.
100% / 0% allo
WT media
iKO media
80% / 20% allo
40% / 60% allo
0% / 100% allo
C
0% / 100% allo
20% / 80% allo
40% / 60% allo
60% / 40% allo
80% / 20% allo
100% / 0% allo
Day 2 post stim.
Day 3 post stim.
CFSE
D
Naive
Day 1 post stim.
Day 2 post stim.
Day 3 post stim.
CD11b (MAC-1)
E
Fold change IFNγ (gMFI ICAM-1 KO treated / gMFI ICAM-1 KO untreated)
Avg. = 0.958, SEM 0.079
1.5
1.0
0.5
0.0
Day 2 post stim.

Figure 3-7: Enhanced ICAM-1 KO effector functions are not due to soluble factors or alternate ICAM-1 binding.

Naïve purified wt OT-I and ICAM-1 KO (iKO) T cells were stimulated *in vitro* using plate-bound H2-K^b:SIINFEKL, recombinant B7-1, and soluble IL-12. **(A)** IL-2 was supplemented to cultures and effector functions determined at each day post activation. gMFI values for wt (*dashed line*, *top value*) and ICAM-1 KO (*black line*, *bottom value*) T cells are shown in flow plots. **(B-C)** Conditioned media from day three wt (*gray filled*) or ICAM-1 KO (*black line*) cultures were used to activate freshly purified wt OT-I T cells at different concentrations of experienced media with fresh alloclone media (experienced media % / alloclone media %) at two and three days post priming. Effector functions and T cell division were determined in (*B*) and (*C*), respectively. **(D)** CD11b (α_M subunit of MAC-1 integrin) kinetics were determined for naïve and activated wt (*gray filled*) and ICAM-1 KO (*black line*) T cells. **(E)** ICAM-1 KO T cells were activated in the absence or presence of anti-LFA-1 blocking antibody (M17/4) for two days and IFNγ expression was monitored. Fold change was determined by using gMFI values for IFNγ and normalizing to the untreated condition for three independent pooled experiments.

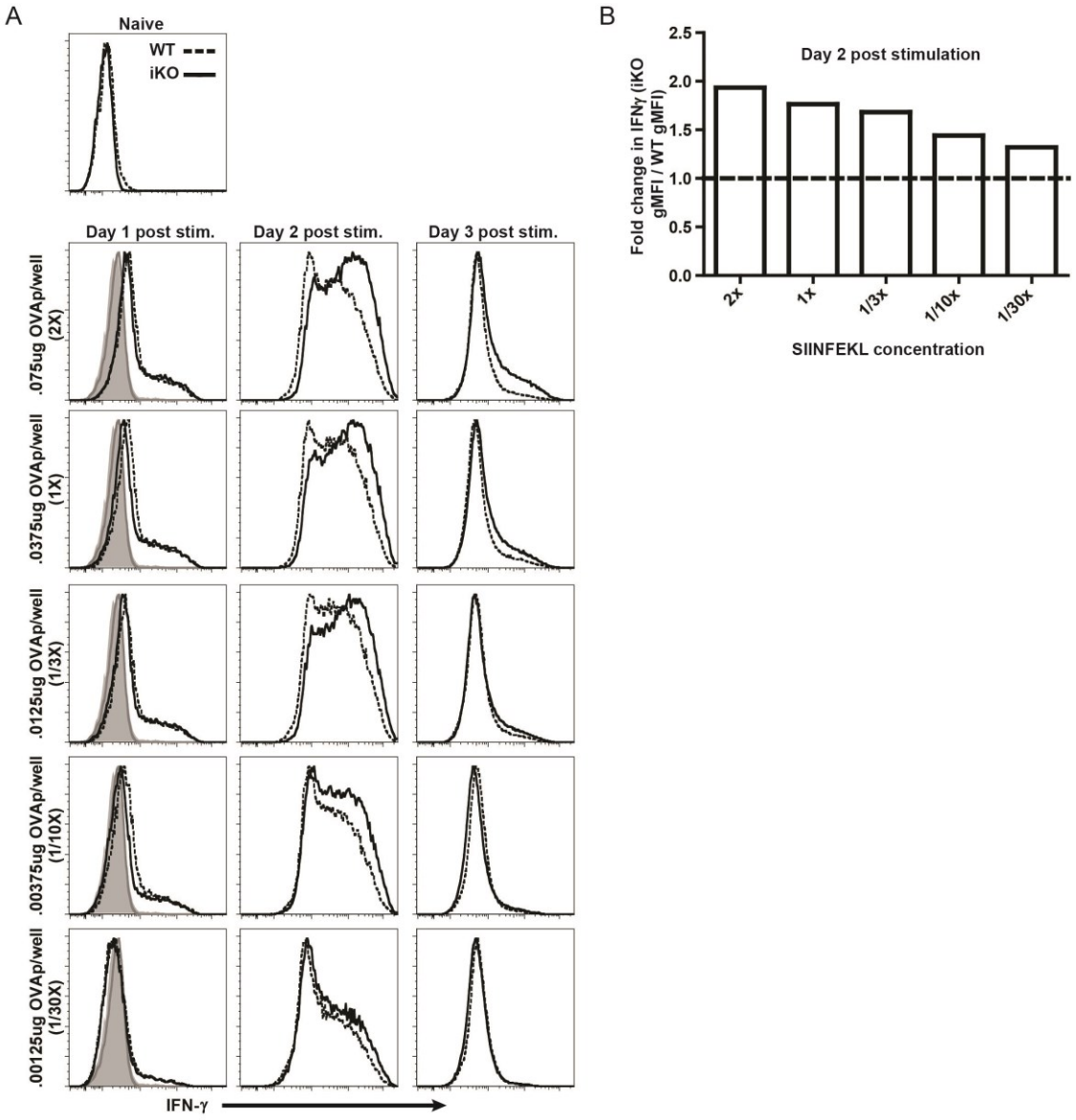
A
Naive
WT
iKO
Day 1 post stim.
Day 2 post stim.
Day 3 post stim.
.075ug OVAp/well (2X)
.0375ug OVAp/well (1X)
.0125ug OVAp/well (1/3X)
.00375ug OVAp/well (1/10X)
.00125ug OVAp/well (1/30X)
IFN-γ
B
Day 2 post stimulation
Fold change in IFNγ (iKO gMFI / WT gMFI)
2.5
2.0
1.5
1.0
0.5
0.0
2x
1x
1/3x
1/10x
1/30x
SIINFEKL concentration

Figure 3-8: Increased effector function in ICAM-1 KO T cells is not dependent upon antigen dosage.

Naïve purified wt OT-I and ICAM-1 KO T cells were stimulated *in vitro* using plate-bound H2-K^b:SIINFEKL, recombinant B7-1, and soluble IL-12. **(A)** Different doses of SIINFEKL were used ranging from 2X (0.075ug OVAp/well) the normal dose to 1/30X (0.00125ug OVAp/well) the normal dose. IFNγ expression was assessed at each dosage at each time point. **(B)** A fold change of IFNγ expression of ICAM-1 KO T cells relative to wt T cells at day two at each SIINFEKL concentration is shown. ICAM-1 KO fold change increases were determined by setting the IFNγ gMFI value for the wt to 1.

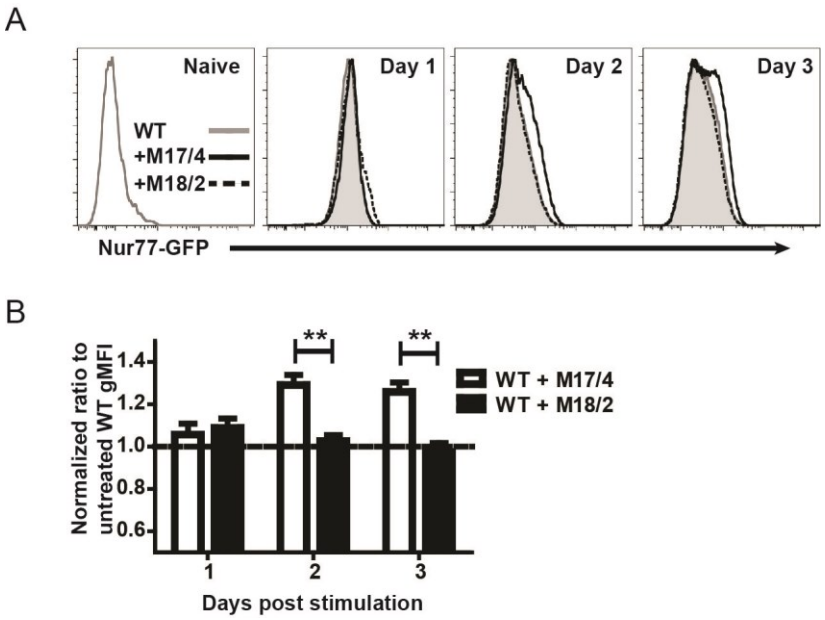

Figure 3-9: Unclustered T cells sense an increased amount of antigen.

Naïve purified Nur77-GFP wt OT-I T cells were stimulated for two days *in vitro* using plate-bound H2-K^{b}:SIINFEKL, recombinant B7-1, and soluble IL-12. Anti-LFA-1 antibodies (M17/4 and M18/2) were used to disrupt or not disrupt clusters, respectively. **(A)** GFP (Nur77-GFP) signal was obtained on naïve and activated T cells over the course of three days. **(B)** GFP (Nur77-GFP) fold-changes for blocking antibody conditions were attained by normalizing to wt untreated gMFI values. Graph shows data pooled from three independent experiments and statistically analyzed using the Student's unpaired two-tailed *t* test (**, p value<0.01).

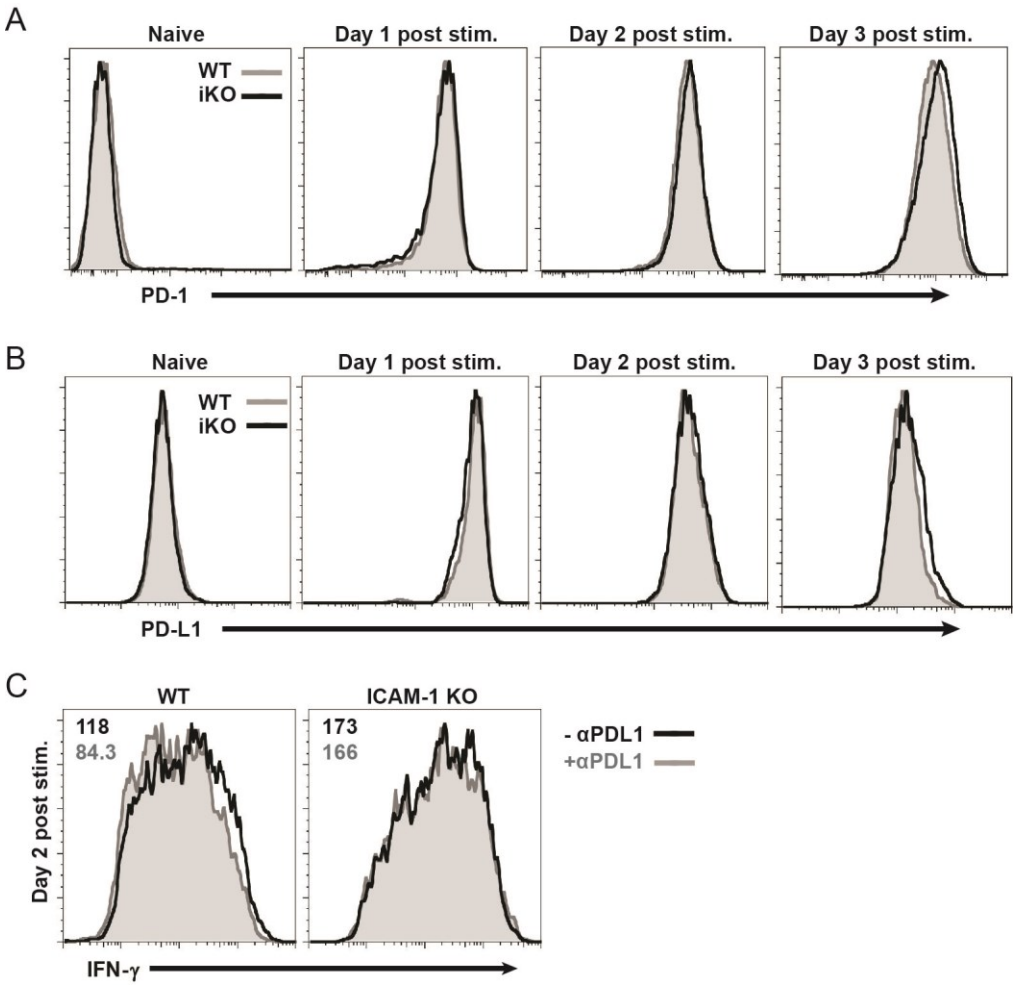

Figure 3-10: T cell cluster immune-inhibition is not mediated through PD-1:PD-L1.

Naïve purified wt OT-I and ICAM-1 KO (iKO) T cells were stimulated for two days *in vitro* using plate-bound H2-K^b:SIINFEKL, recombinant B7-1, and soluble IL-12. **(A)** PD-1 and **(B)** PD-L1 kinetics were tracked on naïve and activated T cells. **(C)** Anti-PD-L1 blocking antibody was added to T cell cultures at time of T cell plating and IFNγ production was analyzed two days post priming on wt and ICAM-1 KO T cells. gMFI values for – anti-PD-L1 antibody (*black line*) and + PD-L1 antibody (*gray line*) conditions are shown in the upper left hand corners of each flow plot.

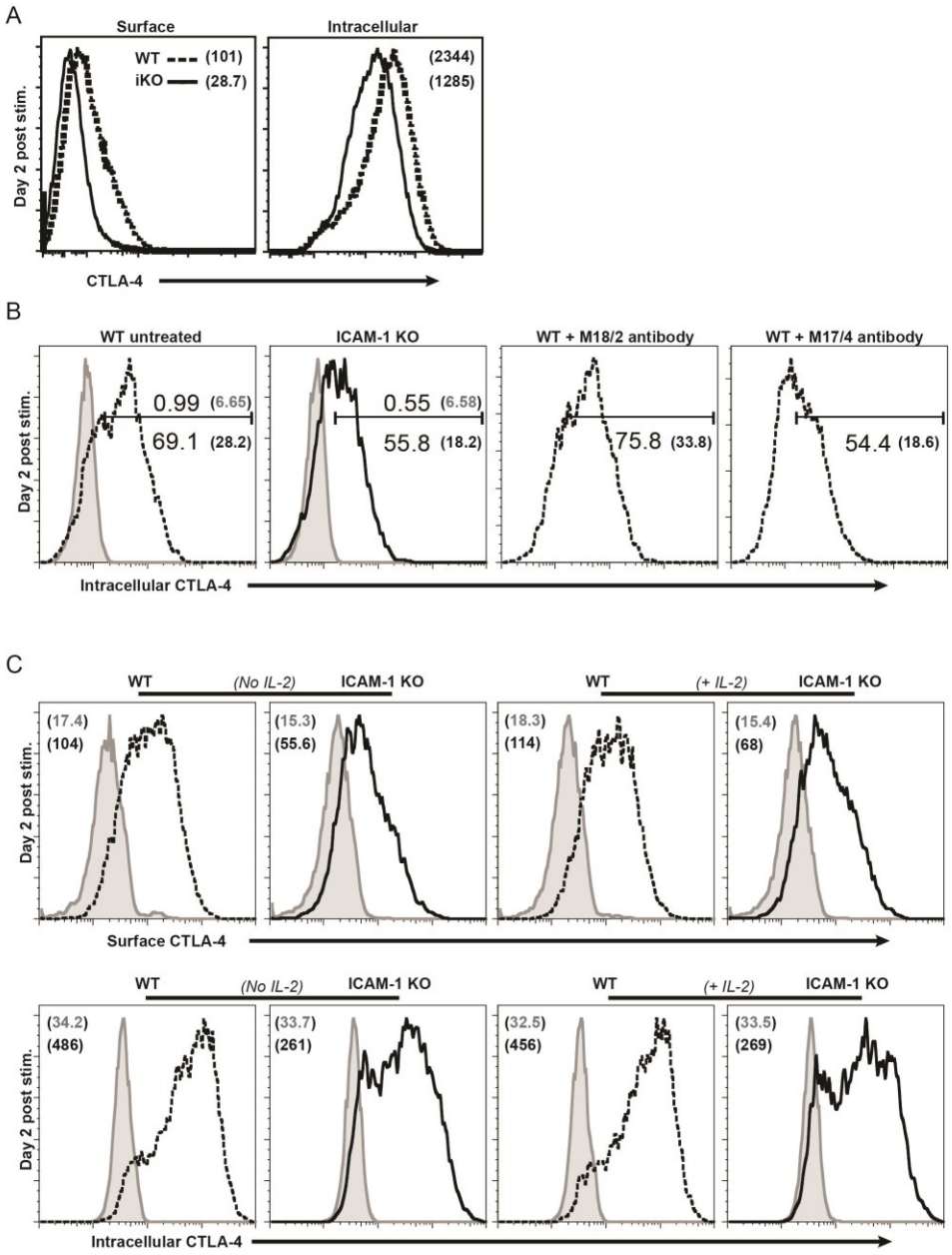
A
Surface
Intracellular
WT (101)
iKO (28.7)
(2344)
(1285)
Day 2 post stim.
CTLA-4
B
WT untreated
ICAM-1 KO
WT + M18/2 antibody
WT + M17/4 antibody
0.99 (6.65)
69.1 (28.2)
0.55 (6.58)
55.8 (18.2)
75.8 (33.8)
54.4 (18.6)
Day 2 post stim.
Intracellular CTLA-4
C
WT
(No IL-2)
ICAM-1 KO
WT
(+ IL-2)
ICAM-1 KO
(17.4)
(104)
(15.3)
(55.6)
(18.3)
(114)
(15.4)
(68)
Day 2 post stim.
Surface CTLA-4
(34.2)
(486)
(33.7)
(261)
(32.5)
(456)
(33.5)
(269)
Intracellular CTLA-4

Figure 3-11: Unclustered T cells show a decrease in overall CTLA-4 expression.

Naïve purified wt OT-I and ICAM-1 KO (iKO) T cells were stimulated for two days *in vitro* using plate-bound H2-K^b:SIINFEKL, recombinant B7-1, and soluble IL-12. **(A)** Surface and intracellular expression of CTLA-4 were obtained. gMFI values for wt (*dashed line*) and ICAM-1 KO (*black line*) T cells are shown in parentheses. **(B)** Intracellular CTLA-4 expression for wt + anti-LFA-1 treatment were attained. Percentages of T cells that are in the positive gate are shown below the gated line and gMFI values for the entire population are shown in the parentheses next to the percentages. Isotype percentages and gMFI values are above the gated line. **(C)** Surface (*top*) and intracellular (*bottom*) CTLA-4 expression in the presence or absence of exogenous IL-2 supplementation. gMFI values for CTLA-4 (*black line*) and isotype (*gray line*) staining are denoted in the upper left hand corner.

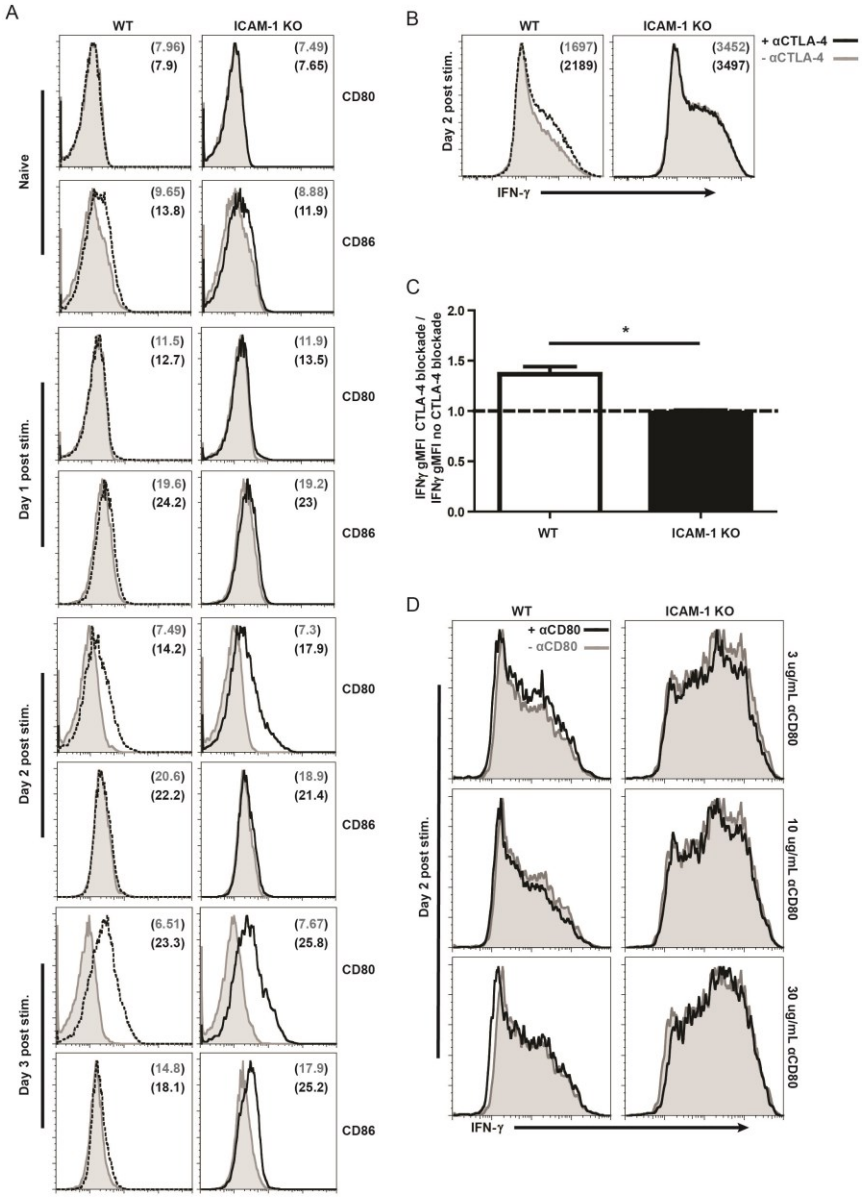
A
WT
ICAM-1 KO
Naive
Day 1 post stim.
Day 2 post stim.
Day 3 post stim.
CD80
CD86
(7.96)
(7.9)
(7.49)
(7.65)
(9.65)
(13.8)
(8.88)
(11.9)
(11.5)
(12.7)
(11.9)
(13.5)
(19.6)
(24.2)
(19.2)
(23)
(7.49)
(14.2)
(7.3)
(17.9)
(20.6)
(22.2)
(18.9)
(21.4)
(6.51)
(23.3)
(7.67)
(25.8)
(14.8)
(18.1)
(17.9)
(25.2)
B
WT
ICAM-1 KO
Day 2 post stim.
(1697)
(2189)
(3452)
(3497)
+ αCTLA-4
- αCTLA-4
IFN-γ
C
IFNγ gMFI CTLA-4 blockade / IFNγ gMFI no CTLA-4 blockade
2.0
1.5
1.0
0.5
0.0
*
WT
ICAM-1 KO
D
WT
ICAM-1 KO
+ αCD80
- αCD80
Day 2 post stim.
3 ug/mL αCD80
10 ug/mL αCD80
30 ug/mL αCD80
IFN-γ

Figure 3-12: T cell cluster immune inhibition is mediated, in part, by CTLA-4.

Naïve purified wt OT-I and ICAM-1 KO (iKO) T cells were stimulated *in vitro* using plate-bound H2-K^b:SIINFEKL, recombinant B7-1, and soluble IL-12. **(A)** CD80 and CD86 kinetics were monitored on naïve and activated T cells. Isotype plots and gMFI are shown in *gray*, while protein staining is shown in black for wt (*dashed*) and ICAM-1 KO (*solid*). **(B)** Day two activated T cells untreated or blocked with 30 µg αCTLA-4 blocking antibody were monitored for IFNγ expression. **(C)** Multiple experiments were pooled and gMFI values for antibody treated wt or ICAM-1 KO T cells were normalized to untreated cultures (*, p value=0.0413). **(D)** Naïve purified wt OT-I and ICAM-1 KO T cells were stimulated *in vitro* using plate-bound H2-K^b:SIINFEKL, recombinant B7-2, and soluble IL-12. Different concentrations of anti-CD80 (3-30 ug/mL) were added (*black line*) or not added (*gray filled*) to each well and two days post priming IFNγ was assessed in both T cell subsets.

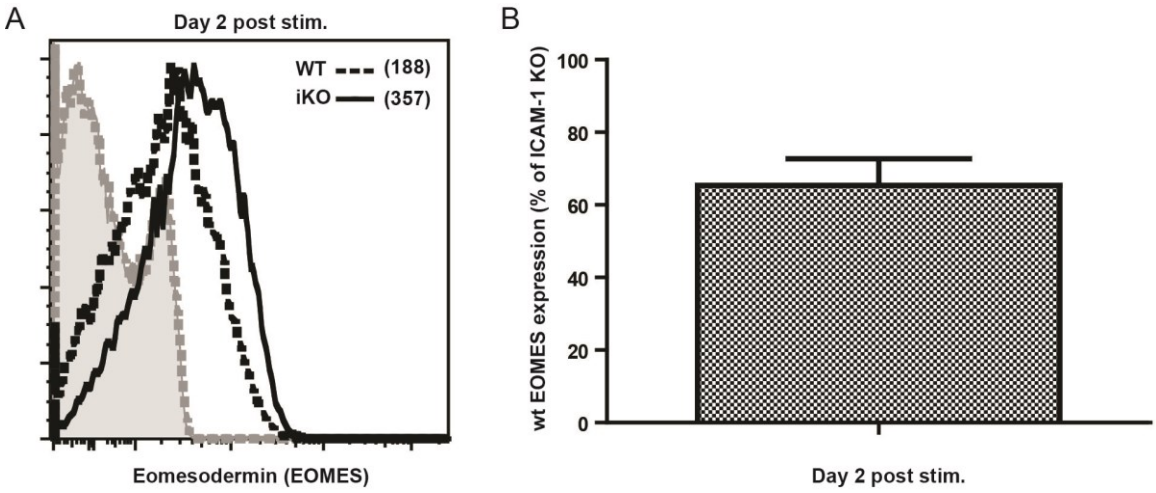

Figure 3-13: Unclustered T cells display enhanced production of the transcription factor eomesodermin (EOMES).

Naïve purified wt OT-I and ICAM-1 KO (iKO) T cells were stimulated for two days *in vitro* using plate-bound H2-K^b:SIINFEKL, recombinant B7-1, and soluble IL-12. **(A)** Intracellular staining for EOMES expression on wt (*dashed line*) and ICAM-1 KO (*black line*) T cells. Isotype controls for wt (*dashed gray line*) and ICAM-1 KO (*gray filled*) T cells are also shown. gMFI values for EOMES expression of one of three independent experiments are displayed in the upper right hand corner. **(B)** An average of three independent experiments quantifying EOMES expression in wt T cells is shown as a % of ICAM-1 KO gMFI expression.

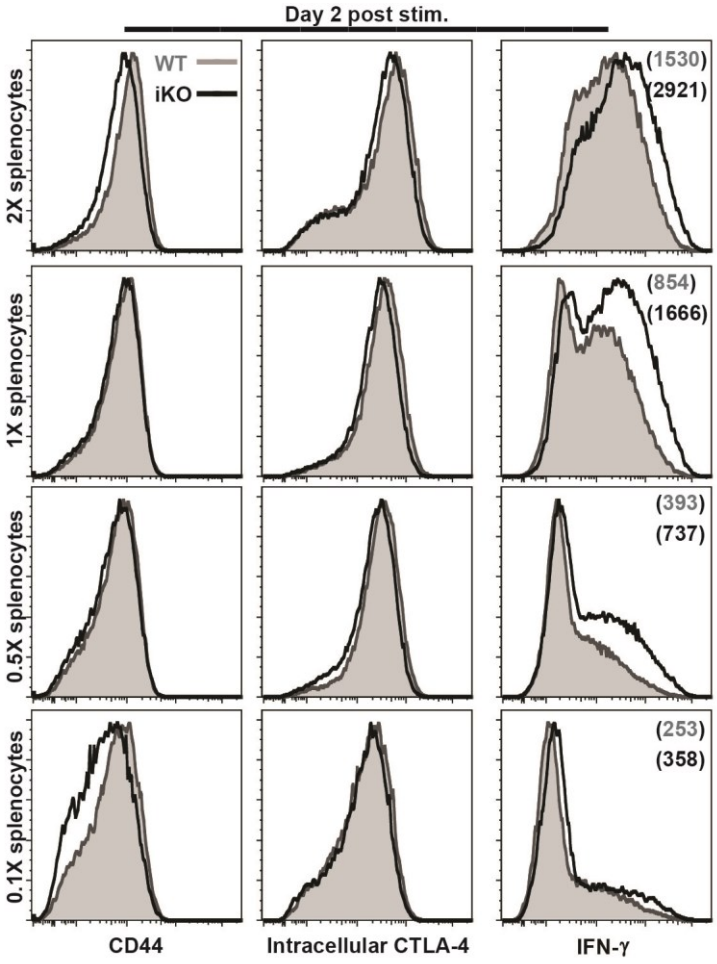

Figure 3-14: ICAM-1 KO T cells display enhanced IFNγ expression when activated with splenocytes *in vitro*.

Naïve purified wt (*gray filled*) and ICAM-1 KO (*black line*) T cells were activated with antigen + C57BL/6 non-transgenic splenocytes at four different splenocyte to T cell ratios (ranging from 2X to 1/10X of the total amount of purified T cells per well) and examined for CD44, intracellular CTLA-4, and IFNγ. gMFI values for IFNγ expression are denoted in the far right flow plots.

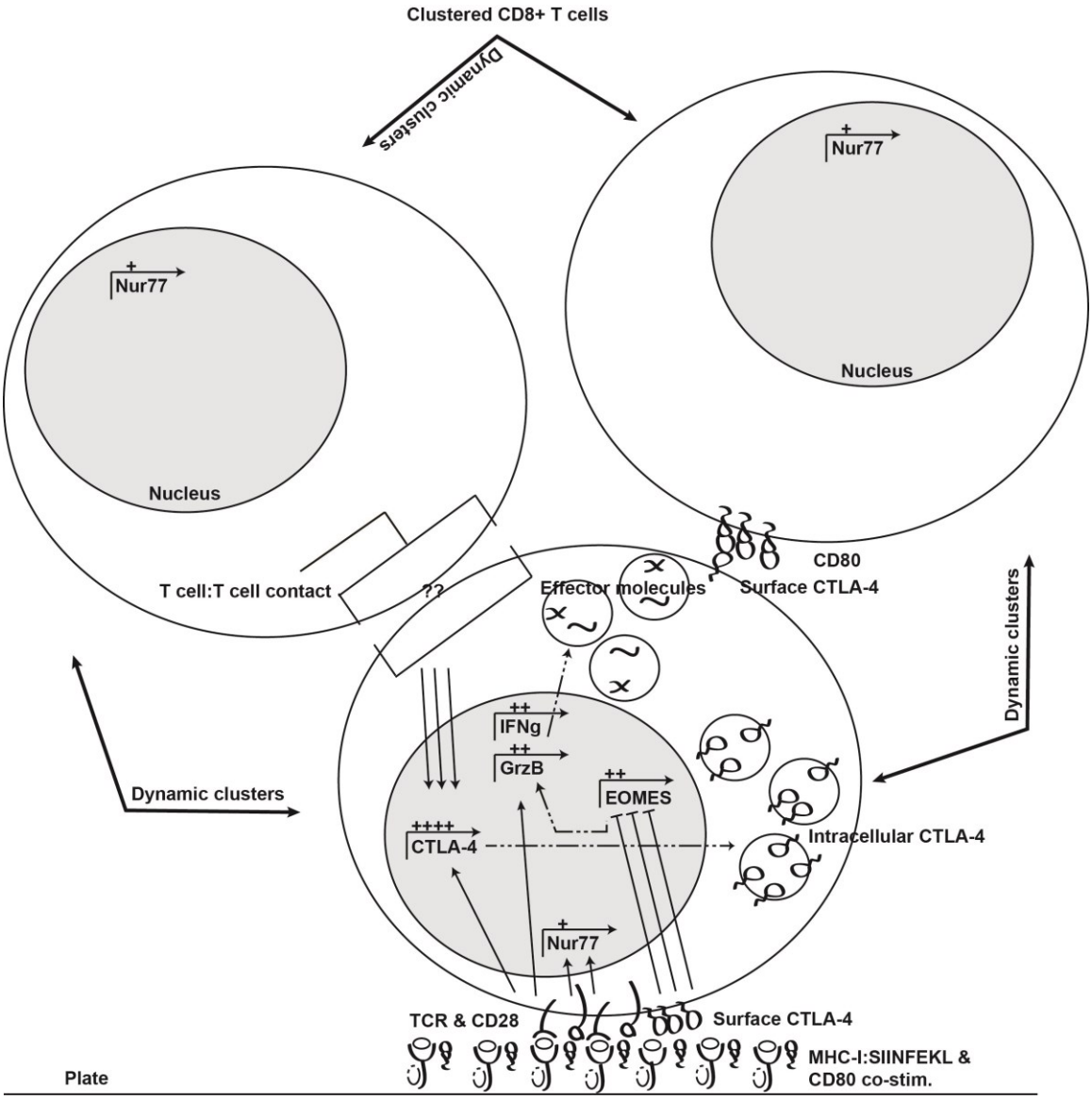
Clustered CD8+ T cells
Dynamic clusters
Nur77
Nucleus
Nur77
Nucleus
T cell:T cell contact
??
CD80
Surface CTLA-4
Effector molecules
Dynamic clusters
Dynamic clusters
IFNg
GrzB
EOMES
CTLA-4
Intracellular CTLA-4
Nur77
TCR & CD28
Surface CTLA-4
MHC-I:SIINFEKL &
CD80 co-stim.
Plate

Figure 3-15: Model of T cell:T cell cluster-induced effector regulation.

Clustered CD8+ T cells regulate effector function by two mechanisms. The first is via TCR stimulation. Clusters are dynamic and arranged in three-dimensional configurations (as evidenced by microscopy and denoted here with bold “dynamic clusters” arrows) and thus are not always in contact with plate bound antigen. These clusters decrease the amount of antigen sensed (as shown by Nur77 expression) and can therefore play a role in tempering effector molecule expression. T cell activation can also influence CTLA-4 expression. The second function of T cell clusters is immunosuppression through contact mediated upregulation of CTLA-4 (denoted by “T cell:T cell contact” (??)). The proteins and signaling mechanisms involved in this upregulation are unknown to date; however supportive evidence has been seen by Fearon and colleagues. This convergence of TCR triggering and T cell:T cell contact leads to an increase in CTLA-4 both intracellularly and at the T cell surface. CTLA-4 leads to EOMES inhibition and therefore the regulation of interferon-γ (IFNg) and granzyme B (GrzB). These regulation events are likely mediated between CTLA-4 on the T cell binding plate bound CD80 using this model; however we cannot completely rule out a T cell:T cell mediated regulation event even though it is difficult to assess. Our splenocyte activation data spectulates that a CD80:CTLA-4 inhibitory event mediated via T cell:T cell contact may occur because ICAM-1 KO T cells activated by splenocytes show normal CTLA-4 levels even though IFNg is increased. Since these T cells cannot cluster, it suggests that the CTLA-4 may not be able to inhibit IFNg production.

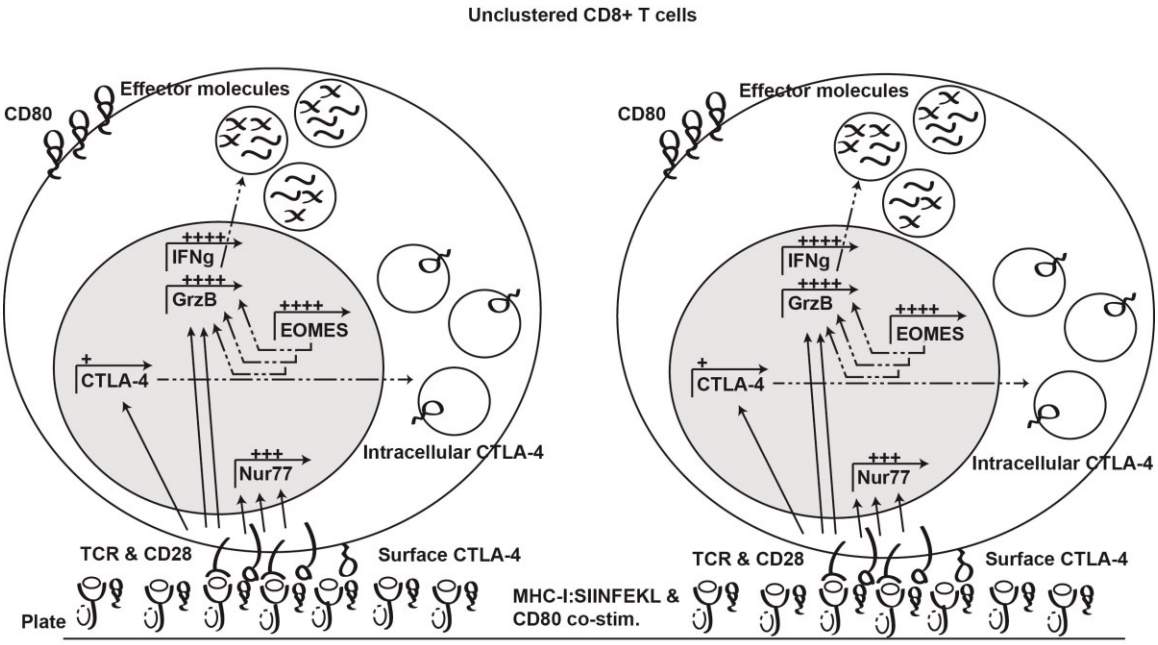

Figure 3-16: Model of effector function in unclustered T cells.

Unlike clustered CD8+ T cells, unclustered T cells are not able to regulate effector function as efficiently. Unclustered T cells sense more antigen than clustered T cells based upon Nur77 and multi-photon microscopy data. This TCR signal contributes to both increased effector molecule expression, as well as a certain amount of CTLA-4 expression. Since ICAM-1 KO T cells (or anti-LFA-1 (M17/4) blockade of wt T cells) disrupt the formation of clusters, we therefore do not observe contact dependent upregulation of CTLA-4. Because of the reduced CTLA-4 expression, unclustered T cells circumvent EOMES inhibition which in turn leads to higher levels of EOMES and increased downstream effector functions. Presumably, the surface CTLA-4 on unclustered T cells could promote some inhibition of EOMES through ligation of plate bound CD80; however, anti-CTLA-4 blockade does not alter IFNg expression on ICAM-1 KO T cells. Therefore, we speculate, that this potential ligation is not enough to induce inhibition, most likely because CTLA-4 expression is low.

CHAPTER 4: The kinetics of immune responses using ICAM-1 deficient CD8+ T cells during *in vivo* activation

INTRODUCTION

A typical CD8+ T cell response after antigenic encounter *in vivo* leads to the rapid generation of an army of effector T cell clones that peaks in total expansion at approximately the same time that the pathogen is cleared. After expansion, T cells contract to 5-10% of the peak T cell pool and persist as memory cells in the host (21, 23, 24). Here the T cells have the ability to quickly reactivate and respond to secondary antigen encounter. Memory T cells are present as a heterogeneous population and reside at many different sites, such as: lymph nodes, spleen, blood, bone marrow, and peripheral tissues (26, 144). Although not completely encompassing and rather simplistic, memory T cells have been historically divided into effector memory ($CD62L^{low}CCR7^{low}$) and central memory ($CD62L^{high}CCR7^{high}$) subsets. Effector memory cells rapidly exert effector functions such as IFNγ production; while, central memory cells are characterized more on the basis of proliferative capabilities but do, however, eventually exert effector functions (7, 25, 26, 144).

The programming of an effector T cell to become a memory T cell has been the topic of much debate. Currently, the dominating argument is that during activation and expansion, T cells are finely tuned to either take on the characteristics of terminal differentiation or memory precursor formation. This programming has been suggested to sprout from several different events over the course of priming, such as: antigen exposure, TCR:MHC-I/peptide strength, time of arrival at site of priming, concentration of third signal, and ligation of co-stimulation proteins to name a few (7, 19, 23). Parsing terminal differentiation from memory precursor formation is currently determined by the

expression of several surface markers, namely the IL-7 receptor α-subunit (CD127) and killer cell lectin-like receptor subfamily G member 1 (KLRG-1). T cells responding to model pathogens such as *Listeria monocytogenes* (LM) and lymphocyte chriomeningitis virus (LCMV) exhibit T cells falling into two major subgroups of CD127 and KLRG-1 expression kinetics. KLRG-1^{high}CD$127^{low\text{-}intermediate}$ are referred to as short-lived effector cells (SLECs) and KLRG-1^{low}CD127^{high} T cells are denoted as memory precursors (MPECs) (23, 26, 30-33). Over the course of infection double positive and double negative populations do arise; however, whether these cells are terminally differentiated, memory-like, hybrid-like, or a cell converting from one population to the other is unclear.

A central event to the production of a viable CD8+ T cell response and the formation of certain T cell subsets is a stable interaction between the T cell and the antigen-laden APC. These interactions, as stated previously, are primarily dependent upon ICAM-1 on an APC binding to LFA-1 integrin expressed by a T cell (75). Scholer *et al*. elegantly revealed that ICAM-1 on DCs is necessary for long-lasting T cell:DC conjugates *in vivo*. They went on to show using wt OT-I CD8+ T cells with targeted antigen delivery that activation, T cell expansion, and target cell killing was normal if ICAM-1 was not present on the DC; however, IFNγ production decreased if ICAM-1 was ablated on a DC (75). Additionally, those authors, as well as others have produced interesting findings demonstrating impairments in T cell memory formation if the APC lacks ICAM-1 (74, 75). Another, more recent study showed using a complete ICAM-1 KO that the ICAM-1 KO T cells that did persist at memory time points post LCMV infection showed a statistical increase in the amount that were SLECs (KLRG-1^{high}CD127^{low}). The authors claimed that ICAM-1, in general, is required for SLEC contraction; as well as, showed corroborate evidence that ICAM-1 (expressed by non T cells) participated in programming the T cell memory pool (76). The current Cox *et al*.

study also performed LCMV infections using wt or ICAM-1 KO hosts, sorted MPECs and SLECs at memory time points and adoptively transferred into new naïve hosts, challenged recipients with LM-gp33 (an LCMV protein), analyzed tetramer specific re-expansion, and discovered that ICAM-1 KO MPEC T cells showed reduced recall abilities (76). These studies did not experiment with T cell:T cell interactions *in vivo*; however, other laboratories have shown that T cell clusters can persist during antigen recognition (85-87, 89) and can even maintain at sites like the brain for extended periods of time (145).

Our objective was to utilize ICAM-1 KO OT-I T cells in an adoptive transfer model, so as to maintain the vital importance of ICAM-1 expression on APCs, to understand the necessity of ICAM-1 on a T cell during *in vivo* priming. Our data show that ICAM-1 is dispensable on T cells for the production of an immune response using both a LM-OVA and an antigen/adjuvant ear challenge model. Interestingly, the loss of ICAM-1 on T cells leads to increased KLRG-1 and granzyme B expression (to varying degrees) at certain time points after antigen/adjuvant administration under high transfer conditions. Additionally, we sought to use our *in vitro* generated ICAM-1 KO effector T cells as an anti-tumor immunotherapeutic approach to mouse melanoma and demonstrated that ICAM-1 KO T cells mediated tumor growth similar to wt OT-I T cells.

MATERIALS AND METHODS

Mice

ICAM-1 deficient mice (B6.129S4-ICAM1^{tm1Jcgr}/J) were generated as previously described (97) and purchased from The Jackson Laboratories (Jackson Laboratory, Bar Harbor, ME). They were backcrossed to the OT-I TCR transgenic on the C57BL/6 background (>10 generations). Colony bred wild-type OT-I mice were used as controls.

Recipient C57BL/6 mice were purchased from The Jackson Laboratories or the National Cancer Institute Mouse Repository (NCI-Frederick, Frederick, MD). Mice were housed and bred under specific-pathogen free conditions and generally used between the ages of 6-12 weeks. Procedures, involving mice, were approved by the Institutional Animal Care and Use Committee at the University of Minnesota – Twin Cities.

Cell preparation

Single cell suspensions of mouse spleens and lymph nodes were prepared by mashing tissues through cell strainers or using an Automated gentleMACS^{TM} Dissociator (Miltenyi Biotec, Auburn, CA) into phosphate buffered saline (PBS)/2% bovine serum. Cell counts were attained using a Countess® Automated Cell Counter (Life Technologies, Grand Island, NY). Purified CD8+ OT-I T cells were obtained by depleting non-CD8+ leukocytes and red blood cells from the bulk population with the following negatively selecting antibodies (FITC conjugated – anti-CD4, anti-B220, anti-CD16/CD32, anti-F4/80, anti-I-A^{b}, anti-Ter119, and anti-CD44 (eBioscience, San Diego, CA and BioLegend, San Diego, CA)), then incubated with anti-FITC microbeads (Miltenyi Biotec), and later applied to a MACS LS column (Miltenyi Biotec). The enriched product was generally ≥95% pure based upon CD8α+Vα2+ staining of 5-10x10^{4} T cells using a FACS Calibur (BD Biosciences, San Jose, CA).

Flow cytometry

For flow cytometry experiments, usually 1-5x10^{6} cells were stained in Hank's balanced salt solution (HBSS)/0.2% sodium azide/2% bovine serum (FACS buffer) for 30 minutes at 4° C. Surface antibody stains, unless stated, were performed at 1:100 dilutions. Antibodies of special interest include KLRG-1 (clone: 2F1, eBioscience) and CD127

(clone: SB/199, BioLegend). Samples were run and collected with a LSRII or Fortessa (BD Biosciences) and analyzed with FlowJo software (Tree Star, Inc., Ashland, OR).

Intracellular staining for flow cytometry

Intracellular (i.c.) staining for granzyme B (clone: GB11, Life Technologies) was performed per manufacturer's instructions using the BD Cytofix/Cytoperm kit (BD Biosciences). Briefly, T cells were stained with surface antibodies, washed with FACS buffer, fixed with 250 µLs of BD Cytofix/Cytoperm, and stored at 4° C for 20 minutes. Cells were then washed twice with 1X BD Perm/Wash buffer, anti-granzyme B added, and cells stored at 4° C. Granzyme B staining was generally performed at a 1:50 dilution for 60 minutes. At which time, cells were washed twice with 1x BD Perm/Wash buffer and resuspended in FACS buffer for flow cytometry.

In vitro T cell stimulation

In vitro activation conditions were designed similarly to previous studies (51, 127). DimerX H-2K^{b}:Ig fusion protein (BD Biosciences) was diluted to 2 µg/mL in sterile PBS and recombinant B7-1/Fc chimeric protein (R&D Systems) was diluted to 0.4 µg/mL in sterile PBS. Flat-bottomed microtiter 96-well plates (Sigma-Aldrich) received 50 µLs of each reagent and incubated for at least 2 hours at room temperature. Wells were washed twice with sterile PBS and once with alloclone media. Alloclone media was RPMI 1640 (Life Technologies) supplemented with 10% fetal calf serum, 4 mM L-glutamine (Mediatech, Inc., Manassas, VA), 0.1 mM nonessential amino acids (Mediatech, Inc.), 1 mM sodium pyruvate (Mediatech, Inc.), 100 U/mL penicillin and streptomycin (Mediatech, Inc.), 10 mM HEPES (Mediatech, Inc.), and 5 µM 2-Mercaptoethanol (Life Technologies). SIINFEKL (0.375 µg/mL) was loaded onto DimerX

H-2K^b:Ig fusion protein by adding 100 µLs/well. Plates were incubated at 37° C for at least 2.5 hours and then washed several times with alloclone. Purified wild-type or ICAM-1 deficient OT-I CD8+ T cells were added at a concentration of 5x10^4 cells/well in a total volume of 210 µLs alloclone supplemented with 0.05 µg/mL of IL-12 (R&D Systems). Plates were then incubated at 37° C until harvested at 24-, 48-, and 72-hour time points.

CFSE labeling

Carboxyfluorescein succinimidyl ester (CFSE; Life Technologies) labeling was performed by adding an equal volume of 10 µM CFSE to T cells (resuspended at 20x10^6/mL in PBS/5% bovine serum). The mixture was vortexed and labeling performed in the dark for 5 minutes. The cell mixture was washed three times with 20-35 mLs PBS/5% bovine serum. Cells were resuspended in PBS/2% bovine serum, counted, and brought to the necessary concentration for injection.

T cell adoptive transfer and LM-OVA infection

Low precursors (5x10^3) of purified wt or ICAM-1 KO OT-I T cells were adoptively transferred intraveneously (i.v.) into congenically different recipients. One day later, mice were infected i.v. with 1.7-3.3x10^3 colony forming units of virulent OVA-expressing *Listeria monocytogenes* (LM-OVA; a generous gift from Dr. Steve Jameson). The LM-OVA was cultured in LB broth supplemented with streptomycin sulfate until an O.D. reading of 0.06-0.1 was attained.

T cell adoptive transfer and antigen / adjuvant ear pinna challenge

High precursors (2.25-5x10^5) of wt or ICAM-1 KO OT-I T cells were adoptively

transferred i.v. into congenically different recipients. One day later, mice were anesthetized with a ketamine/xylazine mixture and challenged with a 10 µL volume of 3 µg OVA emulsified in Incomplete Freund's Adjuvant (IFA; Sigma-Aldrich, St. Louis, MO) into ear pinna. Emulsions were prepared by mixing IFA and PBS/OVA using glass syringes (Popper and Sons, Inc., New Hyde Park, NY) and rapidly freeze thawing multiple times. Emulsifications were transferred from glass syringes into insulin syringes for injections.

B16-OVA melanoma culture, transplantations, and tumor measurements

B16-OVA cells were cultured in alloclone media containing 250µg/mL G418 (Mediatech, Inc.). Cells were thawed, plated, stored in a 37° incubator, and split every couple days. Cells were transplanted into the flank of mice at a concentration of $2x10^5$/injection in PBS. Nine days later 1-$2x10^6$ day three activated wt or ICAM-1 KO effector OT-I T cells were injected i.v. Tumor size was measured (length x width) in mm^2 using calipers at each time point during the experiment.

Statistics

GraphPad Prism version 5.03 software (GraphPad Software, Inc., La Jolla, CA) was utilized to determine statistical significance using Student's unpaired two-tailed *t* test. P value cutoffs and notation were used as follows (unless otherwise denoted in figure captions): *, p value<0.05; **, p value<0.01; ***, p value≤0.0008.

RESULTS

In vitro generated ICAM-1 KO effectors control melanoma burden equal to wt

Adoptive T cell therapy for tumor control was pioneered by Steven Rosenberg's

laboratory over the course of the last several decades and essentially consists of isolating tumor infiltrated lymphocytes (TILs) from tumor, expanding the T cells *ex vivo,* and transfusing the cells back into patients with varying levels of clinical success (146). We speculated that ICAM-1 KO T cells which do not cluster *in vitro* (Fig. 2-6C) but show elevated effector functions (Fig. 3-2A-D) would be prime candidates for anti-tumor adoptive T cell therapy. Using a C57BL/6-derived melanoma cell line expressing the model antigen ovalbumin (B16-OVA), we sought to determine whether activated ICAM-1 KO OT-I CD8+ T cells could regulate tumor better than wt CD8+ OT-I T cells. We transplanted roughly $2x10^5$ B16-OVA cells subcutaneously into the flank of recipient mice and nine days later tumors were measured, mice allocated into groups, and later injected with $1\text{-}2x10^6$ day three activated effector wt or ICAM-1 KO T cells. Tumor burden was measured (in mm^2) with calipers every several days and mice were sacrificed when control (no T cell transfer) tumors were deemed unhealthy. Based upon the tumor growth curves there was control in the T cell transfer conditions and no tumor regulation in the control group (Fig. 4-1[1]). Indeed, there was not a statistical significance between the wt and the ICAM-1 KO transferred conditions.

ICAM-1 KO T cells prime similar to wt T cells after low transfer / in vivo bacterial challenge

The majority of our data utilizing ICAM-1 KO T cells has been performed *in vitro* where T cell clusters have been monitored consistently. Thus, our new objective was to track immune responses *in vivo* using ICAM-1 KO T cells in order to understand the importance of ICAM-1 expression on T cells during activation and expansion to an immunological insult *in vivo*. The majority of previous studies have not adequately pursued this question, either because entire ICAM-1 KO hosts have been used (74, 76),

memory ICAM-1 KO T cells have been transferred into wt mice after being primed in an ICAM-1 deficient environment (76), or wt OT-I T cells have been transferred into ICAM-1 KO hosts in order to address this issue from the opposite perspective (75). We sought to illustrate the necessity of ICAM-1 on a T cell, while keeping ICAM-1 present on APCs in our wt recipient mice.

Our experimental setup consisted of adoptively transferring low physiologically relevant precursor numbers ($5x10^3$) of wt or ICAM-1 KO OT-I T cells intravenously (i.v.) into recipient mice. One day later, host mice were challenged i.v. with virulent Gram-positive *Listeria monocytogenes* expressing ovalbumin (LM-OVA) and the immune response monitored over the course of infection. Using this model pathogen, laboratories have determined that antigen is cleared within 10 days after infection (147). After *in vivo* T cell stimulation, we did not observe differences in the number of T cells recovered (Fig. 4-2A) or effector function, analyzed via granzyme B production (Fig. 4-2B-C) between the wt and ICAM-1 KO T cells at days 6 and 19 post infection. Additionally, there did not appear to be a statistically significant difference in the percentage of MPEC or SLEC populations produced between the wt and ICAM-1 KO T cells at 6 and 19 days post challenge (Fig. 4-2D-E). This data suggests that (under physiological contexts) ICAM-1 on T cells is not necessary for T cell activation, function, and differentiation *in vivo*. More interesting, this data suggests that ICAM-1 KO T cells do not display the same phenotypes between purified single cultures *in vitro* and complex *in vivo* priming conditions. The *in vivo* data complements the mixed culture conditions in which wt and ICAM-1 KO OT-I T cells were cultured together (Fig. 3-5). Based on our current data, we speculate that ICAM-1 KO T cells are interacting with wt (ICAM-1 sufficient) antigen-specific endogenous T cells and potentially clustering because co-clustering can occur *in vitro* (Fig. 3-4A-C).

ICAM-1 KO T cells show differential responses compared to wt T cells after high transfer / antigen / adjuvant ear pinna administration

Our bacterial challenge data suggests that ICAM-1 deficient T cells can respond similarly to wt T cells at low precursor frequencies. This normal response from the ICAM-1 KO OT-I T cells may be due to the ability of the endogenously responding (ICAM-1 sufficient) T cells to expand and form co-clusters with the ICAM-1 KO T cells. Harty and colleagues have shown that titrating increased numbers of precursors into recipients can actually dampen the endogenous response because the adoptively transferred T cells are overwhelming the low endogenous precursors from becoming activated and responding efficiently (1). Thus, we presumed that increasing the precursor number, as well as swapping OVA antigen / Incomplete Freund's Adjuvant (IFA) for virulent LM-OVA, we would be able to not only overwhelm the endogenous response, but also limit the amount of endogenous T cell precursors responding because the mouse is being challenged by a single protein as opposed to a live bacterial infection.

Using a non-soluble antigen deposition (OVA / IFA) ear pinna administration model allowed us to contain the immune response to a single cervical draining lymph node. At day -1, 2.25-5x10^5 OT-I T cells were adoptively transferred i.v. into separate hosts followed by an ear injection of 3 μg OVA emulsified in IFA one day later. Early time points (days 1-4 post challenge (p.c.)) showed similar division between wt and ICAM-1 KO T cells using cell dye dilution (Fig. 4-3A). At day 5 p.c., ICAM-1 KO and wt OT-I T cells showed similar expansion profiles (Fig. 4-3B-C). Expansion kinetics did show some variability between wt and ICAM-1 KO T cells; however, ICAM-1 KO T cells were almost always equal or greater in expansion when compared to wt T cells. Responses occurring after days 4-5 p.c. showed an increase in KLRG-1 expression in

the ICAM-1 KO T cell subset compared to wt in the draining lymph node, spleen, and ear (Fig. 4-3D). At early time points (days 4-5) using this model, KLRG-1 expression is quite low on activated T cells. Granzyme B production was also, for a brief time, increased in the ICAM-1 KO subset compared to wt around day 5 p.c. in the draining lymph node and spleen, but not at the site of challenge in the ear (Fig. 4-3E). Both KLRG-1 and granzyme B expression kinetics displayed some variability among multiple experiments. This data suggests that ICAM-1 deficiency can lead to earlier KLRG-1 and granzyme B expression kinetics, as well as maintained surface KLRG-1 expression, when the endogenous response is potentially overwhelmed by increased initial OT-I precursors. This suggests that ICAM-1 on T cells may help to mediate immune responses *in vivo*.

DISCUSSION

Here we show the role of T cell expressed ICAM-1 during *in vivo* priming and tumor control. Using a bacterial infection model we demonstrate the dispensability of ICAM-1 on T cells for proper priming, activation, acquisition of effector function, and memory generation. However, combining a high transfer and single antigen priming method (which could lead to a response where the transferred cells are the major responders, thereby potentially altering the wt endogenous response and presumably decreasing wt endogenous T cell:ICAM-1 KO T cell clusters) suggests a role for ICAM-1 on T cell differentiation during priming *in vivo*. Finally, highly effective ICAM-1 KO T cells generated *in vitro* do not control mouse melanoma better than clustered wt T cells upon adoptive transfer into tumor bearing recipients; however, we have not adequately tested tumor control between wt and ICAM-1 KO T cell subsets at lower transfer numbers.

Tumor control is not augmented by the lack of ICAM-1 on transferred three day stimulated T cells. Our original speculation, since unclustered ICAM-1 KO T cells can

kill *in vitro* peptide-pulsed thymoma target cells better than wt T cells, that ICAM-1 KO T cells would also be able to contain *in vivo* tumors better than wt. Therefore, we performed tumor control experiments at two different T cell transfer concentrations and determined that there was no difference between the capacity of wt and ICAM-1 KO T cells to regulate tumor growth. It is important to denote that transfer experiments designed to observe T cell maintenance in naïve mice shown in Chapter 3 were performed with day two activated T cells. ICAM-1 KO T cell maintenance kinetics, although diminished compared to wt when activated for two days in culture, were not adequately examined if primed *in vitro* for three days. However, if similar decreased maintenance was observed between day two and day three in the ICAM-1 KO T cells compared to wt under no antigen conditions, then the ICAM-1 KO T cells may have an increased ability to control tumor burden on a per cell basis. Essentially, these data set up the future testing of the hypothesis that primed ICAM-1 KO T cells can control tumor better than wt T cells on a per cell basis. Experimentally, the tumor and maintenance assays are fundamentally different in the sense that antigen is completely absent in the maintenance experiments whereas antigen is obviously present in the tumor mice. Due to the variability among T cell recovery in our tumor experiments, as well as the necessity of separate transfers to understand tumor control, we were not able to clearly gauge whether wt and ICAM-1 KO T cells behaved similarly in tumor bearing mice. The ability to control tumor burden in the ICAM-1 KO T cell transfer condition confirms that ICAM-1 expressed on a T cell surface is not required for migration of T cells to tumor sites.

Much work is being performed to understand the important components needed for optimal CD8+ T cell effector generation. Studies have shown that central memory T cells actually work better at controlling tumor compared to more terminally differentiated

effector memory T cells (146, 148-150). It would be interesting to perform experiments with IL-15 supplemented to the *in vitro* cultures in order to facilitate central memory generation, with the intention of assessing tumor control after central memory T cell transfers. Additionally, we could extend these studies by transferring fewer than $1x10^6$ activated T cells. We hypothesize that we might be able to parse out tumor burden differences between wt and ICAM-1 KO transfers if we decrease the amount of T cells transferred since ICAM-1 KO T cells can kill better on a per cell basis *in vitro*. Even though ICAM-1 KO T cells display enhanced effector function at two and three days post *in vitro* priming, this may not correlate with increased effector abilities after T cell transfer due to environmental differences *in vivo*. Fine tuning cluster disruption *in vitro* for tumor control may hold promise for anti-tumor immunotherapeutics if an efficacious transfer number and relevant tumor model can be utilized.

Understanding the importance of ICAM-1 on T cells during *in vivo* stimulation is crucial for translating our *in vitro* findings to clinical fruition. We employed a bacterial model expressing our model antigen (LM-OVA) to assess the role of T cell expressed ICAM-1 on activation, expansion, effector function, and memory formation. Data from Cox *et al.* show that tetramer specific ICAM-1 KO T cells primed in an ICAM-1 KO host have increased IFNγ production and increased KLRG-1^{high}CD127^{low} T cells at memory time points after acute LCMV infection (76). Thus, we performed similar experiments using LM-OVA. Our observations detailed that effector function (assessed by granzyme B staining) and KLRG-1 expression was similar among wt and ICAM-1 KO T cells at different time points. We also observed comparable memory formation. Cox *et al.* observed KLRG-1 surface expression differences extending out to a time point greater than 150 days p.i (76). These dissimilar results could be due to the lack of ICAM-1 on the APC in their experiments or the infectious agent used to perform the experiments

(LM versus LCMV) which promote an IL-12 (53) or a type I interferon response (54), respectively. Furthermore, we speculate that there is not an observed effector difference between our wt and ICAM-1 KO transfers using this model for two reasons. First, a pathogen such as LM-OVA will induce a large endogenous response that will lead to an army of different T cell clones (in addition to the transferred OT-I T cells) primed to combat the infection. Secondly, we transferred a small number of precursors, thus the ability of ICAM-1 KO T cells to potentially co-cluster under these conditions with endogenously responding T cells is favorable. In order to address these caveats on the *in vivo* T cell activation environment that would limit the endogenously responding T cell clones, we decided to employ a high transfer system in combination with a single protein (OVA) emulsified in adjuvant (IFA) for challenge.

We used this same model in order to overwhelm the endogenous response and potentially ablate as many endogenous wt T cell:ICAM-1 KO OT-I T cell clusters as possible. We did not assess clustering ability via multi-photon microscopy with the ICAM-1 KO T cells using this model system; however, this is an important objective to address in the near future. When ICAM-1 KO T cells were analyzed after OVA / IFA challenge, we observed that ICAM-1 KO T cells expressed an increased amount of both KLRG-1 and granzyme B at certain time points when compared to wt T cells. This result did show some variability from experiment to experiment and the differences in timing may be partially due to the technical difficulty of maintaining a consistent 10 µL injection into the ear pinna. Nonetheless, this result demonstrates that ICAM-1 on activated T cells plays a role in tempering the immune response of primed CD8+ T cells. The enhanced effector function demonstrated herein corroborates the IFNγ findings by Cox *et al* in complete ICAM-1 KO hosts (76). We speculate that when you presumably minimize T cell clustering ability *in vivo* by utilizing high transfer methods and single

protein immunizations that effector function and terminal differentiation can be altered at particular tissue sites for a short period of time. Once these activated T cells (wt or ICAM-1 KO) migrate to the site of immunization (antigen deposition), the ear, we observe no differences in granzyme B expression even though KLRG-1 differences are still observed. This would suggest that SLEC and MPEC populations can be tuned by T cell:T cell contact. We can speculate that during expansion, ICAM-1 KO T cells are not able to bind other ICAM-1 KO T cells that are activating and thus cannot temper effector functions. Multi-photon imaging will need to be used to investigate this hypothesis that might predict that high transfer frequencies can indirectly influence KLRG-1 and granzyme B *in vivo* in ICAM-1 KO T cells by altering wt (ICAM-1 sufficient) responses and/or co-clustering kinetics.

FOOTNOTES

[1] Dr. Eisuke Domae (former post-doctoral fellow in Dr. Yoji Shimizu's laboratory, University of Minnesota – Twin Cities, Minneapolis, MN) provided help with tumor transplantation and tumor growth measurements.

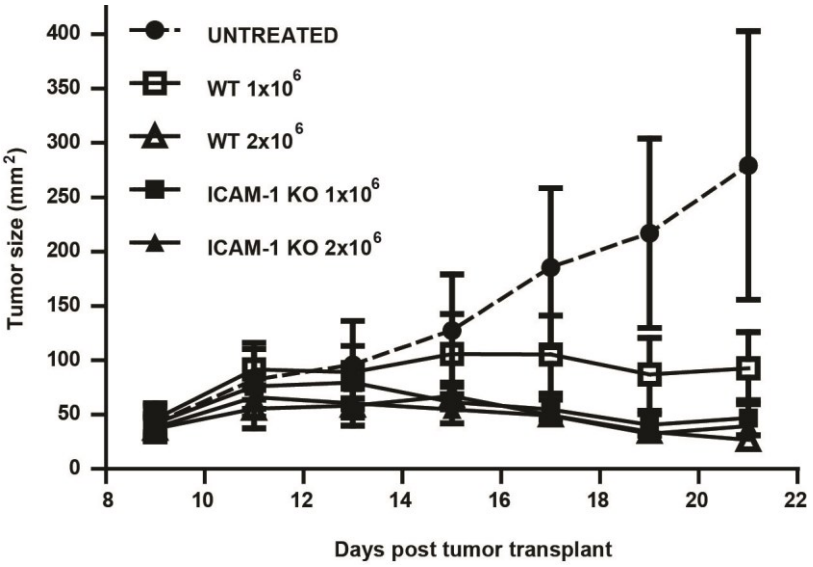

Figure 4-1: Activated ICAM-1 KO effector T cells control tumor burden similar to wt T cells after adoptive transfer.

B16-OVA melanoma cells ($2x10^5$) were injected subcutaneously into recipient mice at day 0. Day 3 *in vitro* activated wt or ICAM-1 KO OT-I CD8+ T cells ($1x10^6$ or $2x10^6$) were adoptively transferred intravenously into tumor bearing mice at day 9. Palpable tumors were grouped so that each condition had similar average tumor sizes before T cell transfer. Tumors were measured starting at day 9 and every other day for the course of the experiment using calipers. Statistical significance (Student's unpaired two-tailed *t* test) was not reached at any time point between wt and ICAM-1 KO $1x10^6$ transfer conditions.

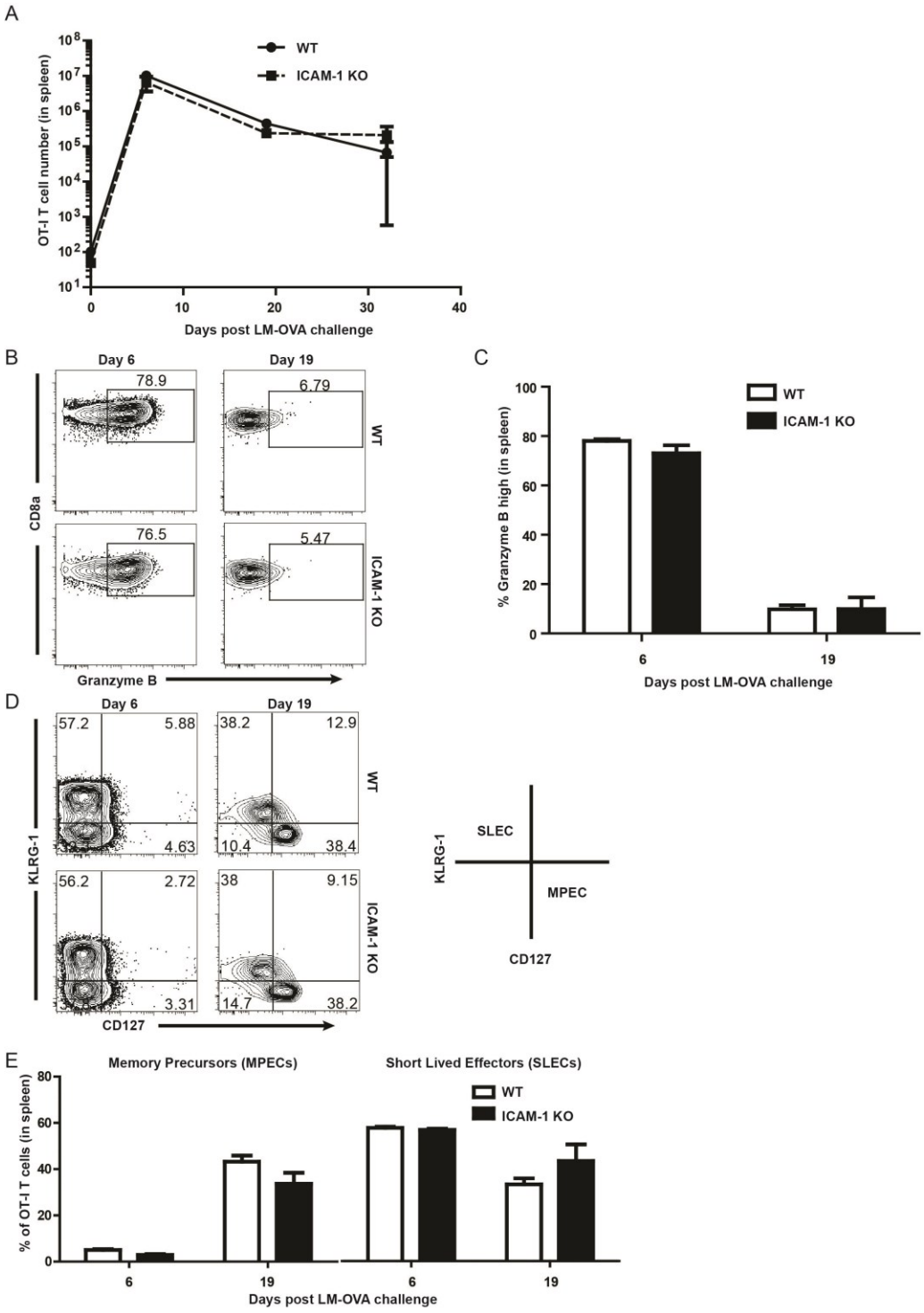
A
WT
ICAM-1 KO
OT-I T cell number (in spleen)
Days post LM-OVA challenge
B
Day 6
Day 19
78.9
6.79
76.5
5.47
WT
ICAM-1 KO
CD8a
Granzyme B
C
WT
ICAM-1 KO
% Granzyme B high (in spleen)
Days post LM-OVA challenge
D
Day 6
Day 19
57.2
5.88
4.63
38.2
12.9
10.4
38.4
56.2
2.72
3.31
38
9.15
14.7
38.2
KLRG-1
CD127
SLEC
MPEC
E
Memory Precursors (MPECs)
Short Lived Effectors (SLECs)
WT
ICAM-1 KO
% of OT-I T cells (in spleen)
Days post LM-OVA challenge

Figure 4-2: ICAM-1 KO T cells respond to LM-OVA infection similarly to wt T cells.

Low precursor frequencies of wt or ICAM-1 KO OT-I CD8+ T cells ($5x10^3$) were adoptively transferred intravenously (i.v.) into recipient mice. One day later, mice were infected with virulent LM-OVA i.v. (*see materials/methods*). **(A)** Response curve of wt and ICAM-1 KO OT-I T cells to LM-OVA in separate hosts. **(B-C)** Representative example and quantification of effector function, assessed by granzyme B production *in vivo*, for wt and ICAM-1 KO T cells at days 6 and 19 post LM-OVA infection. **(D-E)** Representative example and quantification of memory precursors (MPECs; KLRG-$1^{low}CD127^{high}$) and short lived effector cells (SLECs; KLRG-$1^{high}CD127^{low}$) at 6 and 19 days post bacterial infection. Statistical significance (Student's unpaired two-tailed *t* test) was not achieved between the wt and ICAM-1 KO MPEC or SLEC percentages at days 6 and 19 post infection.

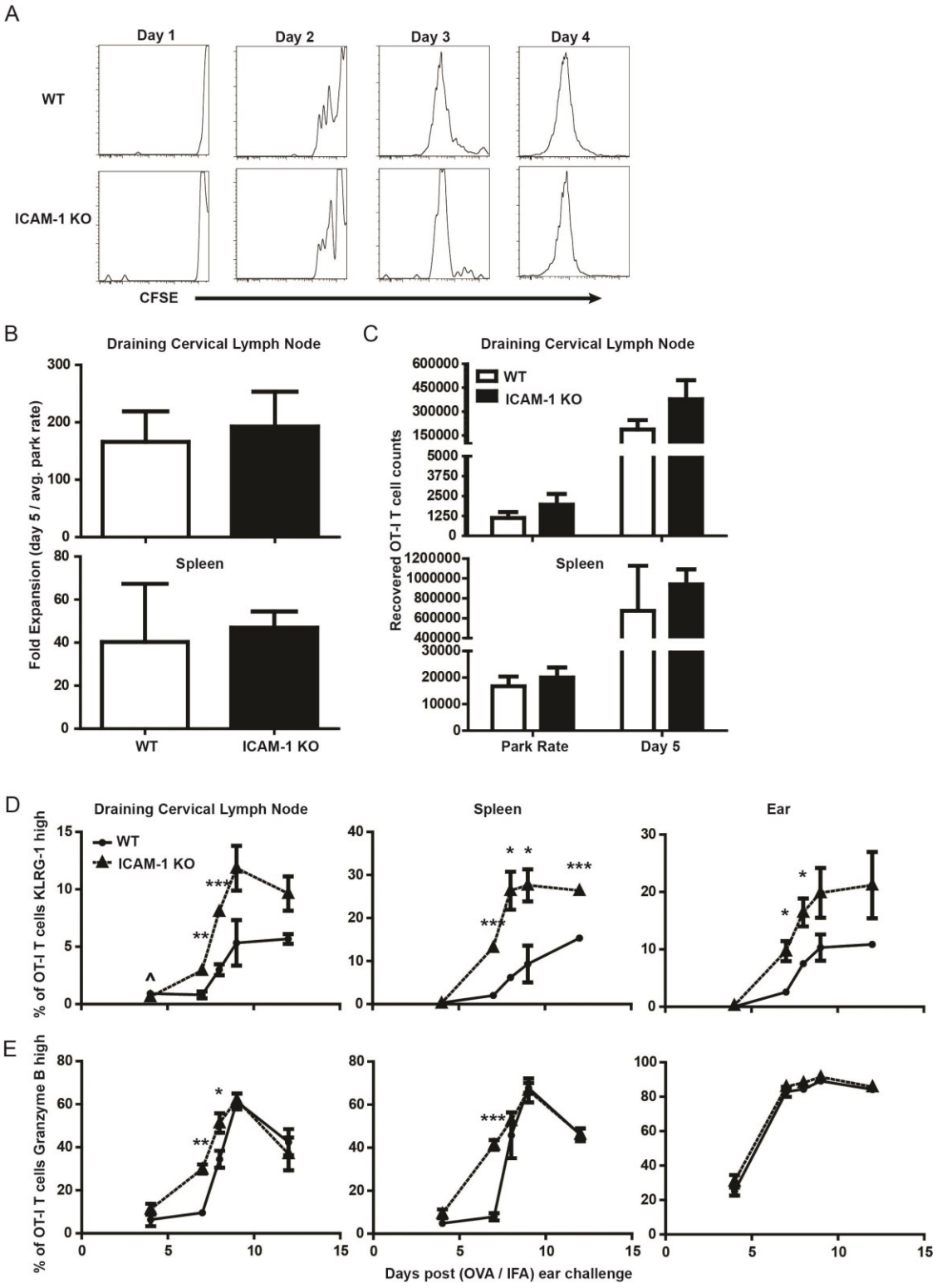
A
Day 1
Day 2
Day 3
Day 4
WT
ICAM-1 KO
CFSE
B
Draining Cervical Lymph Node
Fold Expansion (day 5 / avg. park rate)
Spleen
WT
ICAM-1 KO
C
Draining Cervical Lymph Node
WT
ICAM-1 KO
Recovered OT-I T cell counts
Spleen
Park Rate
Day 5
D
Draining Cervical Lymph Node
Spleen
Ear
% of OT-I T cells KLRG-1 high
E
% of OT-I T cells Granzyme B high
Days post (OVA / IFA) ear challenge

Figure 4-3: ICAM-1 KO T cells show increased KLRG-1 and granzyme B expression after adjuvant / antigen administration into ear pinna

High precursor frequencies of wt or ICAM-1 KO OT-I CD8+ T cells were adoptively transferred intravenously into recipient mice. One day later, mice were challenged with OVA emulsified in IFA (OVA/IFA) into ear pinna (*see materials/methods*). **(A)** CFSE labeled wt or ICAM-1 KO OT-I CD8+ T cells ($2.25\text{-}3.25 \times 10^5$) were transferred and division was monitored 1-4 days post OVA/IFA challenge. Data represents one of two independent dye-labeled experiments. **(B-C)** Approximately 5×10^5 wt or ICAM-1 KO OT-I T cells were transferred and challenged with OVA/IFA. Draining cervical lymph node and spleens were harvested at day 5 and compared to park rate for evaluating fold expansion. Cell numbers of recovered OT-I T cells were also obtained in both tissues. **(D)** KLRG-1 expression and **(E)** granzyme B intracellular expression was also monitored during the response to OVA/IFA by both wt and ICAM-1 KO OT-I T cells. Data represents one of at least four independent experiments ranging in initial OT-I precursor frequency ($2.25\text{-}4 \times 10^5$ cells/injection). Statistical analysis for this experiment was performed using Student's unpaired two-tailed *t* test and comparing the wt T cells to the ICAM-1 T cells with an n=3 mice for each time point (*, p value<0.05; **, p value<0.01; ***, p value≤0.0008; ^, p value<0.05 in the favor of the wt T cells).

CHAPTER 5: CONCLUSION

Understanding the communication systems by which cells of the immune system have evolved to interact with one another is proving to be increasingly complex. The simple idea of T cells interacting with APCs to become primed (151), then interacting with B cells (if a follicular helper CD4+ T cell) to augment humoral immunity (122), and then interacting with an infected target cell (if an effector CD8+ T cell) to clear pathogen (24, 152) is quite minimalistic and does not illustrate a major interaction that has been observed for at least 25 years. T cells are not only interacting with other completely different leukocyte subsets, but they are readily interacting with other antigen experienced T cells (82-89). Recent studies, including the experiments outlined in this dissertation, attempt to understand the necessity of T cell activation clusters and the adhesion molecules that facilitate them. Although evidence for T cell clustering has been around for more than two decades, there has not been precedence to understand the role that activated CD4+ or activated CD8+ T cells might have on one another. Studies looking at how different leukocyte populations co-exist currently overwhelm the literature, but understanding the impact that adjacent CD8+ T cells have on each other during priming is understudied. Thus, we sought to contribute to this gap in knowledge, with the objective of determining whether CD8+ T cell activation clusters play a role in either augmenting or dampening a T cell response. Our data, taken together, supports the hypothesis that CD8+ T cell clusters generated during initial stimulation dampen effector responses and help tune the differentiation of CD8+ T cells.

The results outlined in Chapter 2 contribute to the lack of current knowledge in regards to the adhesive and migratory functions of the integrin ligand, ICAM-1, on the T cell. ICAM-1 was found to be rapidly upregulated after activation in a manner similar to

the early activation marker CD69. Speculatively, the rapid expression of these molecules might be controlled by similar TCR-mediated mechanisms. Thus, the downregulation of $S1P_1$ by CD69 (138) (which suppresses lymph node egress) complements ICAM-1 upregulation which facilitates firm adhesion to other activated T cells, thereby potentially also disrupting lymph node emigration. These two early activation biomarkers, in concert, may play a synergistic role in maintaining T cells at the site of priming for a necessary amount of time.

ICAM-1 was found not to be critical for binding to antigen-pulsed APCs, even though it was completely necessary for promoting T cell:T cell conjugates. This generates the hypothesis as to whether ICAM-1 on a T cell acts as an environmental sensor of lymphocyte density in an activated lymph node with the speculation that in the absence of ICAM-1, T cells might divide more robustly because the environmental gauge that monitors lymphocyte density is ablated. This question is open to further experimental exploration. Based upon steady state T cell profiles, we might have expected an increased proportion of $CD44^{high}$ homeostatically proliferated (131, 132) ICAM-1 deficient CD8+ T cells compared to wild-type; however, this is not the case. Under inflammatory conditions with the antigen/adjuvant ear challenge assays, we most readily recovered similar numbers or increased numbers in the cervical lymph nodes of the ICAM-1 deficient transfers; this result may lend early support to this new environmental sensing hypothesis.

In Chapter 3 we demonstrate that unclustered T cells have augmented effector abilities compared to clustered T cells. We obtained similar results showing that unclustered T cells have an enhanced effector response using both ICAM-1 deficient OT-I T cells and a cluster disrupting anti-LFA-1 antibody with wild-type OT-I T cells. Utilizing wild-type T cells with a blocking antibody is clinically relevant for translational

research in regards to optimizing *in vitro* stimulation conditions in the *ex vivo* expansion of tumor specific lymphocytes obtained from resected tumors for infusion back into cancer patients (146).

In this chapter we also showed two mechanisms by which effector function can be tempered by CD8+ T cell clustering. One mechanism is via decreased antigen sensing because the nature of a T cell cluster (at least *in vitro*) actually allows for a physical separation from plate bound antigen and thus a decrease in an acquired antigen signal. Whether or not this physical separation from antigen occurs *in vivo* is still unknown. However, when T cells expressing ICAM-1 cluster and swarm around an APC in an activated lymph node some activated T cells will be more proximal to antigen compared to others and thus there could be instances in which physical separation from antigen might occur. The second mechanism of interest is one in which contact mediated CTLA-4 expression is increased on clustered T cells, similar to very recent observations by Fearon and colleagues (67), thereby leading to the known downregulation of EOMES which dampens IFN-γ and granzyme B expression (70, 71). Purified ICAM-1 deficient T cells *in vitro* have decreased CTLA-4 and therefore increased EOMES, IFN-γ, granzyme B, and target cell killing.

Since the co-stimulatory reagents B7-1 and B7-2 are adsorbed to the plate for *in vitro* T cell activation, we are not able to state definitely that effector dampening is mediated via CTLA-4:B7 interactions between interacting T cells because the T cell expressed CTLA-4 could also be binding to the B7 molecules on the plate and inducing an inhibitory signal via that route. Additionally, as mentioned in the introduction, a "ligand-independent" model for CTLA-4 inhibitory signals may occur (63); thus the increased amount of wild-type expressed CTLA-4, compared to ICAM-1 deficient T cells, may not even need to be ligated for inhibition of EOMES to occur at least in the purified

T cell cultures. However, the splenocyte activation experiments (Fig. 3-14) showing enhanced effector function on the ICAM-1 deficient T cells even when CTLA-4 levels were comparable to wild-type does not support the “ligand-independent” model of inhibition.

The data illustrated in Fig 3-14 supports the idea that contact mediated upregulation of CTLA-4 on T cells can also be driven by the APC (supporting Fig. 2-3D showing that ICAM-1 deficient T cells do not show defects in binding to antigen-laden APCs compared to wild-type), but the regulation of effector responses still may be controlled by T cell:T cell contact because the ICAM-1 deficient T cells can still not bind one another. We hypothesize that spiking wild-type OT-I T cells into these splenocyte activation cultures would lead to a similar phenotype seen with the mixed cultures of purified T cells which demonstrated that when ICAM-1 deficient T cells co-cluster with wild-type T cells the effector differences are minimized.

Interestingly, the ovalbumin expressing *Listeria monocytogenes* (LM-OVA) infections, shown in Chapter 4, also correlate with the mixed culture studies because it essentially mimics the situation *in vivo* when low precursors of ICAM-1 deficient T cells are transferred and expand in the presence of many LM-OVA antigen specific endogenous (ICAM-1 sufficient) CD8+ T cells. As expected when this study is performed, we do not see differences in MPEC or SLEC skewing, nor do we see differential granzyme B staining between the wild-type and ICAM-1 deficient T cell subsets. However, adoptively transferring high frequencies of ICAM-1 deficient or wild-type OT-I T cells and challenging with antigen/adjuvant in the ear leads to an increase in both the proportion of KLRG-1 expressing T cells and granzyme B expressing T cells in the ICAM-1 deficient subset. We speculate that using a high transfer and single antigen priming strategy could lead to a response whereby the transferred cells are the major

contributors to an immune response and thereby potentially alter the endogenous response (1). If this assumption is valid, our observed phenotype makes sense because increased effector function would correlate with lack of clustering and a lack of T cell:T cell regulation. Presumably, by transferring a high number of ICAM-1 deficient T cells, the potential for clustering with activated endogenous CD8+ T cells is reduced. Further experimentation, particularly effector kinetics with titrations in transfer number and multi-photon microscopy, is needed to definitively validate this hypothesis.

This thesis presents data that supports a role for T cell clusters in dampening CD8+ T cell responses. Clinically, it begs the question whether these clusters can be manipulated *in vivo*. Anti-integrin therapy seems like a plausible option; however, it comes with many risks as evidenced by the withdrawal of the humanized anti-CD11a antibody efalizumab from the market in 2009 (153). Additionally, cellular side effects of anti-integrin antibody treatment may include alterations in both T cell trafficking, as well as APC binding kinetics. Another option may be to inject soluble ICAM-1 (sICAM-1), in the hopes of augmenting a CD8+ effector T cell response by disrupting clusters via saturating ICAM-1 binding sites on LFA-1 so that T cell expressed ICAM-1 cannot ligate LFA-1. This option comes with the caveat that increased sICAM-1 could promote heart disease (98-101), cystic fibrosis (115), multiple sclerosis (116) to name a few. Taking the example of vascular disease and the correlation that high levels of sICAM-1 appear to prognosticate atherosclerotic lesion size (98-101), one might speculate that the sICAM-1 is disrupting T cell clustering during activation and as a result lead to increased IFN-γ produced by effector CD8+ T cells at the site of the lesion, thereby directly influencing lesion size. The link between IFN-γ and cardiovascular disease has been studied and is widely accepted (154). This is another potential area of future study in order to not only understand if CD8+ T cells play a role in heart disease, but to possibly

link T cell clusters, increased sICAM-1, and IFN-γ with a disease that is regarded as the number one killer in the United States.

This dissertation provides a mechanistic framework for the understudied but readily observed phenomenon of T cell:T cell clustering during priming. These studies have laid the groundwork for future *in vivo* experimentation, particularly using multi-photon microscopy to visualize clustering for correlation to effector ability. It also suggests that another layer of immunoinhibition and antigen acquisition results from T cell:T cell crosstalk (or the lack thereof). At the very least, T cell activation clusters do indeed play a crucial role in regulating CD8+ T cell effector responses. Thus, harnessing the knowledge obtained from understanding the temporal and spatial requirements for clustering both *in vitro* and *in vivo* may prove extremely advantageous for future vaccine development and immune-based anti-tumor therapeutics.

REFERENCES

1. Badovinac, V. P., J. S. Haring, and J. T. Harty. 2007. Initial T cell receptor transgenic cell precursor frequency dictates critical aspects of the $CD8^+$ T cell response to infection. *Immunity* 26: 827-841.

2. Blattman, J. N., R. Antia, D. J. Sourdive, X. Wang, S. M. Kaech, K. Murali-Krishna, J. D. Altman, and R. Ahmed. 2002. Estimating the precursor frequency of naive antigen-specific CD8 T cells. *J. Exp. Med.* 195: 657-664.

3. Bousso, P., A. Casrouge, J. D. Altman, M. Haury, J. Kanellopoulos, J. P. Abastado, and P. Kourilsky. 1998. Individual variations in the murine T cell response to a specific peptide reflect variability in naive repertoires. *Immunity.* 9: 169-178.

4. Casrouge, A., E. Beaudoing, S. Dalle, C. Pannetier, J. Kanellopoulos, and P. Kourilsky. 2000. Size estimate of the alpha beta TCR repertoire of naive mouse splenocytes. *J. Immunol.* 164: 5782-5787.

5. Kedzierska, K., E. B. Day, J. Pi, S. B. Heard, P. C. Doherty, S. J. Turner, and S. Perlman. 2006. Quantification of repertoire diversity of influenza-specific epitopes with predominant public or private TCR usage. *J. Immunol.* 177: 6705-6712.

6. Pewe, L. L., J. M. Netland, S. B. Heard, and S. Perlman. 2004. Very diverse CD8 T cell clonotypic responses after virus infections. *J. Immunol.* 172: 3151-3156.

7. Stemberger, C., M. Neuenhahn, V. R. Buchholz, and D. H. Busch. 2007. Origin of CD8+ effector and memory T cell subsets. *Cell Mol. Immunol.* 4: 399-405.

8. Obar, J. J., K. M. Khanna, and L. Lefrancois. 2008. Endogenous naive CD8+ T cell precursor frequency regulates primary and memory responses to infection. *Immunity.* 28: 859-869.

9. Ley, K., C. Laudanna, M. I. Cybulsky, and S. Nourshargh. 2007. Getting to the site of inflammation: the leukocyte adhesion cascade updated. *Nat. Rev. Immunol.* 7: 678-689.

10. DeNucci, C. C., J. S. Mitchell, and Y. Shimizu. 2009. Integrin function in T-cell homing to lymphoid and nonlymphoid sites: getting there and staying there. *Crit Rev. Immunol.* 29: 87-109.

11. Carman, C. V., P. T. Sage, T. E. Sciuto, M. A. De la Fuente, R. S. Geha, H. D. Ochs, H. F. Dvorak, A. M. Dvorak, and T. A. Springer. 2007. Transcellular diapedesis is initiated by invasive podosomes. *Immunity.* 26: 784-797.

12. Vestweber, D. 2007. Adhesion and signaling molecules controlling the transmigration of leukocytes through endothelium. *Immunol. Rev.* 218: 178-196.

13. Millan, J., L. Hewlett, M. Glyn, D. Toomre, P. Clark, and A. J. Ridley. 2006. Lymphocyte transcellular migration occurs through recruitment of endothelial ICAM-1 to caveola- and F-actin-rich domains. *Nat. Cell Biol.* 8: 113-123.

14. Cahalan, M. D., and I. Parker. 2008. Choreography of cell motility and interaction dynamics imaged by two-photon microscopy in lymphoid organs. *Annu. Rev. Immunol.* 26: 585-626.

15. Miller, M. J., S. H. Wei, I. Parker, and M. D. Cahalan. 2002. Two-photon imaging of lymphocyte motility and antigen response in intact lymph node. *Science* 296: 1869-1873.

16. Mandala, S., R. Hajdu, J. Bergstrom, E. Quackenbush, J. Xie, J. Milligan, R. Thornton, G. J. Shei, D. Card, C. Keohane, M. Rosenbach, J. Hale, C. L. Lynch, K. Rupprecht, W. Parsons, and H. Rosen. 2002. Alteration of lymphocyte trafficking by sphingosine-1-phosphate receptor agonists. *Science* 296: 346-349.

17. Cyster, J. G., and S. R. Schwab. 2012. Sphingosine-1-phosphate and lymphocyte egress from lymphoid organs. *Annu. Rev. Immunol.* 30: 69-94.

18. Schwab, S. R., and J. G. Cyster. 2007. Finding a way out: lymphocyte egress from lymphoid organs. *Nat. Immunol.* 8: 1295-1301.

19. Mescher, M. F., J. M. Curtsinger, P. Agarwal, K. A. Casey, M. Gerner, C. D. Hammerbeck, F. Popescu, and Z. Xiao. 2006. Signals required for programming effector and memory development by CD8+ T cells. *Immunol. Rev.* 211: 81-92.

20. Curtsinger, J. M., and M. F. Mescher. 2010. Inflammatory cytokines as a third signal for T cell activation. *Curr. Opin. Immunol.* 22: 333-340.

21. Harty, J. T., and V. P. Badovinac. 2008. Shaping and reshaping CD8+ T-cell memory. *Nat. Rev. Immunol.* 8: 107-119.

22. Russell, J. H., and T. J. Ley. 2002. Lymphocyte-mediated cytotoxicity. *Annu. Rev. Immunol.* 20: 323-370.

23. Kaech, S. M., and E. J. Wherry. 2007. Heterogeneity and cell-fate decisions in effector and memory CD8+ T cell differentiation during viral infection. *Immunity.* 27: 393-405.

24. Williams, M. A., and M. J. Bevan. 2007. Effector and memory CTL differentiation. *Annu. Rev. Immunol.* 25: 171-192.

25. Badovinac, V. P., and J. T. Harty. 2006. Programming, demarcating, and manipulating CD8+ T-cell memory. *Immunol. Rev.* 211: 67-80.

26. Jameson, S. C., and D. Masopust. 2009. Diversity in T cell memory: an embarrassment of riches. *Immunity.* 31: 859-871.

27. Chang, J. T., V. R. Palanivel, I. Kinjyo, F. Schambach, A. M. Intlekofer, A. Banerjee, S. A. Longworth, K. E. Vinup, P. Mrass, J. Oliaro, N. Killeen, J. S. Orange, S. M. Russell, W. Weninger, and S. L. Reiner. 2007. Asymmetric T lymphocyte division in the initiation of adaptive immune responses. *Science* 315: 1687-1691.

28. King, C. G., S. Koehli, B. Hausmann, M. Schmaler, D. Zehn, and E. Palmer. 2012. T cell affinity regulates asymmetric division, effector cell differentiation, and tissue pathology. *Immunity.* 37: 709-720.

29. Stemberger, C., K. M. Huster, M. Koffler, F. Anderl, M. Schiemann, H. Wagner, and D. H. Busch. 2007. A single naive CD8+ T cell precursor can develop into diverse effector and memory subsets. *Immunity.* 27: 985-997.

30. Sarkar, S., V. Kalia, W. N. Haining, B. T. Konieczny, S. Subramaniam, and R. Ahmed. 2008. Functional and genomic profiling of effector CD8 T cell subsets with distinct memory fates. *J. Exp. Med.* 205: 625-640.

31. Kaech, S. M., J. T. Tan, E. J. Wherry, B. T. Konieczny, C. D. Surh, and R. Ahmed. 2003. Selective expression of the interleukin 7 receptor identifies effector CD8 T cells that give rise to long-lived memory cells. *Nat. Immunol.* 4: 1191-1198.

32. Hand, T. W., M. Morre, and S. M. Kaech. 2007. Expression of IL-7 receptor alpha is necessary but not sufficient for the formation of memory CD8 T cells during viral infection. *Proc. Natl. Acad. Sci. U. S. A* 104: 11730-11735.

33. Joshi, N. S., W. Cui, A. Chandele, H. K. Lee, D. R. Urso, J. Hagman, L. Gapin, and S. M. Kaech. 2007. Inflammation directs memory precursor and short-lived effector $CD8^+$ T cell fates via the graded expression of T-bet transcription factor. *Immunity.* 27: 281-295.

34. Kastenmuller, W., M. Brandes, Z. Wang, J. Herz, J. G. Egen, and R. N. Germain. 2013. Peripheral Prepositioning and Local CXCL9 Chemokine-Mediated Guidance Orchestrate Rapid Memory CD8(+) T Cell Responses in the Lymph Node. *Immunity.*

35. Sung, J. H., H. Zhang, E. A. Moseman, D. Alvarez, M. Iannacone, S. E. Henrickson, J. C. de la Torre, J. R. Groom, A. D. Luster, and U. H. Von Andrian. 2012. Chemokine guidance of central memory T cells is critical for antiviral recall responses in lymph nodes. *Cell* 150: 1249-1263.

36. Monks, C. R. F., B. A. Freiberg, H. Kupfer, N. Sciaky, and A. Kupfer. 1998. Three-dimensional segregation of supramolecular activation clusters in T cells. *Nature* 395: 82-86.

37. Xie, J., C. M. Tato, and M. M. Davis. 2013. How the immune system talks to itself: the varied role of synapses. *Immunol. Rev.* 251: 65-79.

38. Cemerski, S., J. Das, E. Giurisato, M. A. Markiewicz, P. M. Allen, A. K. Chakraborty, and A. S. Shaw. 2008. The balance between T cell receptor signaling and degradation at the center of the immunological synapse is determined by antigen quality. *Immunity.* 29: 414-422.

39. Varma, R., G. Campi, T. Yokosuka, T. Saito, and M. L. Dustin. 2006. T cell receptor-proximal signals are sustained in peripheral microclusters and terminated in the central supramolecular activation cluster. *Immunity.* 25: 117-127.

40. Yokosuka, T., K. Sakata-Sogawa, W. Kobayashi, M. Hiroshima, A. Hashimoto-Tane, M. Tokunaga, M. L. Dustin, and T. Saito. 2005. Newly generated T cell receptor microclusters initiate and sustain T cell activation by recruitment of Zap70 and SLP-76. *Nat. Immunol.* 6: 1253-1262.

41. Noel, P. J., L. H. Boise, J. M. Green, and C. B. Thompson. 1996. CD28 costimulation prevents cell death during primary T cell activation. *J. Immunol.* 157: 636-642.

42. Thompson, C. B., T. Lindsten, J. A. Ledbetter, S. L. Kunkel, H. A. Young, S. G. Emerson, J. M. Leiden, and C. H. June. 1989. CD28 activation pathway regulates the production of multiple T-cell-derived lymphokines/cytokines. *Proc. Natl. Acad. Sci. U. S. A* 86: 1333-1337.

43. Gramaglia, I., D. Cooper, K. T. Miner, B. S. Kwon, and M. Croft. 2000. Co-stimulation of antigen-specific CD4 T cells by 4-1BB ligand. *Eur. J. Immunol.* 30: 392-402.

44. van Seventer, G. A., Y. Shimizu, K. J. Horgan, and S. Shaw. 1990. The LFA-1 ligand ICAM-1 provides an important costimulatory signal for T cell receptor-mediated activation of resting T cells. *J. Immunol.* 144: 4579-4586.

45. Sharpe, A. H. 2009. Mechanisms of costimulation. *Immunol. Rev.* 229: 5-11.

46. Chirathaworn, C., J. E. Kohlmeier, S. A. Tibbetts, L. M. Rumsey, M. A. Chan, and S. H. Benedict. 2002. Stimulation through intercellular adhesion molecule-1 provides a second signal for T cell activation. *J. Immunol.* 168: 5530-5537.

47. Curtsinger, J. M., C. S. Schmidt, A. Mondino, D. C. Lins, R. M. Kedl, M. K. Jenkins, and M. F. Mescher. 1999. Inflammatory cytokines provide a third signal for activation of naive CD4+ and CD8+ T cells. *J. Immunol.* 162: 3256-3262.

48. Casey, K. A., and M. F. Mescher. 2007. IL-21 promotes differentiation of naive CD8 T cells to a unique effector phenotype. *J. Immunol.* 178: 7640-7648.

49. Yi, J. S., M. Du, and A. J. Zajac. 2009. A vital role for interleukin-21 in the control of a chronic viral infection. *Science* 324: 1572-1576.

50. Curtsinger, J. M., J. O. Valenzuela, P. Agarwal, D. Lins, and M. F. Mescher. 2005. Type I IFNs provide a third signal to CD8 T cells to stimulate clonal expansion and differentiation. *J. Immunol.* 174: 4465-4469.

51. Agarwal, P., A. Raghavan, S. L. Nandiwada, J. M. Curtsinger, P. R. Bohjanen, D. L. Mueller, and M. F. Mescher. 2009. Gene regulation and chromatin remodeling by IL-12 and type I IFN in programming for CD8 T cell effector function and memory. *J. Immunol.* 183: 1695-1704.

52. Curtsinger, J. M., and M. F. Mescher. 2010. Inflammatory cytokines as a third signal for T cell activation. *Curr. Opin. Immunol.* 22: 333-340.

53. Brombacher, F., A. Dorfmuller, J. Magram, W. J. Dai, G. Kohler, A. Wunderlin, K. Palmer-Lehmann, M. K. Gately, and G. Alber. 1999. IL-12 is dispensable for innate and adaptive immunity against low doses of Listeria monocytogenes. *Int. Immunol.* 11: 325-332.

54. Zhou, S., A. M. Cerny, A. Zacharia, K. A. Fitzgerald, E. A. Kurt-Jones, and R. W. Finberg. 2010. Induction and inhibition of type I interferon responses by distinct components of lymphocytic choriomeningitis virus. *J. Virol.* 84: 9452-9462.

55. Keir, M. E., M. J. Butte, G. J. Freeman, and A. H. Sharpe. 2008. PD-1 and its ligands in tolerance and immunity. *Annu. Rev. Immunol.* 26: 677-704.

56. Francisco, L. M., P. T. Sage, and A. H. Sharpe. 2010. The PD-1 pathway in tolerance and autoimmunity. *Immunol. Rev.* 236: 219-242.

57. Blackburn, S. D., H. Shin, W. N. Haining, T. Zou, C. J. Workman, A. Polley, M. R. Betts, G. J. Freeman, D. A. Vignali, and E. J. Wherry. 2009. Coregulation of CD8+ T cell exhaustion by multiple inhibitory receptors during chronic viral infection. *Nat. Immunol.* 10: 29-37.

58. Takamura, S., S. Tsuji-Kawahara, H. Yagita, H. Akiba, M. Sakamoto, T. Chikaishi, M. Kato, and M. Miyazawa. 2010. Premature terminal exhaustion of Friend virus-specific effector CD8+ T cells by rapid induction of multiple inhibitory receptors. *J. Immunol.* 184: 4696-4707.

59. Wherry, E. J. 2011. T cell exhaustion. *Nat. Immunol.* 12: 492-499.

60. Krummel, M. F., and J. P. Allison. 1995. CD28 and CTLA-4 have opposing effects on the response of T cells to stimulation. *J. Exp. Med.* 182: 459-465.

61. Teft, W. A., M. G. Kirchhof, and J. Madrenas. 2006. A molecular perspective of CTLA-4 function. *Annu. Rev. Immunol.* 24: 65-97.

62. Rudd, C. E., A. Taylor, and H. Schneider. 2009. CD28 and CTLA-4 coreceptor expression and signal transduction. *Immunol. Rev.* 229: 12-26.

63. Walker, L. S., and D. M. Sansom. 2011. The emerging role of CTLA4 as a cell-extrinsic regulator of T cell responses. *Nat. Rev. Immunol.* 11: 852-863.

64. Alegre, M. L., P. J. Noel, B. J. Eisfelder, E. Chuang, M. R. Clark, S. L. Reiner, and C. B. Thompson. 1996. Regulation of surface and intracellular expression of CTLA4 on mouse T cells. *J. Immunol.* 157: 4762-4770.

65. Egen, J. G., and J. P. Allison. 2002. Cytotoxic T lymphocyte antigen-4 accumulation in the immunological synapse is regulated by TCR signal strength. *Immunity.* 16: 23-35.

66. Wang, X. B., C. Y. Zheng, R. Giscombe, and A. K. Lefvert. 2001. Regulation of surface and intracellular expression of CTLA-4 on human peripheral T cells. *Scand. J. Immunol.* 54: 453-458.

67. Thaventhiran, J. E., A. Hoffmann, L. Magiera, M. de la Roche, H. Lingel, M. Brunner-Weinzierl, and D. T. Fearon. 2012. Activation of the Hippo pathway by CTLA-4 regulates the expression of Blimp-1 in the CD8+ T cell. *Proc. Natl. Acad. Sci. U. S. A* 109: E2223-E2229.

68. Schneider, H., E. Valk, S. D. Dias, B. Wei, and C. E. Rudd. 2005. CTLA-4 up-regulation of lymphocyte function-associated antigen 1 adhesion and clustering as an alternate basis for coreceptor function. *Proc. Natl. Acad. Sci. USA* 102: 12861-12866.

69. Pandiyan, P., J. K. Hegel, M. Krueger, D. Quandt, and M. C. Brunner-Weinzierl. 2007. High IFN-gamma production of individual CD8 T lymphocytes is controlled by CD152 (CTLA-4). *J. Immunol.* 178: 2132-2140.

70. Hegel, J. K., K. Knieke, P. Kolar, S. L. Reiner, and M. C. Brunner-Weinzierl. 2009. CD152 (CTLA-4) regulates effector functions of CD8+ T lymphocytes by repressing Eomesodermin. *Eur. J. Immunol.* 39: 883-893.

71. Rudd, C. E. 2009. CTLA-4 co-receptor impacts on the function of Treg and CD8+ T-cell subsets. *Eur. J. Immunol.* 39: 687-690.

72. Pearce, E. L., A. C. Mullen, G. A. Martins, C. M. Krawczyk, A. S. Hutchins, V. P. Zediak, M. Banica, C. B. DiCioccio, D. A. Gross, C. A. Mao, H. Shen, N. Cereb, S. Y. Yang, T. Lindsten, J. Rossant, C. A. Hunter, and S. L. Reiner. 2003. Control of effector CD8+ T cell function by the transcription factor Eomesodermin. *Science* 302: 1041-1043.

73. Wang, W., D. Yu, A. A. Sarnaik, B. Yu, M. Hall, D. Morelli, Y. Zhang, X. Zhao, and J. S. Weber. 2012. Biomarkers on melanoma patient T cells associated with ipilimumab treatment. *J. Transl. Med.* 10: 146.

74. Parameswaran, N., R. Suresh, V. Bal, S. Rath, and A. George. 2005. Lack of ICAM-1 on APCs during T cell priming leads to poor generation of central memory cells. *J. Immunol.* 175: 2201-2211.

75. Scholer, A., S. Hugues, A. Boissonnas, L. Fetler, and S. Amigorena. 2008. Intercellular adhesion molecule-1-dependent stable interactions between T cells and dendritic cells determine CD8+ T cell memory. *Immunity* 28: 258-270.

76. Cox, M. A., S. R. Barnum, D. C. Bullard, and A. J. Zajac. 2013. ICAM-1-dependent tuning of memory CD8 T-cell responses following acute infection. *Proc. Natl. Acad. Sci. U. S. A* 110: 1416-1421.

77. Cambi, A., B. Joosten, M. Koopman, L. F. de, I. Beeren, R. Torensma, J. A. Fransen, M. Garcia-Parajo, F. N. Van Leeuwen, and C. G. Figdor. 2006. Organization of the integrin LFA-1 in nanoclusters regulates its activity. *Mol. Biol. Cell* 17: 4270-4281.

78. Eich, C., I. J. de Vries, P. C. Linssen, B. A. de, J. B. Boezeman, C. G. Figdor, and A. Cambi. 2011. The lymphoid chemokine CCL21 triggers LFA-1 adhesive properties on human dendritic cells. *Immunol. Cell Biol.* 89: 458-465.

79. Kohlmeier, J. E., L. M. Rumsey, M. A. Chan, and S. H. Benedict. 2003. The outcome of T-cell costimulation through intercellular adhesion molecule-1 differs from costimulation through leucocyte function-associated antigen-1. *Immunology* 108: 152-157.

80. Kohlmeier, J. E., M. A. Chan, and S. H. Benedict. 2006. Costimulation of naive human CD4 T cells through intercellular adhesion molecule-1 promotes differentiation to a memory phenotype that is not strictly the result of multiple rounds of cell division. *Immunology* 118: 549-558.

81. Williams, K. M., A. L. Dotson, A. R. Otto, J. E. Kohlmeier, and S. H. Benedict. 2011. Choice of resident costimulatory molecule can influence cell fate in human naive CD4+ T cell differentiation. *Cell Immunol.* 271: 418-427.

82. Rothlein, R., and T. A. Springer. 1986. The requirement for lymphocyte function-associated antigen 1 in homotypic leukocyte adhesion stimulated by phorbol ester. *J. Exp. Med.* 163: 1132-1149.

83. Rothlein, R., M. L. Dustin, S. D. Marlin, and T. A. Springer. 1986. A human intercellular adhesion molecule (ICAM-1) distinct from LFA-1. *J. Immunol.* 137: 1270-1274.

84. Springer, T. A. 1990. Adhesion receptors of the immune system. *Nature* 346: 425-434.

85. Ingulli, E., A. Mondino, A. Khoruts, and M. K. Jenkins. 1997. In vivo detection of dendritic cell antigen presentation to CD4(+) T cells. *J. Exp. Med.* 185: 2133-2141.

86. Hommel, M., and B. Kyewski. 2003. Dynamic changes during the immune response in T cell-antigen-presenting cell clusters isolated from lymph nodes. *J. Exp. Med.* 197: 269-280.

87. Sabatos, C. A., J. Doh, S. Chakravarti, R. S. Friedman, P. G. Pandurangi, A. J. Tooley, and M. F. Krummel. 2008. A synaptic basis for paracrine interleukin-2 signaling during homotypic T cell interaction. *Immunity.* 29: 238-248.

88. Doh, J., and M. F. Krummel. 2010. Immunological synapses within context: patterns of cell-cell communication and their application in T-T interactions. *Curr. Top. Microbiol. Immunol.* 340: 25-50.

89. Ueda, Y., K. Katagiri, T. Tomiyama, K. Yasuda, K. Habiro, T. Katakai, S. Ikehara, M. Matsumoto, and T. Kinashi. 2012. Mst1 regulates integrin-dependent thymocyte trafficking and antigen recognition in the thymus. *Nat. Commun.* 3: 1098.

90. Taylor, P. A., C. J. Lees, S. Fournier, J. P. Allison, A. H. Sharpe, and B. R. Blazar. 2004. B7 expression on T cells down-regulates immune responses through CTLA-4 ligation via T-T interactions [corrections]. *J. Immunol.* 172: 34-39.

91. Roebuck, K. A., and A. Finnegan. 1999. Regulation of intercellular adhesion molecule-1 (CD54) gene expression. *J. Leukoc. Biol.* 66: 876-888.

92. Gahmberg, C. G., L. Valmu, S. Fagerholm, P. Kotovuori, E. Ihanus, L. Tian, and T. Pessa-Morikawa. 1998. Leukocyte integrins and inflammation. *Cell Mol. Life Sci.* 54: 549-555.

93. Van de Stolpe, A., and P. T. Van der Saag. 1996. Intercellular adhesion molecule-1. *J. Mol. Med. (Berl)* 74: 13-33.

94. Jun, C. D., C. V. Carman, S. D. Redick, M. Shimaoka, H. P. Erickson, and T. A. Springer. 2001. Ultrastructure and function of dimeric, soluble intercellular adhesion molecule-1 (ICAM-1). *J. Biol. Chem.* 276: 29019-29027.

95. Lawson, C., and S. Wolf. 2009. ICAM-1 signaling in endothelial cells. *Pharmacol. Rep.* 61: 22-32.

96. Lebedeva, T., M. L. Dustin, and Y. Sykulev. 2005. ICAM-1 co-stimulates target cells to facilitate antigen presentation. *Curr. Opin. Immunol.* 17: 251-258.

97. Xu, H., J. A. Gonzalo, P. Y. St, I. R. Williams, T. S. Kupper, R. S. Cotran, T. A. Springer, and J. C. Gutierrez-Ramos. 1994. Leukocytosis and resistance to septic shock in intercellular adhesion molecule 1-deficient mice. *J. Exp. Med.* 180: 95-109.

98. Bongard, V., A. Elias, S. C. Bal dit, J. Ruidavets, H. Boccalon, L. Drouet, and J. Ferrieres. 2002. Soluble intercellular adhesion molecule-1 is associated with carotid and femoral atherosclerosis but not with intima-media thickness in a population-based sample. *Atherosclerosis* 164: 297-304.

99. Hwang, S. J., C. M. Ballantyne, A. R. Sharrett, L. C. Smith, C. E. Davis, A. M. Gotto, Jr., and E. Boerwinkle. 1997. Circulating adhesion molecules VCAM-1, ICAM-1, and E-selectin in carotid atherosclerosis and incident coronary heart disease cases: the Atherosclerosis Risk In Communities (ARIC) study. *Circulation* 96: 4219-4225.

100. Schmidt, C., J. Hulthe, and B. Fagerberg. 2009. Baseline ICAM-1 and VCAM-1 are increased in initially healthy middle-aged men who develop cardiovascular disease during 6.6 years of follow-up. *Angiology* 60: 108-114.

101. Tanne, D., M. Haim, V. Boyko, U. Goldbourt, T. Reshef, S. Matetzky, Y. Adler, Y. A. Mekori, and S. Behar. 2002. Soluble intercellular adhesion molecule-1 and risk of future ischemic stroke: a nested case-control study from the Bezafibrate Infarction Prevention (BIP) study cohort. *Stroke* 33: 2182-2186.

102. van Den Engel, N. K., E. Heidenthal, A. Vinke, H. Kolb, and S. Martin. 2000. Circulating forms of intercellular adhesion molecule (ICAM)-1 in mice lacking membranous ICAM-1. *Blood* 95: 1350-1355.

103. Stanciu, L. A., and R. Djukanovic. 1998. The role of ICAM-1 on T-cells in the pathogenesis of asthma. *Eur. Respir. J.* 11: 949-957.

104. Robledo, O., A. Papaioannou, B. Ochietti, C. Beauchemin, D. Legault, A. Cantin, P. D. King, C. Daniel, V. Y. Alakhov, E. F. Potworowski, and Y. St-Pierre. 2003. ICAM-1 isoforms: specific activity and sensitivity to cleavage by leukocyte elastase and cathepsin G. *Eur. J. Immunol.* 33: 1351-1360.

105. King, P. D., E. T. Sandberg, A. Selvakumar, P. Fang, A. L. Beaudet, and B. Dupont. 1995. Novel isoforms of murine intercellular adhesion molecule-1 generated by alternative RNA splicing. *J. Immunol.* 154: 6080-6093.

106. Hu, X., S. R. Barnum, J. E. Wohler, T. R. Schoeb, and D. C. Bullard. 2010. Differential ICAM-1 isoform expression regulates the development and progression of experimental autoimmune encephalomyelitis. *Mol. Immunol.* 47: 1692-1700.

107. Sligh, J. E., Jr., C. M. Ballantyne, S. S. Rich, H. K. Hawkins, C. W. Smith, A. Bradley, and A. L. Beaudet. 1993. Inflammatory and immune responses are impaired in mice deficient in intercellular adhesion molecule 1. *Proc. Natl. Acad. Sci. USA* 90: 8529-8533.

108. Pluskota, E., Y. Chen, and S. E. D'Souza. 2000. Src homology domain 2-containing tyrosine phosphatase 2 associates with intercellular adhesion molecule 1 to regulate cell survival. *J. Biol. Chem.* 275: 30029-30036.

109. Thompson, P. W., A. M. Randi, and A. J. Ridley. 2002. Intercellular adhesion molecule (ICAM)-1, but not ICAM-2, activates RhoA and stimulates c-fos and rhoA transcription in endothelial cells. *J. Immunol.* 169: 1007-1013.

110. Lyck, R., Y. Reiss, N. Gerwin, J. Greenwood, P. Adamson, and B. Engelhardt. 2003. T-cell interaction with ICAM-1/ICAM-2 double-deficient brain endothelium in vitro: the cytoplasmic tail of endothelial ICAM-1 is necessary for transendothelial migration of T cells. *Blood* 102: 3675-3683.

111. Shaulian, E., and M. Karin. 2001. AP-1 in cell proliferation and survival. *Oncogene* 20: 2390-2400.

112. Maeda, Y., J. Chihara, F. Horiuchi, J. Miyatake, Y. Tatsumi, F. Urase, K. Irimajiri, S. Nakajima, and A. Horiuchi. 1996. Elevated levels of soluble ICAM-1 in serum of patients with acute myeloid leukemia undergoing bone marrow transplantation. *Am. J. Hematol.* 52: 227-228.

113. Kostler, W. J., S. Tomek, T. Brodowicz, A. C. Budinsky, M. Flamm, M. Hejna, M. Krainer, C. Wiltschke, and C. C. Zielinski. 2001. Soluble ICAM-1 in breast cancer: clinical significance and biological implications. *Cancer Immunol. Immunother.* 50: 483-490.

114. Shijubo, N., K. Imai, S. Aoki, M. Hirasawa, H. Sugawara, H. Koba, M. Tsujisaki, T. Sugiyama, Y. Hinoda, A. Yachi, and . 1992. Circulating intercellular adhesion molecule-1 (ICAM-1) antigen in sera of patients with idiopathic pulmonary fibrosis. *Clin. Exp. Immunol.* 89: 58-62.

115. De, R., V, A. Oliva, B. Messore, B. Grosso, C. Mollar, and E. Pozzi. 1998. Circulating adhesion molecules in cystic fibrosis. *Am. J. Respir. Crit Care Med.* 157: 1234-1239.

116. McDonnell, G. V., S. A. McMillan, J. P. Douglas, A. G. Droogan, and S. A. Hawkins. 1999. Serum soluble adhesion molecules in multiple sclerosis: raised sVCAM-1, sICAM-1 and sE-selectin in primary progressive disease. *J. Neurol.* 246: 87-92.

117. Marlin, S. D., D. E. Staunton, T. A. Springer, C. Stratowa, W. Sommergruber, and V. J. Merluzzi. 1990. A soluble form of intercellular adhesion molecule-1 inhibits rhinovirus infection. *Nature* 344: 70-72.

118. Prasad, A. S. 2009. Zinc: role in immunity, oxidative stress and chronic inflammation. *Curr. Opin. Clin. Nutr. Metab Care* 12: 646-652.

119. Bourdillon, M. C., R. N. Poston, C. Covacho, E. Chignier, G. Bricca, and J. L. McGregor. 2000. ICAM-1 deficiency reduces atherosclerotic lesions in double-knockout mice (ApoE(-/-)/ICAM-1(-/-)) fed a fat or a chow diet. *Arterioscler. Thromb. Vasc. Biol.* 20: 2630-2635.

120. Rosette, C., R. B. Roth, P. Oeth, A. Braun, S. Kammerer, J. Ekblom, and M. F. Denissenko. 2005. Role of ICAM1 in invasion of human breast cancer cells. *Carcinogenesis* 26: 943-950.

121. Burbach, B. J., R. B. Medeiros, K. L. Mueller, and Y. Shimizu. 2007. T cell receptor signaling to integrins. *Immunol. Rev.* 218: 65-81.

122. Crotty, S. 2011. Follicular helper CD4 T cells (TFH). *Annu. Rev. Immunol.* 29: 621-663.

123. Qi, H., J. L. Cannons, F. Klauschen, P. L. Schwartzberg, and R. N. Germain. 2008. SAP-controlled T-B cell interactions underlie germinal centre formation. *Nature* 455: 764-769.

124. Sanders, R. W., E. C. de Jong, C. E. Baldwin, J. H. Schuitemaker, M. L. Kapsenberg, and B. Berkhout. 2002. Differential transmission of human immunodeficiency virus type 1 by distinct subsets of effector dendritic cells. *J. Virol.* 76: 7812-7821.

125. Wang, J. H., C. Kwas, and L. Wu. 2009. Intercellular adhesion molecule 1 (ICAM-1), but not ICAM-2 and -3, is important for dendritic cell-mediated human immunodeficiency virus type 1 transmission. *J. Virol.* 83: 4195-4204.

126. Buckle, A.-M., and N. Hogg. 1990. Human memory T cells express intercellular adhesion molecule- 1 which can be increased by interleukin 2 and interferon-gamma. *Eur. J. Immunol.* 20: 337-341.

127. Xiao, Z., K. A. Casey, S. C. Jameson, J. M. Curtsinger, and M. F. Mescher. 2009. Programming for CD8 T cell memory development requires IL-12 or type I IFN. *J. Immunol.* 182: 2786-2794.

128. Kavanaugh, A. F., E. Lightfoot, P. E. Lipsky, and N. Oppenheimer-Marks. 1991. Role of CD11/CD18 in adhesion and transendothelial migration of T cells: analysis utilizing CD18-deficient T cell clones. *J. Immunol.* 146: 4149-4156.

129. Andrew, D. P., J. P. Spellberg, H. Takimoto, R. Schmits, T. W. Mak, and M. M. Zukowski. 1998. Transendothelial migration and trafficking of leukocytes in LFA-1-deficient mice. *Eur. J. Immunol.* 28: 1959-1969.

130. Windish, H. P., P. L. Lin, J. T. Mattila, A. M. Green, E. O. Onuoha, L. P. Kane, and J. L. Flynn. 2009. Aberrant TGF-beta signaling reduces T regulatory cells in ICAM-1-deficient mice, increasing the inflammatory response to Mycobacterium tuberculosis. *J. Leukoc. Biol.* 86: 713-725.

131. Hamilton, S. E., M. C. Wolkers, S. P. Schoenberger, and S. C. Jameson. 2006. The generation of protective memory-like CD8+ T cells during homeostatic proliferation requires CD4+ T cells. *Nat. Immunol.* 7: 475-481.

132. Surh, C. D., and J. Sprent. 2008. Homeostasis of naive and memory T cells. *Immunity.* 29: 848-862.

133. Burbach, B. J., R. Srivastava, R. B. Medeiros, W. E. O'Gorman, E. J. Peterson, and Y. Shimizu. 2008. Distinct regulation of integrin-dependent T cell conjugate

formation and NF-kB activation by the adapter protein ADAP. *J. Immunol.* 181: 4840-4851.

134. Mueller, K. L., M. S. Thomas, B. J. Burbach, E. J. Peterson, and Y. Shimizu. 2007. Adhesion and degranulation promoting adapter protein (ADAP) positively regulates T cell sensitivity to antigen and T cell survival. *J. Immunol.* 179: 3559-3569.

135. Miller, M. J., S. H. Wei, M. D. Cahalan, and I. Parker. 2003. Autonomous T cell trafficking examined in vivo with intravital two-photon microscopy. *Proc. Natl. Acad. Sci. U. S. A* 100: 2604-2609.

136. Shibaki, A., and S. I. Katz. 2002. Induction of skewed Th1/Th2 T-cell differentiation via subcutaneous immunization with Freund's adjuvant. *Exp. Dermatol.* 11: 126-134.

137. Ruetten, H., C. Thiemermann, and M. Perretti. 1999. Upregulation of ICAM-1 expression on J774.2 macrophages by endotoxin involves activation of NF-kappaB but not protein tyrosine kinase: comparison to induction of iNOS. *Mediators. Inflamm.* 8: 77-84.

138. Shiow, L. R., D. B. Rosen, N. Brdickova, Y. Xu, J. An, L. L. Lanier, J. G. Cyster, and M. Matloubian. 2006. CD69 acts downstream of interferon-alpha/beta to inhibit S1P1 and lymphocyte egress from lymphoid organs. *Nature* 440: 540-544.

139. Moran, A. E., K. L. Holzapfel, Y. Xing, N. R. Cunningham, J. S. Maltzman, J. Punt, and K. A. Hogquist. 2011. T cell receptor signal strength in Treg and iNKT cell development demonstrated by a novel fluorescent reporter mouse. *J. Exp. Med.* 208: 1279-1289.

140. Obar, J. J., and L. Lefrancois. 2010. Early signals during CD8 T cell priming regulate the generation of central memory cells. *J. Immunol.* 185: 263-272.

141. Qureshi, O. S., S. Kaur, T. Z. Hou, L. E. Jeffery, N. S. Poulter, Z. Briggs, R. Kenefeck, A. K. Willox, S. J. Royle, J. Z. Rappoport, and D. M. Sansom. 2012. Constitutive clathrin-mediated endocytosis of CTLA-4 persists during T cell activation. *J. Biol. Chem.* 287: 9429-9440.

142. Boise, L. H., A. J. Minn, P. J. Noel, C. H. June, M. A. Accavitti, T. Lindsten, and C. B. Thompson. 1995. CD28 costimulation can promote T cell survival by enhancing the expression of Bcl-XL. *Immunity.* 3: 87-98.

143. Watts, T. H. 2010. Staying alive: T cell costimulation, CD28, and Bcl-xL. *J. Immunol.* 185: 3785-3787.

144. Woodland, D. L., and J. E. Kohlmeier. 2009. Migration, maintenance and recall of memory T cells in peripheral tissues. *Nat. Rev. Immunol.* 9: 153-161.

145. Wakim, L. M., A. Woodward-Davis, and M. J. Bevan. 2010. Memory T cells persisting within the brain after local infection show functional adaptations to their tissue of residence. *Proc. Natl. Acad. Sci. U. S. A* 107: 17872-17879.

146. Restifo, N. P., M. E. Dudley, and S. A. Rosenberg. 2012. Adoptive immunotherapy for cancer: harnessing the T cell response. *Nat. Rev. Immunol.* 12: 269-281.

147. Pamer, E. G. 2004. Immune responses to Listeria monocytogenes. *Nat. Rev. Immunol.* 4: 812-823.

148. Klebanoff, C. A., L. Gattinoni, P. Torabi-Parizi, K. Kerstann, A. R. Cardones, S. E. Finkelstein, D. C. Palmer, P. A. Antony, S. T. Hwang, S. A. Rosenberg, T. A. Waldmann, and N. P. Restifo. 2005. Central memory self/tumor-reactive CD8+ T cells confer superior antitumor immunity compared with effector memory T cells. *Proc. Natl. Acad. Sci. U. S. A* 102: 9571-9576.

149. Berger, C., M. C. Jensen, P. M. Lansdorp, M. Gough, C. Elliott, and S. R. Riddell. 2008. Adoptive transfer of effector CD8+ T cells derived from central memory cells establishes persistent T cell memory in primates. *J. Clin. Invest* 118: 294-305.

150. Chapuis, A. G., J. A. Thompson, K. A. Margolin, R. Rodmyre, I. P. Lai, K. Dowdy, E. A. Farrar, S. Bhatia, D. E. Sabath, J. Cao, Y. Li, and C. Yee. 2012. Transferred melanoma-specific CD8+ T cells persist, mediate tumor regression, and acquire central memory phenotype. *Proc. Natl. Acad. Sci. U. S. A* 109: 4592-4597.

151. Mempel, T. R., S. E. Henrickson, and U. H. Von Andrian. 2004. T-cell priming by dendritic cells in lymph nodes occurs in three distinct phases. *Nature* 427: 154-159.

152. Purbhoo, M. A., D. J. Irvine, J. B. Huppa, and M. M. Davis. 2004. T cell killing does not require the formation of a stable mature immunological synapse. *Nat. Immunol.* 5: 524-530.

153. Major, E. O. 2010. Progressive multifocal leukoencephalopathy in patients on immunomodulatory therapies. *Annu. Rev. Med.* 61: 35-47.

154. Schroecksnadel, K., B. Frick, C. Winkler, and D. Fuchs. 2006. Crucial role of interferon-gamma and stimulated macrophages in cardiovascular disease. *Curr. Vasc. Pharmacol.* 4: 205-213.